AD-A074 395 ARMY ELECTRONICS RESEARCH AND DEVELOPMENT COMMAND WS--ETC F/G 4/2
RELATIONSHIPS BETWEEN IR EXTINCTION, ABSORPTION, AND LIQUID WAT--ETC(U)
AUG 79 R G PINNICK, S G JENNINGS, P CHYLEK

UNCLASSIFIED ERADCOM/ASL-TR-0037 NL

| OF |
AD-
A074395

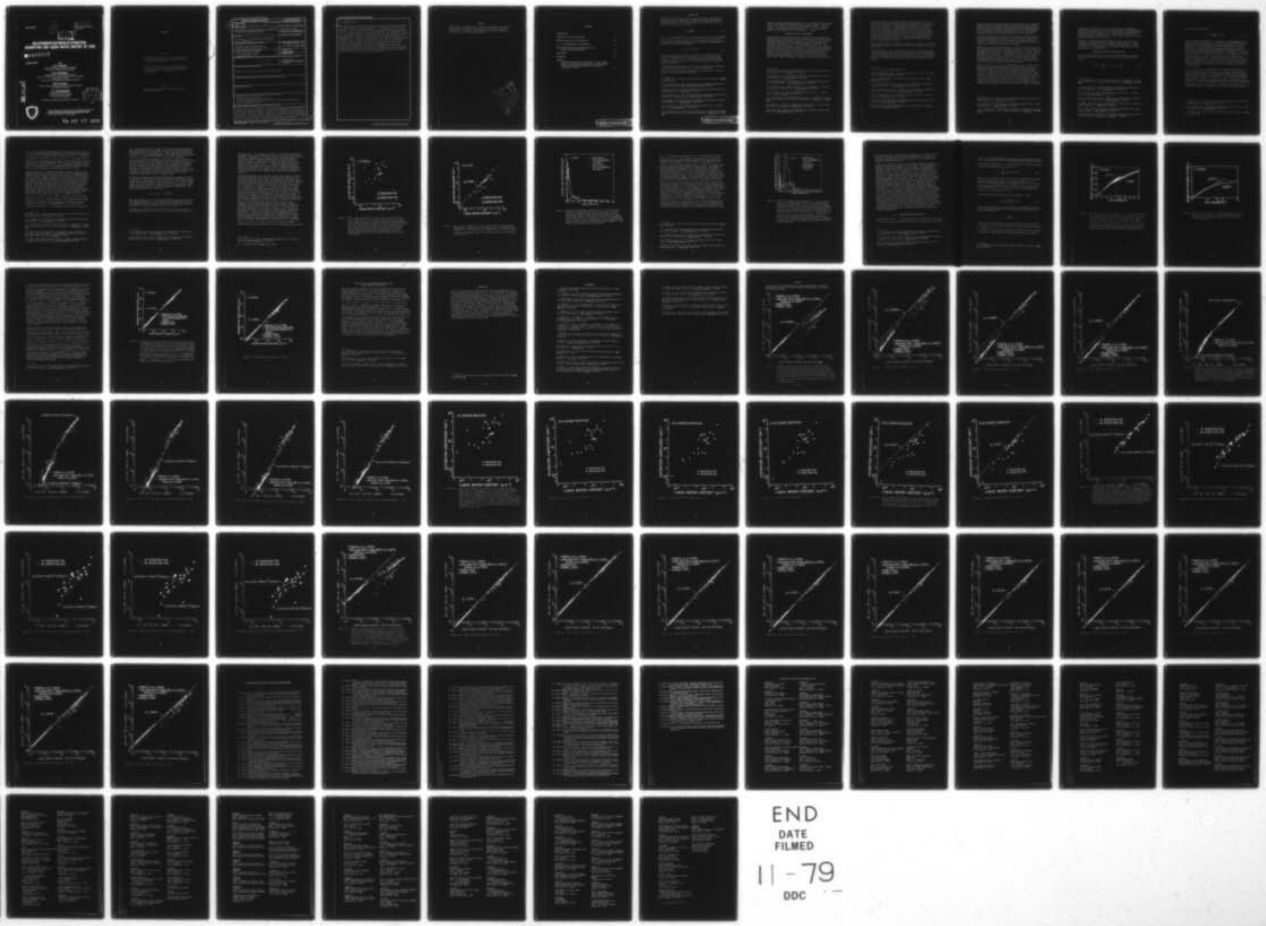

END
DATE
FILMED
11-79
DDC

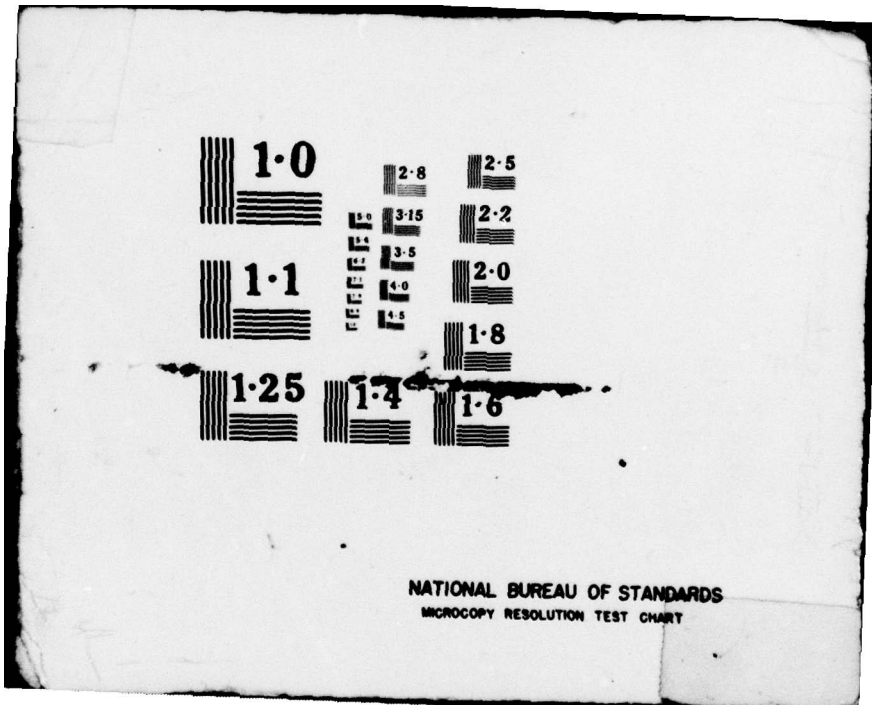
1·0
1·1
1·25
1·4
1·6
1·8
2·0
2·2
2·5
2·8
3·15
3·5
4·0
4·5
NATIONAL BUREAU OF STANDARDS
MICROCOPY RESOLUTION TEST CHART

ASL-TR-0037

AD

Reports Control Symbol
OSD 1366

LEVEL II

RELATIONSHIPS BETWEEN IR EXTINCTION, ABSORPTION, AND LIQUID WATER CONTENT OF FOGS

AD A074395

August 1979

By

R.G. PINNICK
US Army Atmospheric Sciences Laboratory
White Sands Missile Range, NM 88002

S.G. JENNINGS*
Department of Pure and Applied Physics
University of Manchester Institute of Science and Technology
Manchester, England
*Visiting US Army Atmospheric Sciences Laboratory

PETR CHÝLEK
Center for Earth and Planetary Physics, Harvard University
Cambridge, MA 02138

H.J. AUVERMANN
Physical Science Laboratory
New Mexico State University
Las Cruces, NM 88003

Approved for public release; distribution unlimited

US Army Electronics Research and Development Command
ATMOSPHERIC SCIENCES LABORATORY
White Sands Missile Range, NM 88002

NOTICES

Disclaimers

The findings in this report are not to be construed as an official Department of the Army position, unless so designated by other authorized documents.

The citation of trade names and names of manufacturers in this report is not to be construed as official Government indorsement or approval of commercial products or services referenced herein.

Disposition

Destory this report when it is no longer needed. Do not return it to the originator.

SECURITY CLASSIFICATION OF THIS PAGE (When Data Entered)

REPORT DOCUMENTATION PAGE

READ INSTRUCTIONS BEFORE COMPLETING FORM

1. REPORT NUMBER: ERADCOM/ASL-TR-0037	2. GOVT ACCESSION NO.
3. RECIPIENT'S CATALOG NUMBER	
4. TITLE (and Subtitle): RELATIONSHIPS BETWEEN IR EXTINCTION, ABSORPTION, AND LIQUID WATER CONTENT OF FOGS.	5. TYPE OF REPORT & PERIOD COVERED: R&D Technical Report
	6. PERFORMING ORG. REPORT NUMBER
7. AUTHOR(s): R. G. Pinnick, S. G. Jennings, Petr Chylek, and H. J. Auvermann	8. CONTRACT OR GRANT NUMBER(s)
9. PERFORMING ORGANIZATION NAME AND ADDRESS: Atmospheric Sciences Laboratory, White Sands Missile Range, NM 88002	10. PROGRAM ELEMENT, PROJECT, TASK AREA & WORK UNIT NUMBERS: DA Task No. 1L161102B53A-13
11. CONTROLLING OFFICE NAME AND ADDRESS: US Army Electronics Research and Development Command, Adelphi, MD 20783	12. REPORT DATE: August 1979
	13. NUMBER OF PAGES: 19
14. MONITORING AGENCY NAME & ADDRESS (if different from Controlling Office)	15. SECURITY CLASS. (of this report): UNCLASSIFIED
	15a. DECLASSIFICATION/DOWNGRADING SCHEDULE

16. DISTRIBUTION STATEMENT (of this Report)

Approved for public release; distribution unlimited.

17. DISTRIBUTION STATEMENT (of the abstract entered in Block 20, if different from Report)

18. SUPPLEMENTARY NOTES

19. KEY WORDS (Continue on reverse side if necessary and identify by block number)

Infrared extinction in fog
Visibility and infrared extinction in fog
Relations between infrared extinction and liquid water content in fog
Infrared absorption in fog

20. ABSTRACT (Continue on reverse side if necessary and identify by block number)

It is well known that atmospheric fog and haze particles degrade the performance of DOD electro-optical sensors. A quantitative assessment of these effects unfortunately requires knowledge of droplet size distributions, which generally have complex spacial and temporal variations. The problem would be simplified considerably if estimates of the radiative properties of fog and haze particles could be made without detailed knowledge of their size distributions. In this report, an attempt is made to find relationships between the radiative

DD FORM 1 JAN 73 1473 EDITION OF 1 NOV 65 IS OBSOLETE

SECURITY CLASSIFICATION OF THIS PAGE (When Data Entered)

20. ABSTRACT (cont)

properties of fogs and hazes (in particular the volume extinction and absorption coefficients) and their liquid water content, that are relatively independent of droplet size distribution. It is found that definite relationships exist only at particular infrared wavelengths. At wavelengths around $\lambda = 11\mu m$, a linear relation exists between extinction and liquid water content, and at wavelengths around $\lambda = 3.8\mu m$, $9.5\mu m$ similar relations between fog and haze absorption coefficient and liquid water content exist that are nearly independent of the droplet size distribution. Thus the results suggest unique relations between integrated liquid water content along a path in fog and transmission (at $\lambda \doteq 11\mu m$) along that path (neglecting multiple scatter effects and forward scatter corrections), and between fog liquid water content at a particular point and the infrared emission (at $\lambda \doteq 3.8\mu m$, $9.5\mu m$) at that point. Finally, the correlation of visible and infrared extinction is investigated empirically using 341 droplet size distribution measurements made under a variety of meteorological conditions.

PREFACE

We gratefully acknowledge John A. Garland, Environmental and Medical Sciences Division, Harwell, who supplied his raw data of fog size distributions. One author (Petr Chýlek) was partially supported by a grant from the US Army Research Office.

CONTENTS

INTRODUCTION

Chýlek[1] has recently shown that a linear relationship, independent of the form of the size distribution, should exist between the infrared extinction around $\lambda = 11\mu m$ and the liquid water content of fogs. The relation can be written in the form

$$\sigma_e = \frac{3\pi c}{2\rho\lambda} W, \tag{1}$$

where σ_e is the volume extinction coefficient measured at the wavelength λ, W is the liquid water content, ρ is the density of water, and the coefficient c is equal to the slope of a straight line approximating the efficiency factor for extinction Q_e by

$$Q_e (x, \lambda) \doteq c(\lambda)x. \tag{2}$$

The size parameter x is defined by the ratio of the particle circumference to the wavelength. An approximate value of the coefficient $c(\lambda)$ at $\lambda = 11\mu m$ is $c \doteq 0.31$. The conditions under which the approximation (2) is valid and the derivation of the relation (1) have been discussed elsewhere.[1]

In this report the validity of relation (1) is verified by calculating the volume extinction coefficient σ_e and the liquid water content W for 341 different fog droplet size distributions[2-7] measured under various meteorological situations.

---

[1]P. Chýlek, 1978, "Extinction and Liquid Water Content of Fogs," J Atmos Sci, 35:296-300

[2]J. A. Garland, 1971, "Some Fog Droplet Size Distributions Obtained by an Impaction Method," Quart J Roy Meteorol Soc, 97:483-494

[3]M. Kumai, 1973, "Arctic Fog Droplet Size Distribution and Its Effect on Light Attenuation," J Atmos Sci, 30:635-643

[4]J. A. Garland et al., 1973, "A Study of the Contribution of Pollution to Visibility in a Radiation Fog," Atmos Environ, 7:1079-1092

[5]B. A. Kunkel, 1971, "Fog Drop-Size Distributions Measured with a Laser Hologram Camera," J Appl Meteorol, 10:482-486

[6]W. T. Roach et al., 1976, "The Physics of Radiation Fog: I-a Field Study," Q J Roy Meteorol Soc, 102:313-333

[7]R. G. Pinnick et al., 1978, "Vertical Structure in Atmospheric Fog and Haze and Its Effect on IR and Visible Extinction," J Atmos Sci, 35:2020-2032

Further, a linear relationship, similar to (1), is shown to exist between the infrared absorption coefficient in the spectral regime λ = 3.5 to 5.3μm, λ = 8 to 10μm, and the liquid water content of fogs. Thus for example, the absorption coefficient of fogs at λ = 3.8μm is uniquely related to their extinction and absorption at λ = 10μm.

SELECTED FOG SIZE DISTRIBUTIONS

Relatively few reliable measurements of fog droplet size distributions have been made, particularly for which numerical data is available. The fog measurements used here were judged to be reliable and were chosen to represent a wide range of fog conditions ranging from maritime and continental advection fogs[3,5,2] to inland radiation fogs.[2,4,6,7] The early work on evolving fogs near the Atlantic Ocean in France and stable inland fog and haze near Paris by Arnulf et al.[8] was not used because it was not possible to obtain true droplet distributions from their figures. Arnulf et al. captured droplets onto spider threads (for which the capture coefficient depends on droplet size) but give only the uncorrected droplet distribution data. Results of the pioneering work of May,[9] using a specially designed two-stage impactor, were not used since

---

[3]M. Kumai, 1973, "Arctic Fog Droplet Size Distribution and Its Effect on Light Attenuation," J Atmos Sci, 30:635-643

[5]B. A. Kunkel, 1971, "Fog Drop-Size Distributions Measured with a Laser Hologram Camera," J Appl Meteorol, 10:482-486

[2]J. A. Garland, 1971, "Some Fog Droplet Size Distributions Obtained by an Impaction Method," Q J Roy Meteorol Soc, 97:483-494

[4]J. A. Garland et al., 1973, "A Study of the Contribution of Pollution to Visibility in a Radiation Fog," Atmos Environ, 7:1079-1092

[6]W. T. Roach et al., 1976, "The Physics of Radiation Fog: I-a Field Study," Q J Roy Meteorol Soc, 102:313-333

[7]R. G. Pinnick et al., 1978, "Vertical Structure in Atmospheric Fog and Haze and Its Effect on IR and Visible Extinction," J Atmos Sci, 35:2020-2032

[8]A. Arnulf et al., 1957, "Transmission by Haze and Fog in the Spectral Region 0.35 to 10 Microns," J Opt Soc Am, 47:491-498

[9]K. R. May, 1961, "Fog Droplet Sampling Using a Modified Impactor Technique," Q J Roy Meteorol Soc, 87:535-548

the numerical data are no longer available.* Measurements of valley fog drop sizes obtained by exposing gelatin-coated slides to a stream of foggy air by Pilié et al.[10] were deemed not credible since the distributions were normalized to simultaneous measurements of extinction coefficient derived by a transmissometer. Fog drop measurements made with a light-scattering counter by Eldridge[11] were not utilized since errors in his measurements are suspected because of nonisokinetic sampling. The inlet of his counter was only 1 cm in diameter and became wet during the sampling process. In addition, some unexplained differences were caused by a dilution apparatus Eldridge used for high droplet concentration conditions.

Three different sampling techniques were employed to obtain the fog size distributions utilized in this study: impaction, holographic, and light scattering.

Garland,[2] Garland et al.,[4] and Roach et al.[6] used a modified two-stage Casella impactor designed by May[9] mounted horizontally in a wind tunnel to provide isokinetic sampling. Corrections to the collection efficiency based on the penetration curves of the impactor[12] were applied to the raw data. The size range of sensitivity of this device is 0.3 to 72μm radius.

---

*K. R. May, private communication, 1978

[10]R. J. Pilié, 1975, "The Life Cycle of Valley Fog. Part II: Fog Microphysics," J Appl Meteorol, 14:364-374

[11]R. G. Eldridge, 1961, "A Few Fog Drop-Size Distributions," J Appl Meteorol, 18:671-676

[2]J. A. Garland, 1971, "Some Fog Droplet Size Distributions Obtained by an Impaction Method," Q J Roy Meteorol Soc, 97:483-494

[4]J. A. Garland et al., 1973, "A Study of the Contribution of Pollution to Visibility in a Radiation Fog," Atmos Environ, 7:1079-1092

[6]W. T. Roach et al., 1976, "The Physics of Radiation Fog: I-a Field Study, Q J Roy Meteorol Soc, 102:313-333

[9]K. R. May, 1961, "Fog Droplet Sampling Using a Modified Impactor Technique," Q J Roy Meteorol Soc, 87:535-548

[12]K. R. May, 1945, "The Cascade Impactor: An Instrument for Sampling Aerosols," J Sci Instr, 22:187-195

Kumai[3] also used a two-stage impactor to measure advection fog droplets formed over the Arctic Ocean at Point Barrow, Alaska, together with a gelatin-coated glass slide collection plate whose collection efficiency was calculable as a function of wind velocity. Also, imprint-droplet correction factors were applied to obtain true sizes. The combined methods yielded drop size concentration from 2.2 to 64μm radius.

In general, the primary deficiency of the impaction technique, besides requiring laborious data reduction, is the uncertainty in number concentration determination for near-micrometer and submicrometer size droplets. In addition, the size limit of detectability is about 0.3μm radius using conventional microscopy techniques.

Kunkel[5] used a laser hologram technique to measure droplets in advection fog propagating inland during nighttime at Otis Air Force Base, MA. The hologram camera was capable of sampling volumes of 4.5 cm^3 at a rate of five samples per minute, in a near-isokinetic fashion, and with minimal disturbance to the droplets. Droplets with radii of 2 to 40μm were detected. Because of the small number of droplets (normally < 50) in the distributions reported by Kunkel, all 17 of the reported droplet distributions were averaged together, which in any case represent only a 3-minute interval, to obtain a single distribution.

Finally, the radiation fog and haze measurements made by Pinnick et al.[7] during wintertime in West Germany with a commercially available light-scattering counter (the "Knollenberg" Classical Scattering Aerosol Spectrometer manufactured by Particle Measurement Systems, Boulder, CO) were used. This device works on the principle that as aerosol flows through an illuminated volume, light scattered by single droplets into a particular solid angle is measured and used to determine particle size by pulse height analyzing response pulses. Determination of droplet size from the response is indirect because of the dependence of the response on factors other than droplet size, namely, droplet refractive index and the lens geometry of the optical system. Particular attention

---

[3]M. Kumai, 1973, "Arctic Fog Droplet Size Distribution and Its Effect on Light Attenuation," J Atmos Sci, 30:635-643

[5]B. A. Kunkel, 1971, "Fog Drop-Size Distributions Measured with a Laser Hologram Camera," J Appl Meteorol, 10:482-486

[7]R. G. Pinnick et al., 1978, "Vertical Structure in Atmospheric Fog and Haze and Its Effect on IR and Visible Extinction," J Atmos Sci, 35:2020-2032

was given to the calibration of this instrument using monodisperse particles of different sizes and refractive indexes. The manufacturer's advertised calibration was not used. Rather, droplet size distributions were determined by redefining the size pulse height channels as described in detail by Pinnick et al.[7] This counter is sensitive to water droplets with radii of 0.23 to 16μm.

Altogether, 341 different size distributions were used to check the validity of equation (1) in the atmospheric window around λ = 11μm; 25 fog distributions were taken from Garland[2] and Roach et al.,[6] 6 from Garland et al.,[4] 20 from Kumai,[3] 1 from Kunkel,[5] and 289 fog and haze distributions from Pinnick et al.[7]

NUMERICAL RESULTS FOR FOG EXTINCTION

A Mie scattering program and index of refraction of water as given by Hale and Querry[13] were used to calculate the volume extinction coefficient

$$\sigma_e(\lambda) = \pi \int r^2 \quad Q_e \ (\lambda, r) \quad n(r)dr \qquad (3)$$

---

[7]R. G. Pinnick et al., 1978, "Vertical Structure in Atmospheric Fog and Haze and Its Effect on IR and Visible Extinction," J Atmos Sci, 35:2020-2032

[2]J. A. Garland, 1971, "Some Fog Droplet Size Distributions Obtained by an Impaction Method," Q J Roy Meteorol Soc, 97:483-494

[6]W. T. Roach et al., 1976, "The Physics of Radiation Fog: I-a Field Study," Q J Roy Meteorol Soc, 102:313-333

[4]J. A. Garland et al., 1973, "A Study of the Contribution of Pollution to Visibility in a Radiation Fog," Atmos Environ, 7:1079-1092

[3]M. Kumai, 1973, "Arctic Fog Droplet Size Distribution and Its Effect on Light Attenuation," J Atmos Sci, 30:635-643

[5]B. A. Kunkel, 1971, "Fog Drop-Size Distributions Measured with a Laser Hologram Camera," J Appl Meteorol, 10:482-486

[13]G. M. Hale and M. R. Querry, 1973, "Optical Constants of Water in the 200 nm to 20μm Wavelength Region," Appl Opt, 12:555-563

and the liquid water content

$$W = \frac{4}{3}\pi\rho \int r^3\, n(r)dr \qquad (4)$$

for the previously mentioned 341 fog and haze size distributions n(r) at several different wavelengths λ. The numerical integrations were performed only over the range of particle radii measured for each size distribution, under the assumption that the differential size distribution n(r) is constant within each measured particle size channel. In other words, the measured distributions were not extended to larger or smaller particle sizes and were not smoothed. The results at λ = 0.55μm, 1.2μm, 4μm, and 11μm, together with the $Q_e = cx$ approximation [equation (1)], are shown in figure 1. Additional results at other infrared wavelengths are shown in the appendix, figures A-1 through A-4. The Kumai[3] or Kunkel[5] results at λ = 0.55μm and 1.2μm have not been included since the contribution of particles with r ≲ 2μm (which neither Kumai nor Kunkel measured) to extinction at these wavelengths is suspected as being excessive.

At λ = 11μm the $Q_e = cx$ approximation is a good approximation for all size distributions except those with a large number of droplets with radii r > 14μm.[1] Some fog size distributions used in our calculations contained droplets with r > 14μm; however, their contribution generally did not dominate either the extinction σ_e or the liquid water content W. Consequently, the linear relationship (1) between the volume extinction coefficient σ_e and the liquid water content W is expected to be reasonably well satisfied at λ = 11μm. Results of numerical calculations confirming the validity of equation (1) at λ = 11μm are shown in figure 1d.

---

[3]M. Kumai, 1973, "Arctic Fog Droplet Size Distribution and Its Effect on Light Attenuation," J Atmos Sci, 30:635-643

[5]B. A. Kunkel, 1971, "Fog Drop-Size Distributions Measured with a Laser Hologram Camera," J Appl Meteorol, 10:482-486

[1]P. Chýlek, 1978, "Extinction and Liquid Water Content of Fogs," J Atmos Sci, 35:296-300

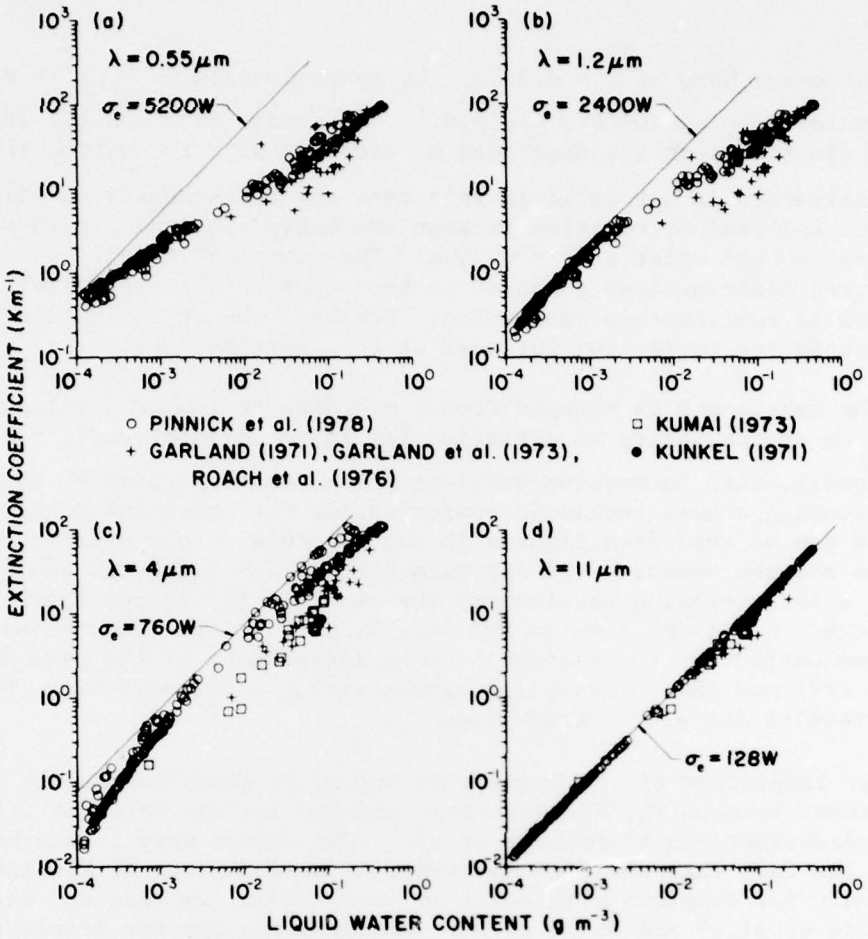

Figure 1. Variation of extinction coefficient with liquid water content in atmospheric fog and haze for 341 size distribution measurements made at different geographic locales and under a variety of meteorological conditions. In the infrared spectral region around λ = 11μm (d), there exists a linear size distribution independent relation between the volume extinction coefficient σ_e and the liquid water content W of the form of eq. (1). Consequently, the results of all measurements are close to a straight line. The predicted relation between extinction σ_e and liquid water content W according to eq. (1) is shown by the straight line, where σ_e is in km^{-1} and W is in g m^{-3}. On the other hand at λ = 0.55μm (a), the Q_e = cx approximation is not satisfied and no unambiguous relation between the extinction and liquid water content exists. The large spread of the points in the graph shows that the extinction coefficient is a function of the size distribution as well as of the liquid water content. As the wavelength is increased to λ = 1.2μm (b) and λ = 4μm (c), the Q_e = cx approximation is satisfied for larger droplets and the relation (1) shown by the straight lines is becoming a more realistic approximation for hazes and fogs.

On the other hand at $\lambda = 0.55\mu m$, the approximation $Q_e = cx$ is valid only for water droplets with $r \leq 0.5\mu m$.[1] Since most haze and all fog droplet size distributions are dominated by droplets with $r > 0.5\mu m$, the $Q_e = cx$ approximation is not valid in this case and consequently no size distribution independent relation between the extinction and liquid water content should exist at $\lambda = 0.55\mu m$. The numerical results based on the measured distributions compared to the equation (1) approximation in figure 1a confirm this conclusion. Further, the approximation grossly overestimates extinction for most of the distributions.

As the wavelength is changed from $\lambda = 0.55\mu m$ to longer wavelengths, the $Q_e = cx$ approximation is satisfied for larger droplet radii r. Consequently, with increasing wavelength the relation given by equation (1) is becoming a more realistic approximation for hazes and fogs. This trend can be seen from figures 1b and 1c, showing the numerical calculations and the equation (1) approximation at $\lambda = 1.2\mu m$ and $4\mu m$. Note that with increasing wavelengths the relation (1) better approximates the exact numerical results and finally at $\lambda = 11\mu m$ (figure 1d) the volume extinction coefficient becomes independent of the size distribution n(r) and the relation (1) agrees within a factor 2 with the numerical results for all distributions.

Closer inspection of the results in figure 1d shows noticeably better agreement between the Mie numerical results and the relation (1) for the size distributions of Pinnick et al.[7] The reason very likely has to do with the fact that the size distribution measurements of Pinnick et al. are only for droplets with radii up to $r = 16\mu m$, whereas the Garland,[2] Garland et al.,[4] and Roach et al.[6] measurements are for droplets with radii

---

[1]P. Chýlek, 1978, "Extinction and Liquid Water Content of Fogs," J Atmos Sci, 35:296-300

[7]R. G. Pinnick et al., 1978, "Vertical Structure in Atmospheric Fog and Haze and Its Effect on IR and Visible Extinction," J Atmos Sci, 35:2020-2032

[2]J. A. Garland, 1971, "Some Fog Droplet Size Distributions Obtained by an Impaction Method," Q J Roy Meteorol Soc, 97:483-494

[4]J. A. Garland et al., 1973, "A Study of the Contribution of Pollution to Visibility in a Radiation Fog," Atmos Environ, 7:1079-1092

[6]W. T. Roach et al., 1976, "The Physics of Radiation Fog: I-a Field Study," Q J Roy Meteorol Soc, 102:313-333

up to r = 72μm; the Kumai[3] measurements are for droplets with radii up to r = 64μm, and the Kunkel[5] measurement is for droplets with radii up to r = 40μm. Since the maximum radius condition for the Q_e = cx approximation leading to relation (1) is for r_m = 14μm at λ = 11μm, none of the Pinnick et al. distributions can strongly violate this condition as no particles with r > 16μm were measured. Thus, the better agreement of the numerical results for the Pinnick et al. distributions with the relation (1) at λ = 11μm (and also at λ = 4μm [figure 1c]) may be partly a consequence of their inability to measure droplets with r > 16μm.

Another qualification concerning the results in figure 1 bears on the assumption that all fog and haze particles consist of homogeneous water droplets and have complex refractive indexes of water. Haze particles in particular may contain a significant volume fraction of contaminants such as sea salt or ammonium sulfate. The crucial question here is to what degree the particle refractive index is affected by such contaminants. The formation of fog is known to require atmospheric relative humidity (RH) to be near 100 percent. For the haze data appearing in figure 1, the relative humidity was close to 100 percent.[7] Hänel[14] and Hänel and Bullrich[15] have studied the effect of RH variations on mean complex refractive indexes of maritime and urban aerosols. Hänel[14] found that for RH $\geq$ 95 percent the real and imaginary parts of the complex refractive index n_{re} and n_{im} at λ = 0.55μm have values $1.33 \leq n_{re} \leq 1.36$ and $0 \leq n_{im} \leq 0.006$. Examination of Mie efficiency factors Q_e (m, x) for refractive indexes in this range shows the assumption that m = 1.33-0i in Mie calculations of extinction according to equation (3) and the Q_e = cx approximation (1) is a good one. At wavelengths longer than λ = 0.55μm, Hänel and Bullrich's formulae show

---

[3]M. Kumai, 1973, "Arctic Fog Droplet Size Distribution and Its Effect on Light Attenuation," J Atmos Sci, 30:635-643

[5]B. A. Kunkel, 1971, "Fog Drop-Size Distributions Measured with a Laser Hologram Camera," J Appl Meteorol, 10:482-486

[7]R. G. Pinnick et al., 1978, "Vertical Structure in Atmospheric Fog and Haze and Its Effect on IR and Visible Extinction," J Atmos Sci, 35:2020-2032

[14]C. Hänel, 1976, "The Properties of Atmospheric Aerosol Particles as Functions of Relative Humidity at Thermodynamic Equilibrium with the Surrounding Moist Air," Adv in Geophys, 19:73-188

[15]G. Hänel and K. Bullrich, 1978, "Physico - Chemical Property Models of Tropospheric Aerosol Particles," Beitr Phys Atmos 51:129-138

that, providing RH values are higher than 95 percent, both maritime and urban aerosol mean refractive indexes are again not markedly different from those of water. For example at λ = 11μm, from Hanel and Bullrich's formulae the real and imaginary parts of the complex index are predicted to be $1.153 \leq n_{re} \leq 1.207$ and $0.0968 \leq n_{im} \leq 0.109$, compared to $m = 1.153 - 0.0968i$ for pure water. The effect of these refractive index variations in Mie calculations of extinction coefficient according to equations (3) and (1) are estimated to be not more than 10 percent. For fog, an additional argument can be made to support the assumption that the particle refractive indexes can be approximated by those of pure water. The argument is that the liquid mass content of fogs is on the order of 0.005 g m^{-3} or greater, and thus the volume fraction of any contaminant in fog droplets must necessarily be small so that the refractive indexes must be close to those of water.

Because of the Army's interest in relating infrared properties of fogs to atmospheric visibility (or visible extinction), the extinction versus liquid water content data have been plotted in the form of extinction at various infrared wavelengths λ versus extinction at λ = 0.55μm. These numerical results, together with empirical power-law expressions fitted to the numerical results, are shown in figures A-5 through A-11. The empirical expressions are of the form

$$\sigma_e(\lambda) = a[\sigma_e(\lambda = 0.55\mu m)]^b$$

where the parameters a and b are constants depending only on the particular infrared wavelength λ. The empirical power-law expressions are of only marginal value, as in general there is no unique relation between extinction in the infrared and extinction at λ = 0.55μm.

To examine more closely the fog results in figure 1 in terms of fog type, attention has been restricted to data of Garland,[2] Garland et al.,[4]

---

[2]J. A. Garland, 1971, "Some Fog Droplet Size Distributions Obtained by an Impaction Method," Q J Roy Meteorol Soc, 97:483-494

[4]J. A. Garland et al., 1973, "A Study of the Contribution of Pollution to Visibility in a Radiation Fog," Atmos Environ, 7:1079-1092

and Roach et al.[6] The reasons are twofold: first, these measurements were made during fogs occurring under distinctly different meteorological conditions. Altogether, 37 different fogs were measured during a 5-year period under the gamut of meteorological conditions found in England. Secondly, measurements were made for a sufficiently broad range of particle sizes ($0.3\mu m < r < 72\mu m$) that errors in extinction and liquid water content due to the presence of larger and smaller droplets are estimated to be small. Of the 37 measured distributions, 3 were not used because the raw data were not available, 3 because ice crystals were present in the samples, and 5 because fog type was not specified.

The Garland and Roach et al. fog data, which already appear in figure 1, have been divided into two classes: radiation fog and advection fog. Garland has cautioned* that although the radiation fogs clearly formed in situ by radiation cooling, some fogs classified as advection type may have been mature radiation fogs transported by the wind from a distant area of formation. In any case, the data are replotted according to this classification in figure 2 ($\lambda = 0.55\mu m$) and figure 3 ($\lambda = 11\mu m$). At $\lambda = 0.55\mu m$, it is evident that radiation fogs are generally more effective scatterers, and hence more effective in reducing visibility, than advection fogs with the same liquid water content. To show the reason for this result, the differential extinction coefficients of a radiation fog (figure 2, solid circle) and an advection fog (figure 2, solid square) measurement with about the same liquid water content have been plotted versus particle radius (figure 4). Because the plots are made on a linear-linear scale, the areas under the curves are a measure of the corresponding extinction coefficients. Thus the radiation fog extinction coefficient ($35\ km^{-1}$) is more than twice the advection fog extinction coefficient ($15.8\ km^{-1}$). For the radiation fog, small droplets, let us say with $r \leq 3\mu m$, are very numerous and contribute 60 percent of the extinction without making a significant contribution to liquid water content. On the other hand for the advection fog, a broader size distribution is found and these smaller particles contribute only 6 percent of the extinction at $\lambda = 0.55\mu m$. Both the radiation and the advection fog size distributions strongly violate the maximum radius condition allowed in the $Q_e = cx$ approximation ($r_m = 0.5\mu m$ at $\lambda = 0.55\mu m$), so there is no reason to expect a unique relation between extinction at $\lambda = 0.55\mu m$ and liquid water content.

---

[6]W. T. Roach et al., 1976, "The Physics of Radiation Fog: I-a Field Study," Q J Roy Meteorol Soc, 102:313-333

*J. A. Garland, private communication, 1978

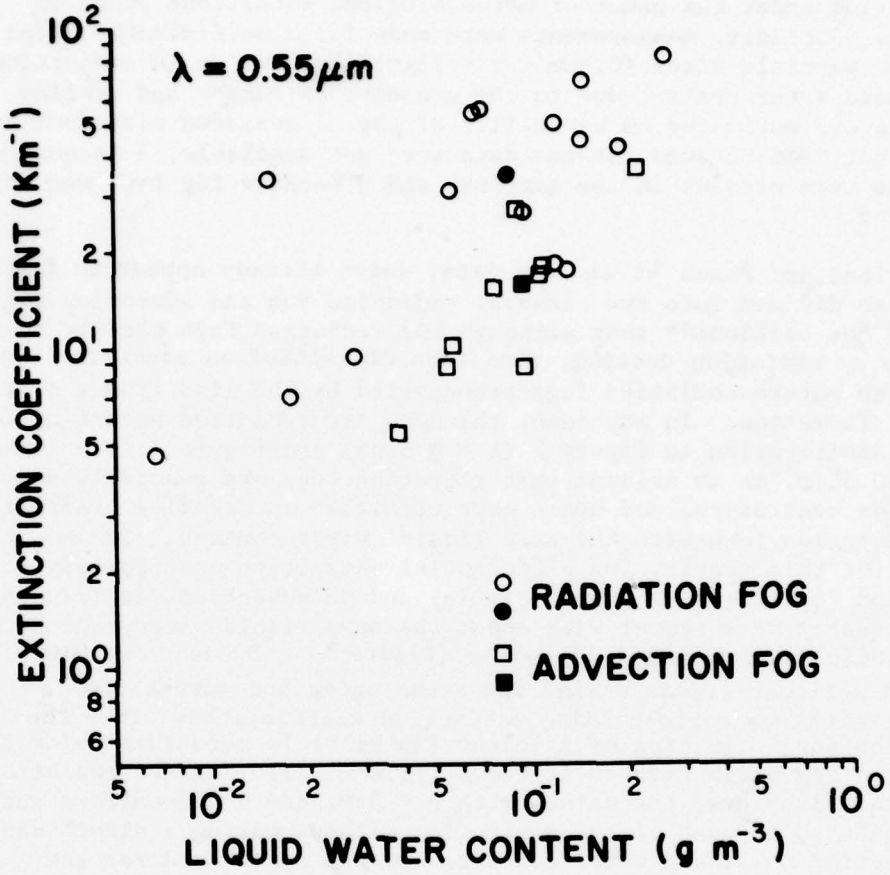

Figure 2. Same as fig. 1a except only the fog data of Garland, Garland et al., and Roach et al. are shown. The extinction and liquid water contents calculated from the 26 measured size distributions are divided according to radiation (circles) or advection (squares) fog. The figure shows that radiation fogs are generally more effective scatterers than advection fogs with the same liquid water content because they contain more droplets in the Mie resonance region that contribute a significant part of the extinction but contribute only a marginal amount to the liquid water content.

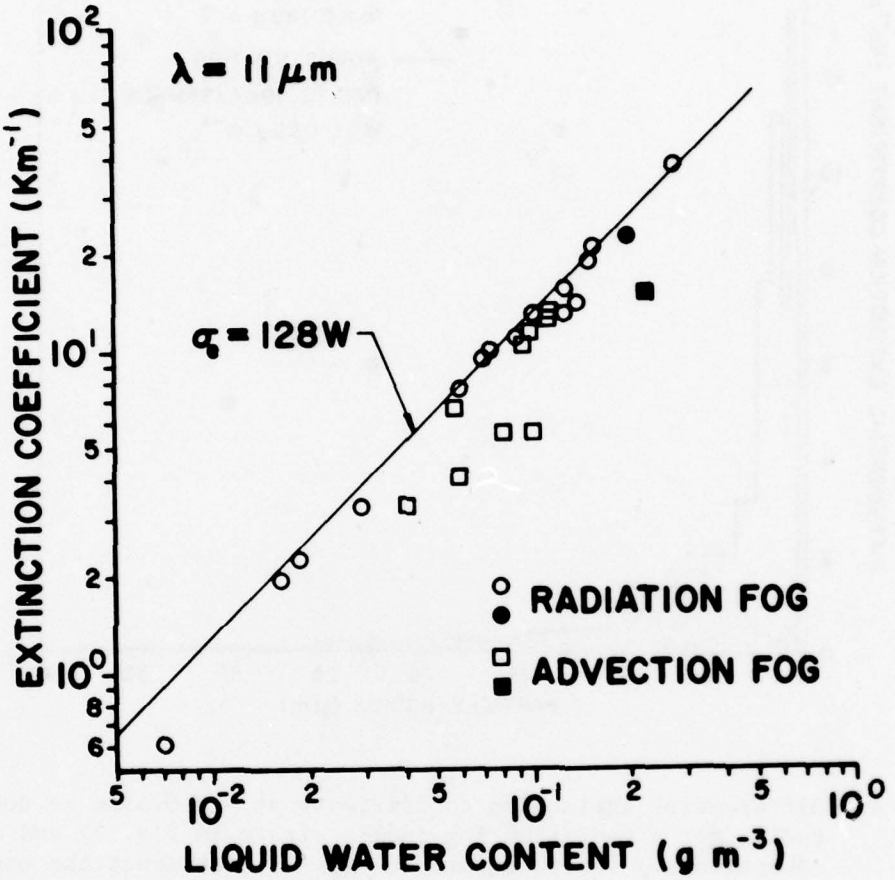

Figure 3. Same as fig. 2 except for λ = 11μm. The predicted relation between extinction and liquid water content given by eq. (1) is shown by the straight line. Because the $Q_e = cx$ approximation is generally better satisfied for radiation fogs, those points fall closer to the straight line prediction.

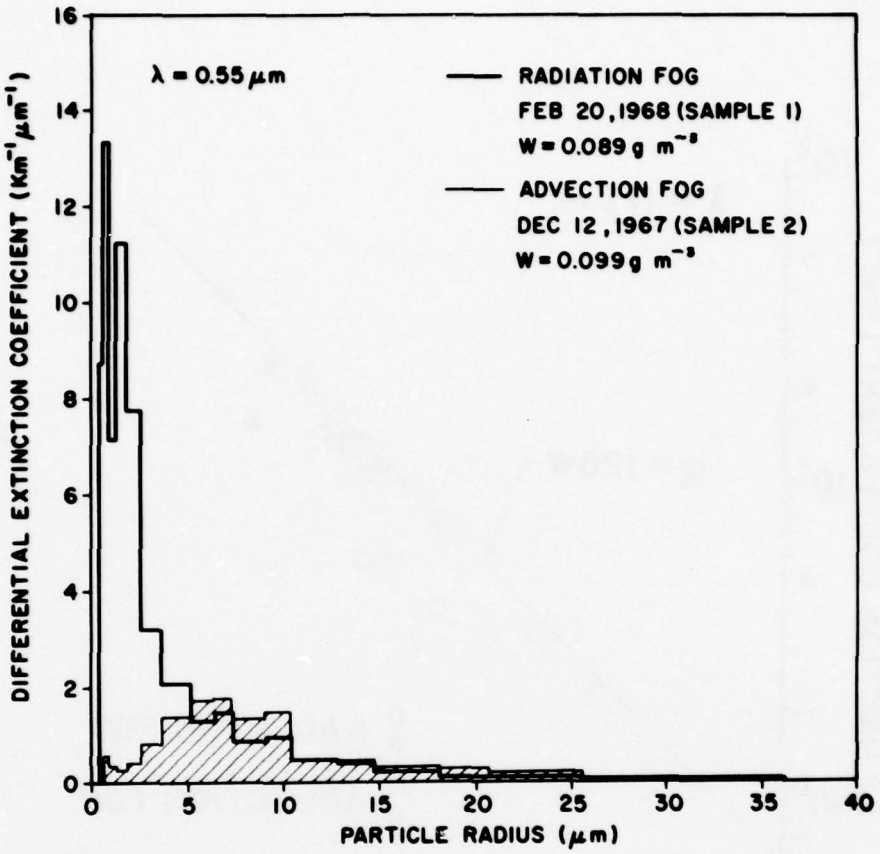

Figure 4. Differential extinction coefficients at λ = 0.55μm vs droplet radius for a radiation fog (solid circle in fig. 2) and an advection fog (solid square in fig. 2) with about the same liquid water content. The areas under the curves are a measure of the total extinction coefficients (35 km^{-1} for the radiation fog vs 15.8 km^{-1} for the advection fog). For the radiation fog, 60% of the extinction is contributed by droplets having $r \leq 3\mu m$, compared to only 6% for the advection fog.

At λ = 11μm (figure 3), although the Q_e = cx approximation is within a factor of about 2 for both radiation and advection fog results, the approximation is generally in better agreement with the radiation fog results. The explanation is that the Q_e = cx approximation is only strictly valid providing fog droplets have $r \lesssim 14\mu m$,[1] and radiation fogs better satisfy this condition than do advection fogs. The degree to which this maximum radius condition is violated can be determined for two fog examples from figure 5. The figure shows the differential extinction coefficient at λ = 11μm for a radiation fog (figure 3 solid circle) and an advection fog (figure 3 solid square) again having about the same liquid water content. For the radiation fog, 69 percent of the extinction arises from droplets with radii less than the maximum value r_m = 14μm, while for the advection fog this value drops to 33 percent.

A survey of all the differential extinction coefficient versus particle radius graphs similar to those shown in figure 5 for the radiation fogs of Garland[2], Garland et al.,[4] and Roach et al.[6] in figure 3 shows that in all cases extinction at λ = 11μm is dominated by droplets with $r \leq 14\mu m$. On the other hand, a survey of the differential extinction coefficient graphs for the advection fogs presented in figure 3, and also the advection fogs of Kumai,[3] shows that for about half of the distributions, extinction at λ = 11μm is dominated by droplets with $r > 14\mu m$. Since the extinction efficiency factor for these larger particles is overestimated by the Q_e = cx approximation (see figure 3 of ref 1), the numerical calculation of the extinction for these advection fogs falls below the equation (1) prediction in figure 3. For the remaining half of the advection fogs, droplets with $r \leq 14\mu m$ dominate extinction and the points fall within 20 percent of the equation (1) prediction. Thus,

---

[1]P. Chýlek, 1978, "Extinction and Liquid Water Content of Fogs," J Atmos Sci, 35:296-300

[2]J. A. Garland, 1971, "Some Fog Droplet Size Distributions Obtained by an Impaction Method," Q J Roy Meteorol Soc, 97:483-494

[4]J. A. Garland et al., 1973, "A Study of the Contribution of Pollution to Visibility in a Radiation Fog," Atmos Environ, 7:1079-1092

[6]W. T. Roach et al., 1976, "The Physics of Radiation Fog: I-a Field Study," Q J Roy Meteorol Soc, 102:313-333

[3]M. Kumai, 1973, "Arctic Fog Droplet Size Distribution and Its Effect on Light Attenuation," J Atmos Sci, 30:635-643

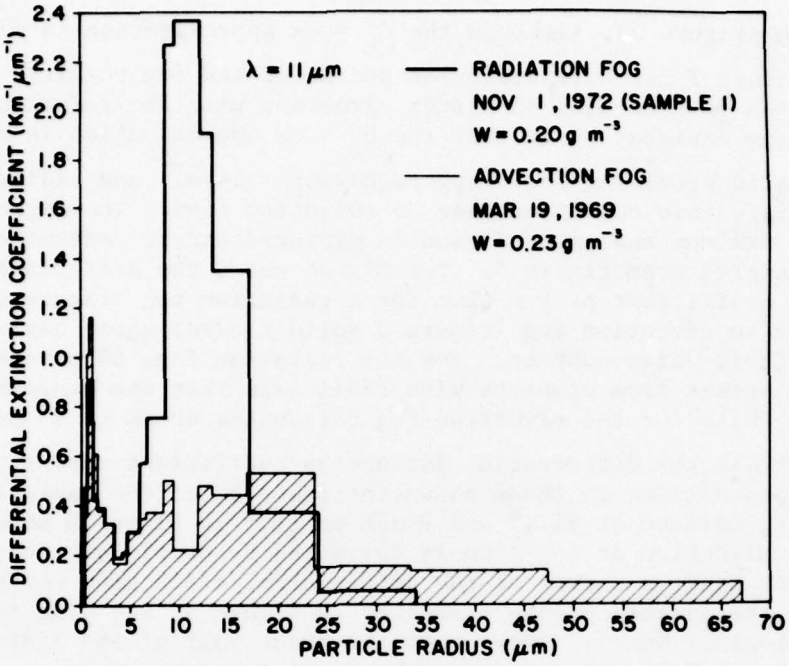

Figure 5. Differential extinction coefficients at λ = 11μm vs droplet radius for a radiation fog (solid circle in fig. 3) and an advection fog (solid square in fig. 3) with about the same liquid water content. The total extinction for the radiation fog is 22.6 km^{-1} compared to 15.0 km^{-1} for the advection fog. The fraction of extinction contributed by droplets with $r \leq$ 14μm (the maximum value allowed in the $Q_e = cx$ approximation) is 69% for the radiation fog, decreasing to 33% for the advection fog. Thus the prediction between extinction (at λ = 11μm) and liquid water content (given by eq. (1) and shown in fig. 3) is a better approximation for radiation fogs than for advection fogs.

while droplets with $r \leq 14\mu m$ dominate extinction at $\lambda = 11\mu m$ for radiation fog, this is not always the case for advection fog, where the presence of larger droplets partially destroys the size distribution independent linear relation (1).

To show the transition of the extinction versus liquid water content results for wavelengths between $\lambda = 0.55\mu m$ and $\lambda = 11\mu m$, included in the appendix (figures A-12 through A-17) are numerical calculations of extinction versus liquid water content for the fog distributions of Garland,[2] Garland et al.,[4] and Roach et al.[6] for $\lambda = 1.2\mu m$, $3\mu m$, $4\mu m$, $5\mu m$, $8\mu m$, and $10\mu m$. Again, because of the Army's interest in relating visibility to infrared extinction in fogs, these Garland and Roach results are replotted in the form of extinction coefficient at various infrared wavelengths versus extinction at $\lambda = 0.55\mu m$ (appendix, figures A-18 through A-24). The results are divided according to fog type (radiation and advection) in each figure. In addition to the Mie-calculated numerical results, empirical power-law relationships are shown that relate extinction at a particular infrared wavelength to extinction at $\lambda = 0.55\mu m$. These power-law relationships, which appear as straight lines in figures A-18 through A-24, represent a least square fit to the numerical results for radiation fogs and for the advection fogs. Because of the relatively large spread in the numerical result data points, the empirical relations derived from these data points are rather precarious, and should therefore be used only as a rough indication of the wavelength variation of extinction coefficient in radiation and advection fogs. These figures show that extinction in advection fogs tends to be more neutral (wavelength independent) than in radiation fogs (completely neutral extinction would correspond to a 45-degree line in figures A-18 through A-24). Such a result is expected because advection fogs generally have a broader distribution of droplet sizes than do radiation fogs.

$Q_a = c'x$ APPROXIMATION FOR ABSORPTION

Realizing that the $Q_e = cx$ approximation works reasonably well for fog at $\lambda \cong 11\mu m$, and for haze at shorter wavelengths, an investigation was made to

---

[2]J. A. Garland, 1971, "Some Fog Droplet Size Distributions Obtained by an Impaction Method," Q J Roy Meteorol Soc, 97:483-494

[4]J. A. Garland et al., 1973, "A Study of the Contribution of Pollution to Visibility in a Radiation Fog," Atmos Environ, 7:1079-1092

[6]W. T. Roach et al., 1976, "The Physics of Radiation Fog: I-a Field Study," Q J Roy Meteorol Soc, 102:313-333

see if a similar approximation for fog droplet absorption might hold in the λ = 3 to 5μm and λ = 8 to 12μm atmospheric window spectral regions.

The absorption coefficient σ_a for a polydispersion of droplets described by the size distribution n(r) is given by

$$\sigma_a = \int \pi r^2 Q_a(m,x)\ n(r)\ dr \qquad (5)$$

where Q_a (m,x) is the Mie efficiency factor for absorption for a water droplet with refractive index m (λ) and size parameter $x = 2\pi r/\lambda$. Plots of the efficiency factor for absorption Q_a vs x for λ = 3.8 and 9.5μm are shown in figures 6 and 7. As Chýlek[1] found for extinction, the efficiency factor for absorption Q_a can be well approximated by $Q_a\ (x,\lambda) \doteq c'(\lambda)x$, providing $x \leq x_m$.

Using this linear approximation for Q_a in equation (5) gives

$$\sigma_a = \frac{3\pi c'}{2\lambda} \int \frac{4\pi r^3}{3}\ n(r)dr. \qquad (6)$$

Thus, explicit dependence on the size distribution disappears and leads to the absorption coefficient being linearly related to liquid water content W according to

$$\sigma_a = \frac{3\pi c'}{2\lambda\rho} W. \qquad (7)$$

As in the case of extinction, the restriction that $x \leq x_m$ need not be strictly satisfied, but water droplets with radii greater than the value $r_m = \frac{\lambda x_m}{2\pi}$ must not contribute excessively to either absorption or liquid water content. Numerical values of the maximum radii r_m at various

---

[1]P. Chýlek, 1978, "Extinction and Liquid Water Content of Fogs," J Atmos Sci, 35:296-300

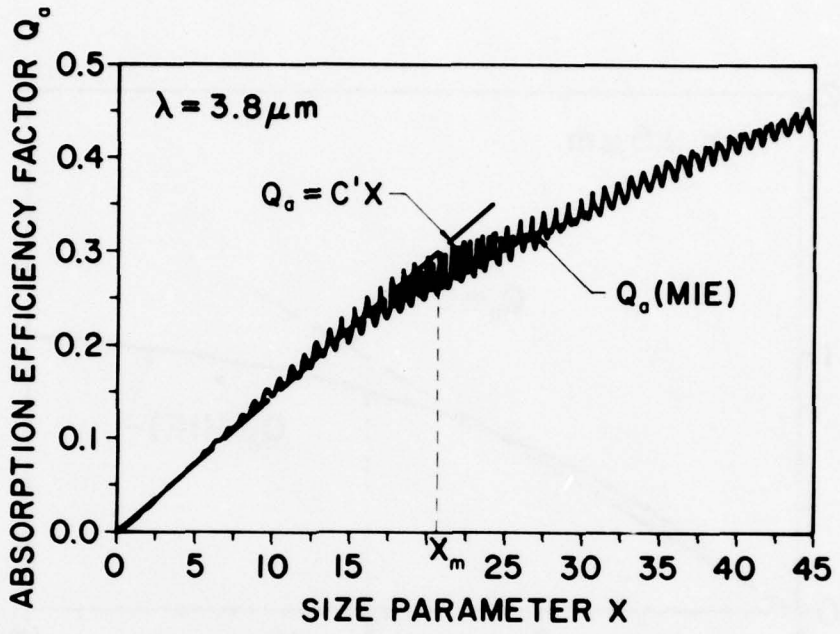

Figure 6. The efficiency factor for absorption Q_a for water versus droplet size parameter x at a wavelength λ = 3.8μm (index of refraction m = 1.364 - 0.0034i). The efficiency factor can be approximated by a straight line $Q_a = c'x$ providing $x \leq x_m$. The approximation overestimates the exact value of Q_a for some size parameters, but underestimates it for others. These two errors tend to cancel, leading to the absorption coefficient being linearly related to liquid water content according to eq. (7).

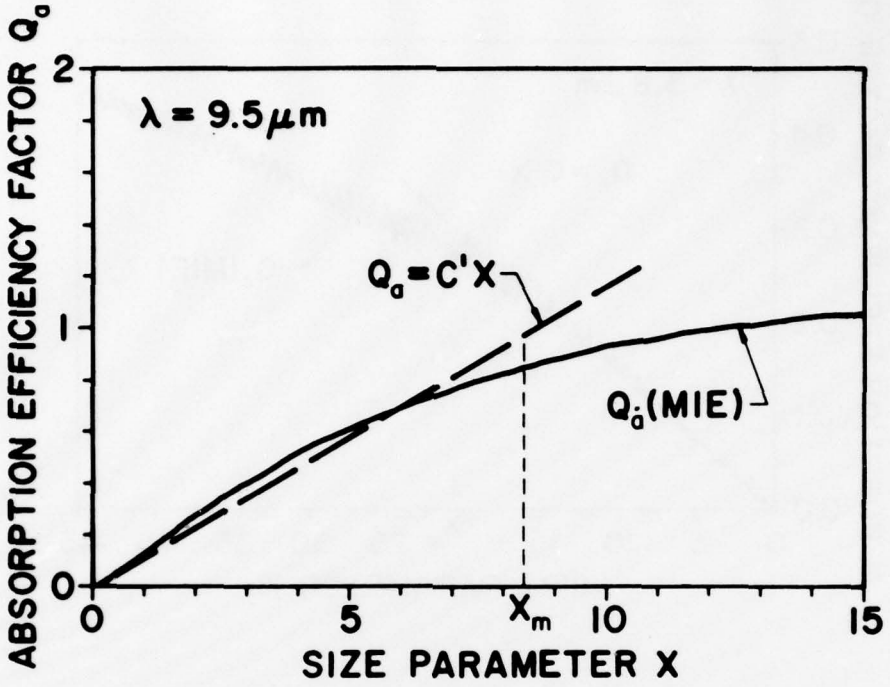

Figure 7. Same as fig. 6 except for λ = 9.5μm (index of refraction of water m = 1.243 - 0.0443i). The efficiency factor for absorption can again be approximated by a straight line Q_a = c'x providing $x \leq x_m$.

wavelengths λ, as well as the slope c' of a straight line approximating Q_a for $x \leq x_m$, are given in table 1. Also given are values of the quantity $\frac{3\pi c'}{2\lambda\rho}$ which if multiplied by the liquid water content give the absorption coefficient. In order that these predicted relationships (and maximum radius conditions) between droplet absorption and liquid water content may be compared to the corresponding results for extinction, the values of x_m, r_m, etc., for the $Q_e = cx$ approximation[1] for extinction also appear in table 1. The values of x_m, r_m, and c for extinction are sometimes slightly different from those of Chýlek[1] since there is some leeway in the subjective procedure for approximating the efficiency factor $Q_e(x)$ by a linear function of size parameter x. The table shows that the limiting radius r_m depends strongly on wavelength and is in general markedly different for absorption and extinction at a particular wavelength. An exception is at $\lambda = 9.5\mu m$, where the limiting radii are $r_m = 13\mu m$ for absorption as compared to $r_m = 12.5\mu m$ for extinction. Thus for fog droplet distributions that have radii $r < 12.5\mu m$ (i.e., most radiation fogs) from table 1 a prediction can be made that absorption contributes 29 percent of the extinction at $\lambda = 9.5\mu m$, independent of the form of the droplet size distribution. However, there is obviously no unique relation between fog absorption and extinction for all wavelengths.

Since the $Q_e = cx$ approximation for extinction at $\lambda = 11\mu m$, which requires droplets have maximum radius $r_m = 14\mu m$, is adequate for atmospheric fog, the $Q_a = c'x$ approximation for absorption should be adequate for fog at selected wavelengths also having $r_m \approx 14\mu m$. Table 1 shows that wavelengths $\lambda = 3.8\mu m$, $4\mu m$, $5.3\mu m$, and $9.5\mu m$ either satisfy or nearly satisfy this criterion. Therefore, a linear relation might be expected between fog absorption and fog liquid water content according to equation (7), independent of the droplet size distribution, for these particular wavelengths.

---

[1]P. Chýlek, 1978, "Extinction and Liquid Water Content of Fogs," J Atmos Sci, 35:296-300

TABLE 1. PARAMETERS FOR THE LINEAR RELATION BETWEEN IR ABSORPTION, EXTINCTION, AND LIQUID WATER CONTENT OF FOGS

At a given wavelength λ the efficiency factor for absorption Q_a (and extinction Q_e) can be approximated by a straight line $Q_a = c'x$ ($Q_e = cx$) for size parameters $x \leq x_m$. The values of x_m and c' (and c) are determined from the efficiency curves (see for example figs. 6 and 7). If we know the maximum radius r_m of droplets in a given size distribution, from the table we can find the wavelength λ at which a linear relationship between absorption (or extinction) and liquid water content exists, and the appropriate value of the parameter c' (or c). The value of the quantity $\frac{3\pi c'}{2\lambda\rho}$ (or $\frac{3\pi c}{2\lambda\rho}$) multiplied by the liquid water content W gives the absorption coefficient σ_a (or extinction coefficient σ_e).

	ABSORPTION				EXTINCTION			
λ (μm)	x_m	$r_{m(\mu m)}$	c'	$\frac{3\pi c'}{2\lambda\rho}$ ($cm^2 g^{-1}$)	x_m	$r_{m(\mu m)}$	c	$\frac{3\pi c}{2\lambda\rho}$ ($cm^2 g^{-1}$)
3.0	2.3	1.1	0.58	9.1×10^3	3.2	1.5	0.85	13.3×10^3
3.5	14	8.0	0.037	0.50 "	5.9	3.3	0.72	9.6 "
3.8	21	13	0.015	0.18 "	6.5	4.0	0.66	8.2 "
4.0	22	14	0.018	0.22 "	6.7	4.3	0.64	7.6 "
4.5	14	10	0.047	0.49 "	7.0	5.0	0.59	6.1 "
5.0	14	11	0.044	0.41 "	7.2	5.8	0.56	5.3 "
5.3	16	14	0.035	0.31 "	7.5	6.3	0.56	5.0 "
8.0	7.6	9.7	0.10	0.61 "	7.3	9.3	0.51	3.0 "
8.5	8.2	11	0.11	0.60 "	7.9	10.7	0.45	2.5 "
9.0	8.0	12	0.11	0.57 "	8.0	11.5	0.44	2.3 "
9.5	8.4	13	0.12	0.58 "	8.2	12.5	0.41	2.0 "
10.0	7.0	11	0.13	0.60 "	8.8	14	0.38	1.8 "
10.5	6.0	10	0.16	0.70 "	8.6	14	0.33	1.5 "
11.0	4.1	7.2	0.21	0.93 "	8.1	14	0.31	1.3 "
11.5	3.1	5.7	0.30	1.26 "	5.0	9.1	0.37	1.5 "
12.0	2.3	4.5	0.42	1.65 "	4.9	9.3	0.44	1.7 "
12.5	1.9	3.7	0.58	2.2 "	3.7	7.3	0.58	2.2 "

To check this contention, a Mie scattering program was used to calculate the volume absorption coefficient $\sigma_a(\lambda)$ according to equation (5) for the previously mentioned 341 fog and haze size distributions at several different wavelengths. As in the extinction calculations, particle refractive indexes of water have been assumed, and thus refractive index differences that might be caused by the presence of contaminants such as sea salt and ammonium sulfate have been neglected. The results at λ = 3.8 and 9.5μm plotted as a function of fog liquid water content together with the $Q_a = c'x$ approximation (7) are shown in figures 8 and 9. The figures show that although the numerical results are slightly better approximated at λ = 3.8μm as compared to λ = 9.5μm, at both wavelengths the linear relation (7) is within a factor 2.5 of the numerical results for all 341 fog and haze size distributions. Examination of results at numerous other infrared wavelengths (given in the appendix, figures A-25 through A-37) shows that even though the maximum radius condition is sometimes violated, for λ = 3.5 to 5.3μm, and 8 to 10μm all numerical results for the 341 fog distributions are within a factor 2.5 of the predictions between absorption and liquid water content given by relation (7) and listed in table 1, and in most cases the agreement is within a factor 2. However, at wavelengths λ = 10.5 to 12μm, the numerical results differ by as much as a factor 4 from the linear relation (7).

Previously Platt[16] found an approximate linear relation between the absorption coefficient σ_a at λ = 11μm and liquid water content W of nonprecipitating stratocumulus clouds. Platt performed Mie calculations on 25 measured cloud droplet distributions, plotted the values of σ_a at λ = 11μm versus W, did a least squares fit through the resulting data points, and obtained $\sigma_a = 76.5$ W, comparing modestly well with the equation (7) prediction from table 1 of $\sigma_a = 93$ W, where the absorption is in km^{-1} and the liquid water content in g m^{-3}. The reason for the over-prediction of the absorption is that a significant number of droplets in Platt's distributions have radii greater than 7.2μm, the maximum value allowable in the $Q_a = c'x$ approximation at λ = 11μm. Had Platt chosen a slightly shorter wavelength, say λ = 9.5μm, he would have found an even better correlation of absorption and liquid water content, as well as better agreement with our linear prediction (7), since the maximum radius restriction is more nearly satisfied for clouds at the shorter wavelength.

---

[16]C. M. R. Platt, 1976, "Infrared Absorption and Liquid Water Content in Stratocumulus Clouds," Q J Roy Meteorol Soc, 102:553-561

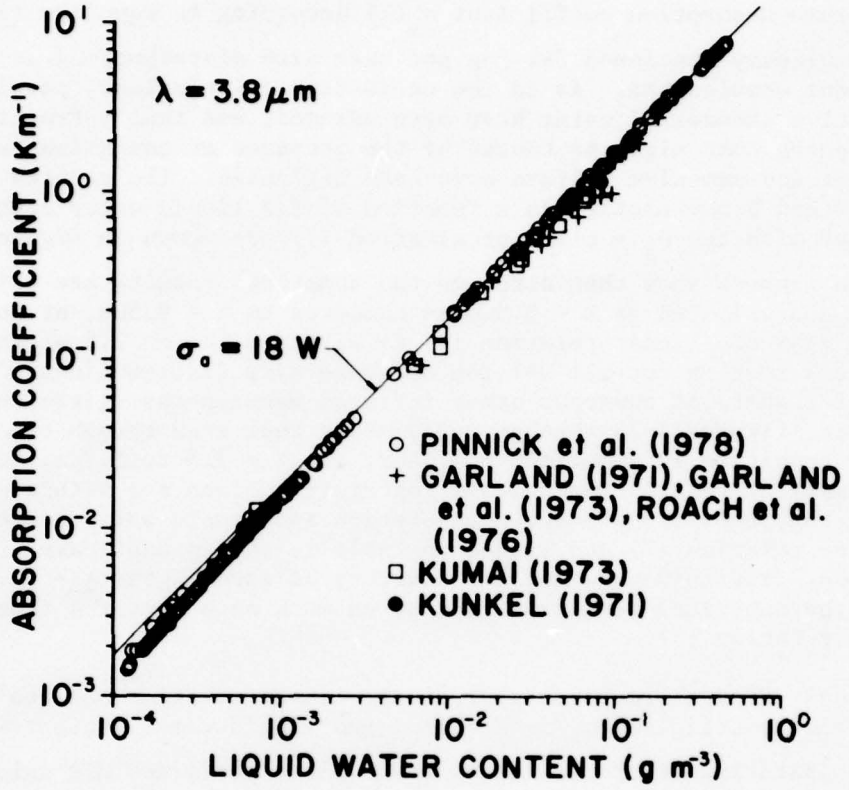

Figure 8. Variation of absorption coefficient with liquid water content in atmospheric fog and haze for 341 size distribution measurements made at different geographic locales and under a variety of meteorological conditions. In the infrared region around $\lambda = 3.8\mu m$, there exists a linear size distribution independent relation between the volume absorption coefficient σ_a and the liquid water content W of the form of eq. (7). Consequently, the results of all measurements are close to a straight line. The predicted relation between absorption σ_a and liquid water content W according to eq. (7) is shown by the straight line, where σ_a is in km^{-1} and W is in g m^{-3}.

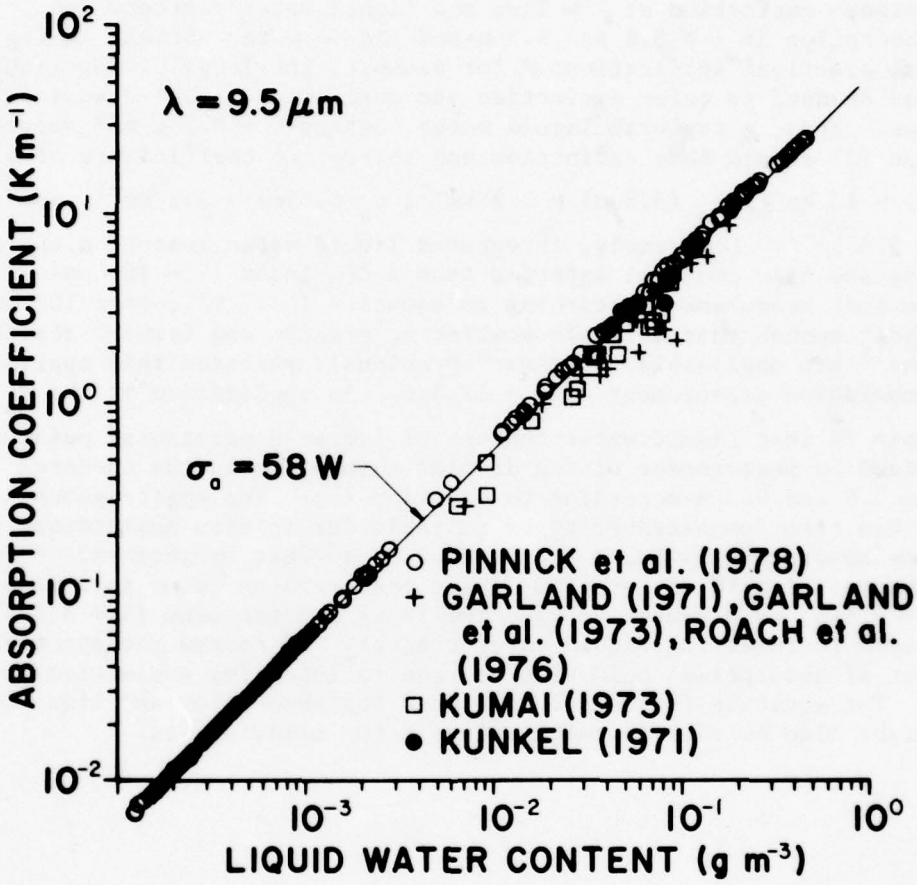

Figure 9. Same as figure 8 except for λ = 9.5μm.

APPLICATION OF EXTINCTION-ABSORPTION-LIQUID WATER CONTENT RELATIONSHIPS

The unique linear relationship, which is independent of the size distribution, between extinction at $\lambda \cong 11\mu m$ and liquid water content, and between absorption at $\lambda \cong 3.8$ and $9.5\mu m$ and liquid water content in fog has several practical applications. For example, knowledge of fog liquid water could be used to infer extinction and absorption at selected infrared wavelengths. Thus, a fog with liquid water content $W = 0.1\ g\ m^{-3}$ according to equation (1) should have extinction and absorption coefficients of σ_e ($\lambda = 11\mu m$) = $13\ km^{-1}$, σ_a ($3.8\mu m$) = $1.8\ km^{-1}$, $\sigma_a(5.3\mu m) = 3.1\ km^{-1}$, and σ_a ($9.5\mu m$) = $5.8\ km^{-1}$. Conversely, integrated liquid water content along a path in fog and haze could be inferred from a CO_2 laser ($\lambda = 10.6\mu m$) transmissometer measurement according to equation (1). Of course the path must be short enough that multiple scattering effects and forward scattering corrections[17] are negligible. Carlon[18] previously realized this application for a transmission measurement at $\lambda = 12.5\mu m$. An application of the $\sigma_a - W$ relationship is that liquid water content of fog at a particular point could be determined by measurement of fog droplet absorption in the spectral region $\lambda \cong 3.8$ and $9.5\mu m$ according to equation (7). The spectrophone technique has been demonstrated to be suitable for in situ measurement of particulate absorption by Bruce and Pinnick,[19] so that measurement of fog droplet absorption with either a CO_2 laser spectrophone tuned to a wavelength $\lambda \cong 9.5\mu m$, or a deuterium fluoride laser spectrophone ($\lambda \cong 3.8\mu m$) could be used to infer fog liquid water content. Of course the spectrophone measurement of absorption could also be used to infer fog extinction at $\lambda \cong 11\mu m$. The equation (7) relation between fog absorption and liquid water content might also be used in calculation of fog emissivities.

---

[17]A. Deepak and M. A. Box, 1978, "Forward Scattering Corrections for Optical Extinction Measurements in Aerosol Media. 2: Polydispersions," Appl Opt 17:3169-3176

[18]H. R. Carlon et al., 1977, "Infrared Extinction Spectra of Some Common Liquid Aerosols," Appl Opt, 16:1598-1605

[19]C. W. Bruce and R. G. Pinnick, 1977, "In-situ Measurements of Aerosol Absorption with a Resonant CW Laser Spectrophone," Appl Opt, 16:1762-1765

CONCLUSIONS

Chýlek's[1] prediction of a linear relation, which is independent of the size distribution, between extinction at $\lambda \cong 11\mu m$ and liquid water content of fog has been verified within a factor 2 for 341 different fog and haze droplet distributions measured under a variety of meteorological conditions. The prediction generally works better for radiation fogs than advection fogs. A similar linear relation between fog droplet absorption at $\lambda \cong 3.8$ and $9.5\mu m$ and liquid water content has been derived and validated using the same 341 distributions. However, there exists no size distribution independent relation between extinction in the visible ($\lambda \cong 0.55\mu m$) and fog liquid water content. Three practical applications of these findings are suggested: (1) inference of fog integrated liquid water content along a path by measurement of laser transmission (at $\lambda \cong 11\mu m$) across that path; (2) inference of fog liquid water content at a particular point from measurement of fog droplet absorption with a deuterium fluoride or CO_2 laser spectrophone, and (3) calculation of fog emissivities in the infrared from knowledge of fog liquid water content.

---

[1]P. Chýlek, 1978, "Extinction and Liquid Water Content of Fogs," J Atmos Sci, 35:296-300

REFERENCES

1. Chýlek, Petr, 1978, "Extinction and Liquid Water Content of Fogs," J Atmos Sci, 35:296-300.

2. Garland, J. A., 1971, "Some Fog Droplet Size Distributions Obtained by an Impaction Method," Quart J Roy Meteorol Soc, 97:483-494.

3. Kumai, Motoi, 1973, "Arctic Fog Droplet Size Distribution and Its Effect on Light Attenuation," J Atmos Sci, 30:635-643.

4. Garland, J. A., J. R. Branson, and L. C. Cox, 1973, "A Study of the Contribution of Pollution to Visibility in a Radiation Fog," Atmos Environ, 7:1079-1092.

5. Kunkel, B. A., 1971, "Fog Drop-Size Distributions Measured with a Laser Hologram Camera," J Appl Meteorol, 10:482-486.

6. Roach, W. T., R. Brown, S. J. Caughey, J. A. Garland, and C. J. Readings, 1976, "The Physics of Radiation Fog: I - a Field Study," Q J Roy Meteorol Soc, 102:313-333.

7. Pinnick, R. G., D. L. Hoihjelle, G. Fernandez, E. B. Stenmark, J. D. Lindberg, S. G. Jennings, and G. B. Hoidale, 1978, "Vertical Structure in Atmospheric Fog and Haze and Its Effects on IR and Visible Extinction," J Atmos Sci, 35:2020-2032.

8. Arnulf, A., J. Bricard, E. Curé, and C. Véret, 1957, "Transmission by Haze and Fog in the Spectral Region 0.35 to 10 Microns," J Opt Soc Am, 47:491-498.

9. May, K. R., 1961, "Fog Droplet Sampling Using a Modified Impactor Technique," Quart J Roy Meteorol Soc, 87:535-548.

10. Pilié, R. J., 1975, "The Life Cycle of Valley Fog. Part II: Fog Microphysics," J Appl Meteorol, 14:364-374.

11. Eldridge, R. G., 1961, "A Few Fog Drop-Size Distributions," J Appl Meteorol, 18:671-676.

12. May, K. R., 1945, "The Cascade Impactor: An Instrument for Sampling Aerosols," J Sci Instr, 22:187-195.

13. Hale, G. M., and M. R. Querry, 1973, "Optical Constants of Water in the 200 nm to 20μm Wavelength Region," Appl Opt, 12:555-563.

14. Hänel, G., 1976, "The Properties of Atmospheric Aerosol Particles as Functions of Relative Humidity at Thermodynamic Equilibrium with the Surrounding Moist Air," Adv in Geopys, 19:73-188.

15. Hänel, G., and K. Bullrich, 1978, "Physico - Chemical Property Models of Tropospheric Aerosol Particles," Beitr Phys Atmos, 51:129-138.

16. Platt, C. M. R., 1976, "Infrared Absorption and Liquid Water Content in Stratocumulus Clouds," Q J Roy Meteorol Soc, 102:553-561.

17. Deepak, Adarsh, and M. A. Box, 1978, "Forward Scatting Corrections for Optical Extinction Measurements in Aerosol Media. 2: Polydispersions," Appl Opt, 17:3169-3176.

18. Carlon, H. R., D. Anderson, M. Milham, T. Tarnove and R. Frickel, 1977, "Infrared Extinction Spectra of some Common Liquid Aerosols," Appl Opt, 16:1598-1605.

19. Bruce, C. W., and R. G. Pinnick, 1977, "In-situ Measurements of Aerosol Absorption with a Resonant CW Laser Spectrophone," Appl Opt, 16:1762-1765.

APPENDIX

FOG AND HAZE EXTINCTION COEFFICIENT VS LIQUID WATER CONTENT, IR EXTINCTION COEFFICIENT VS VISIBLE EXTINCTION COEFFICIENT, AND ABSORPTION COEFFICIENT VS LIQUID WATER CONTENT

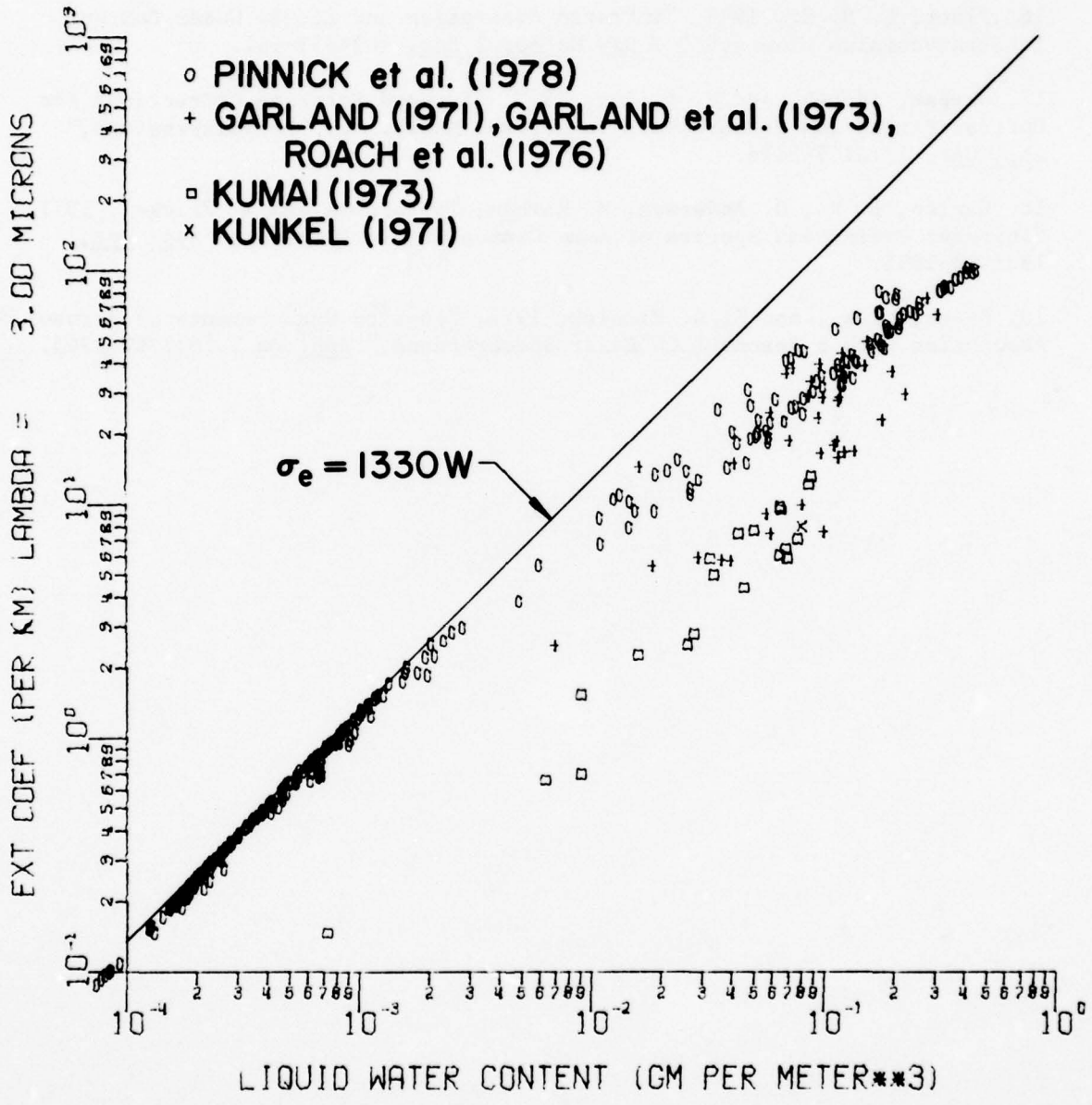

Figure A-1. Variation of extinction coefficient (at λ = 3.0μm) with liquid water content in atmospheric fog and haze for 341 size distribution measurements made at different geographic locales and under a variety of meteorological conditions. The large spread of the points in the graph shows that the extinction coefficient is a function of the size distribution as well as of the liquid water content. The predicted relation between extinction σ_e and liquid water content W according to eq. (1) is shown by the straight line, where σ_e is in km^{-1} and W is in g m^{-3}.

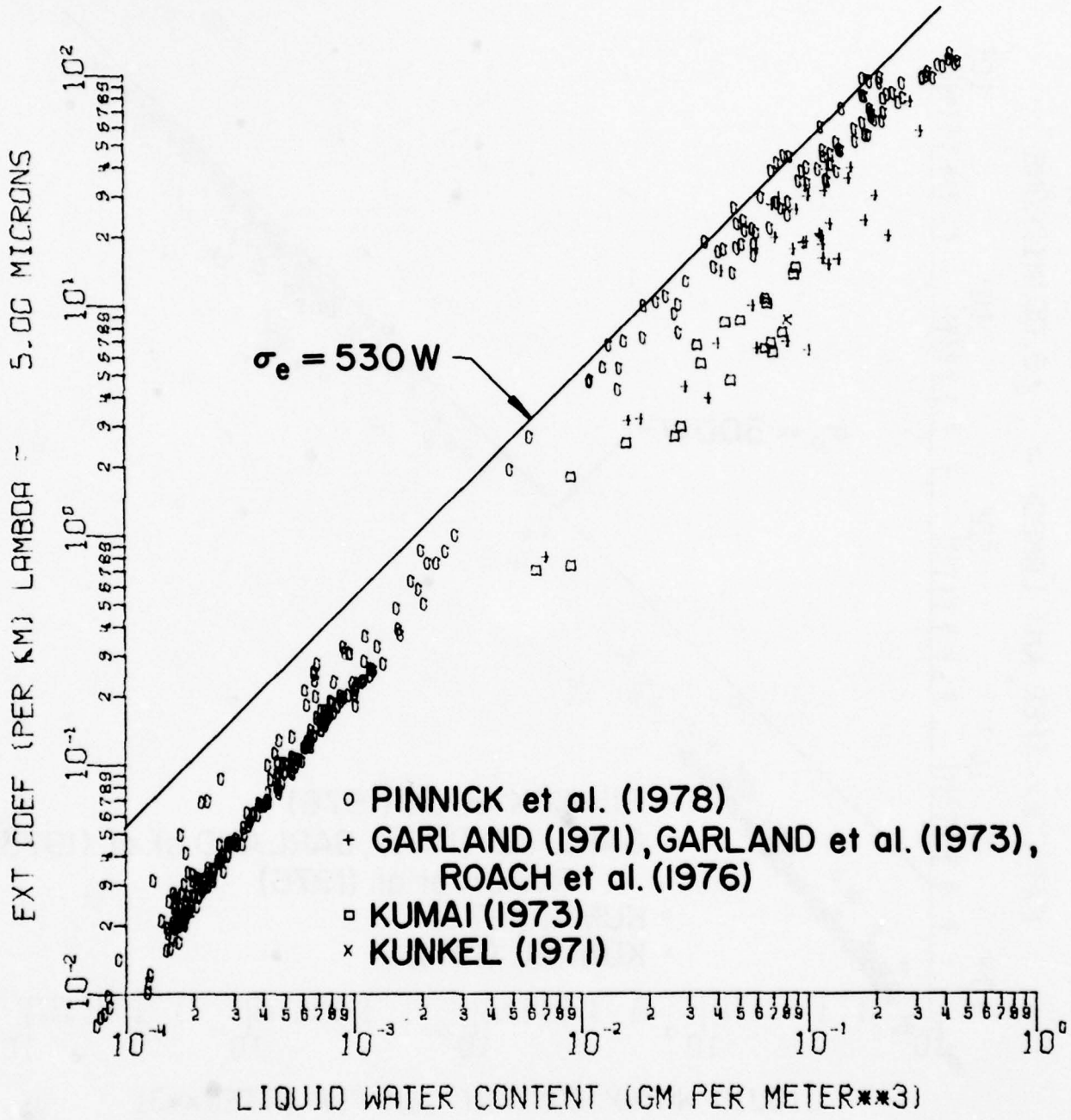

Figure A-2. Same as figure A-1 except for λ = 5μm.

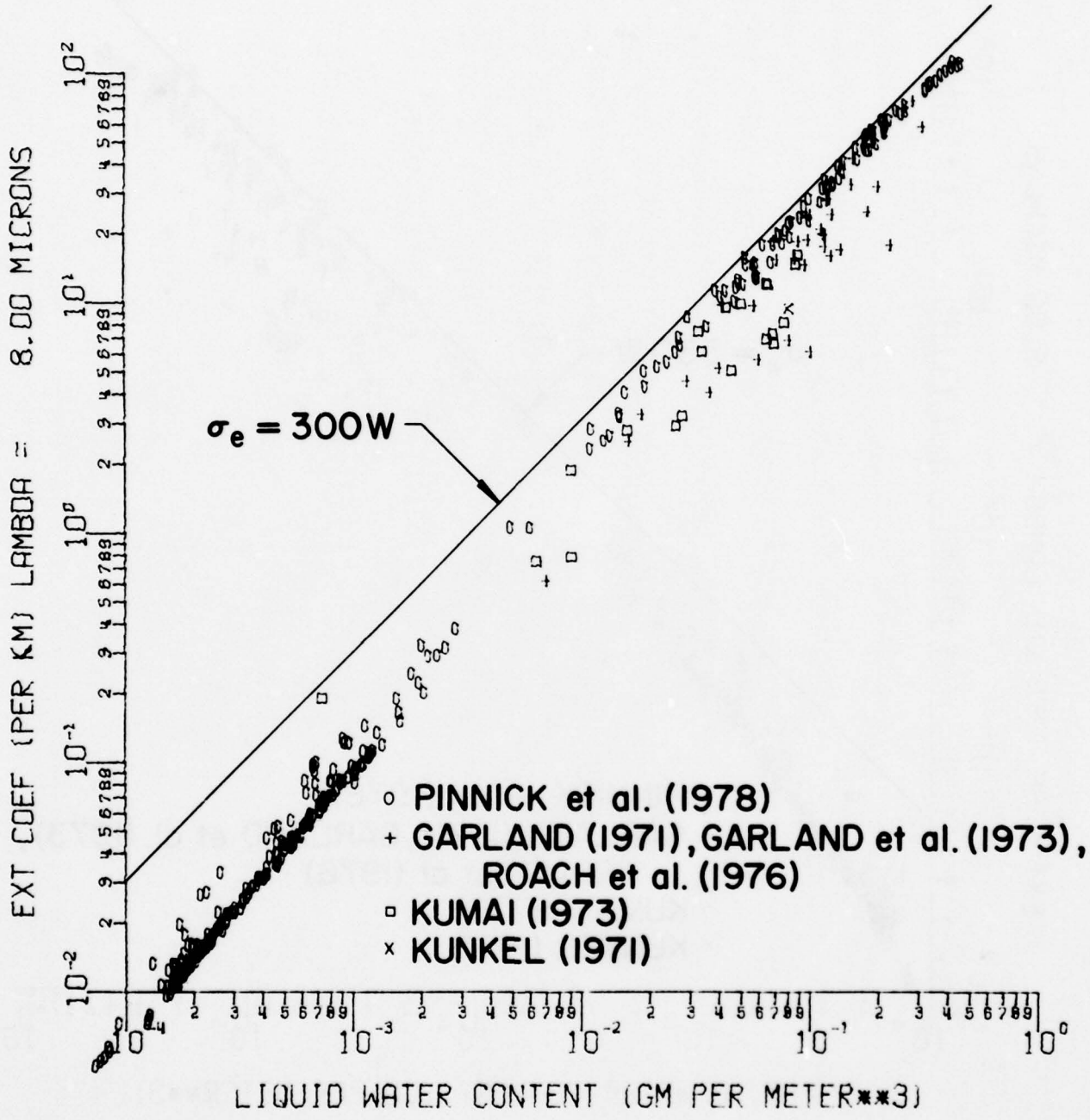

Figure A-3. Same as figure A-1 except for λ = 8μm.

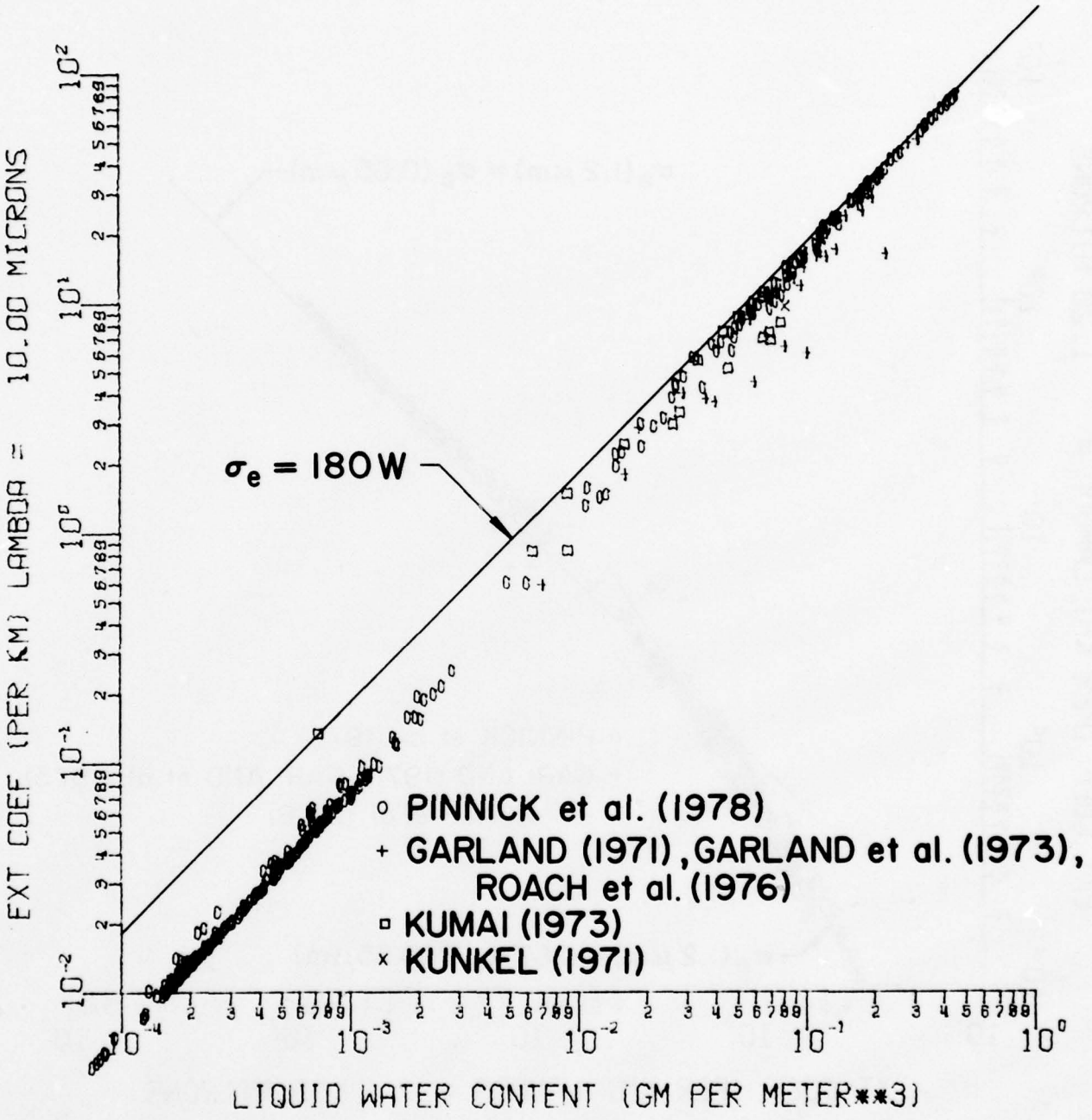

Figure A-4. Same as figure A-1 except for λ = 10μm.

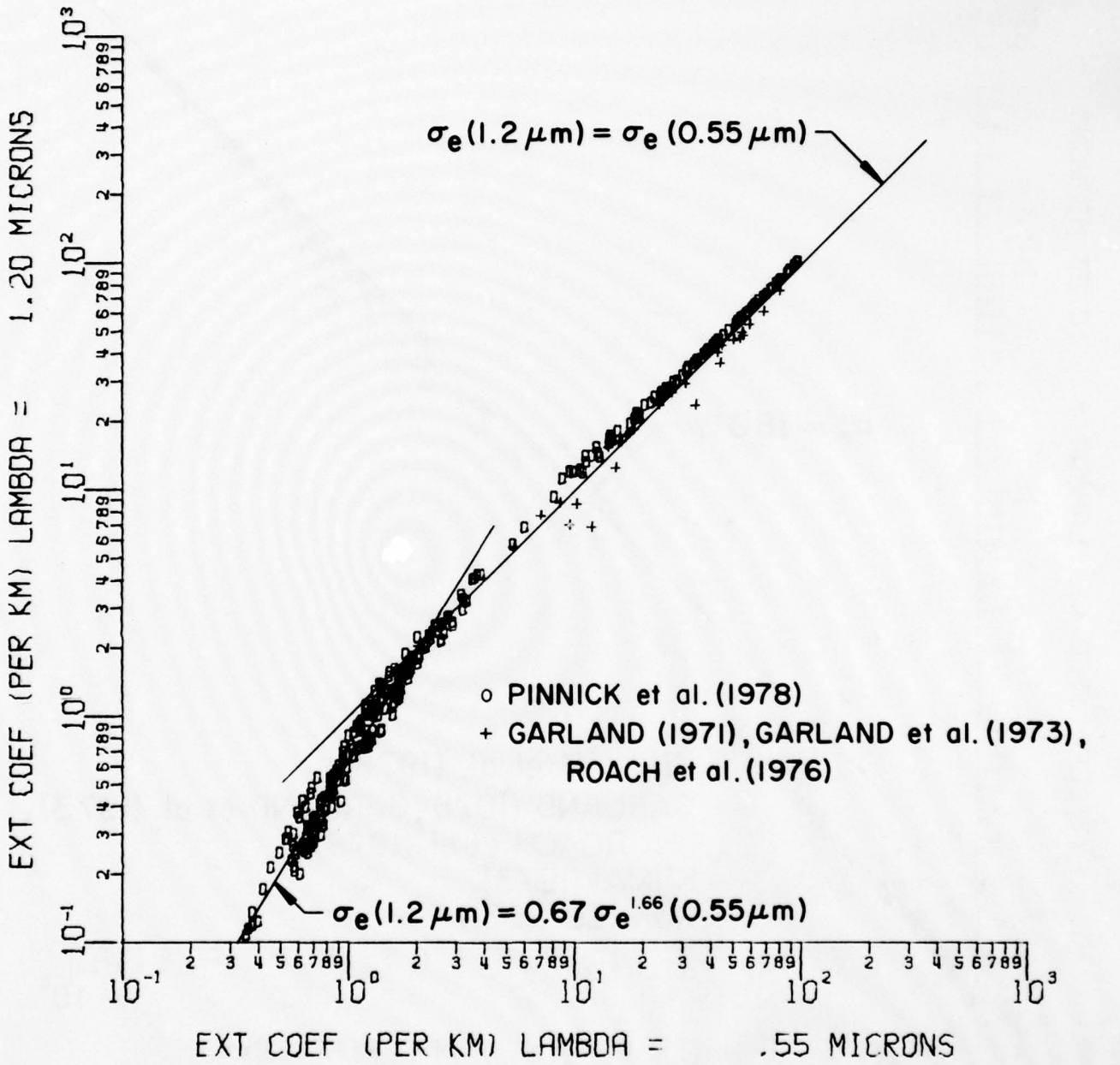

Figure A-5. Variation of the infrared extinction coefficient at λ = 1.2μm with visible extinction coefficient (λ = 0.55μm) in atmospheric fog and haze for 341 size distribution measurements made at different geographic locales and under a variety of meteorological conditions. The spread of the points in the graph shows that the infrared extinction coefficient is a function of the size distribution as well as of the visible extinction coefficient. Also shown are empirical power-law relationships fit to the Mie-calculated points.

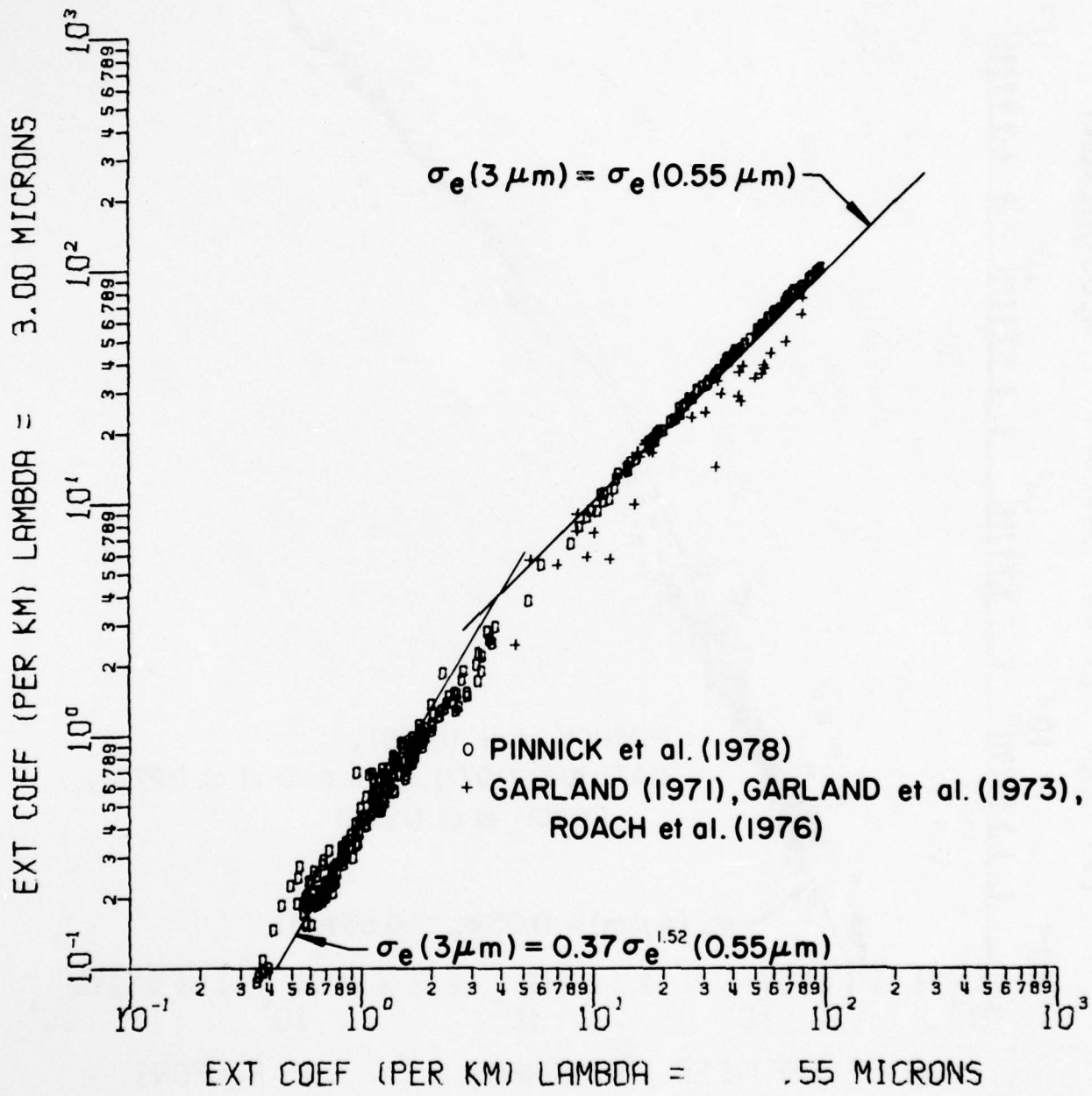

Figure A-6. Same as figure A-5 except for the infrared wavelength λ = 3μm.

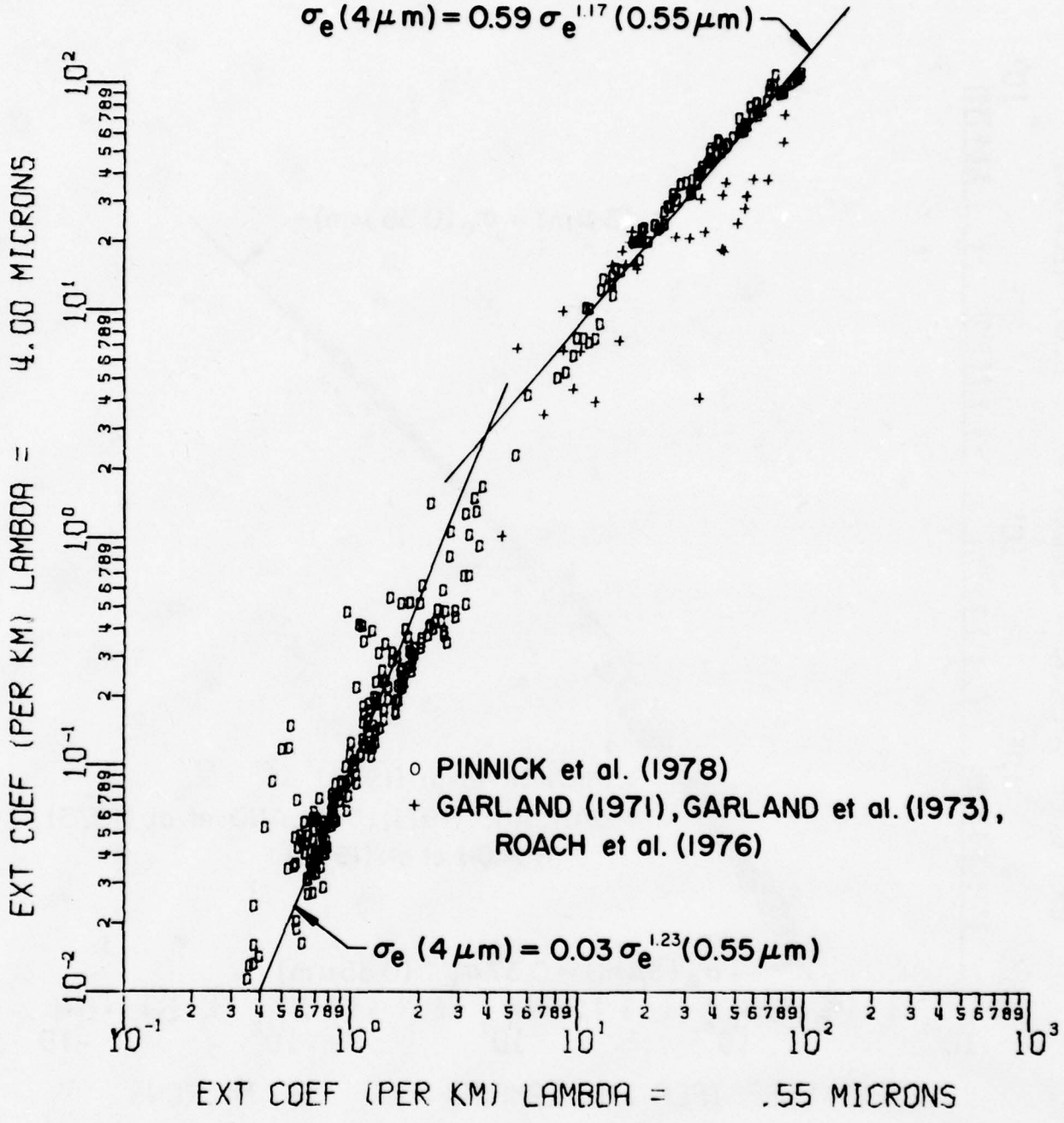

Figure A-7. Same as figure A-5 except for the infrared wavelength λ = 4μm.

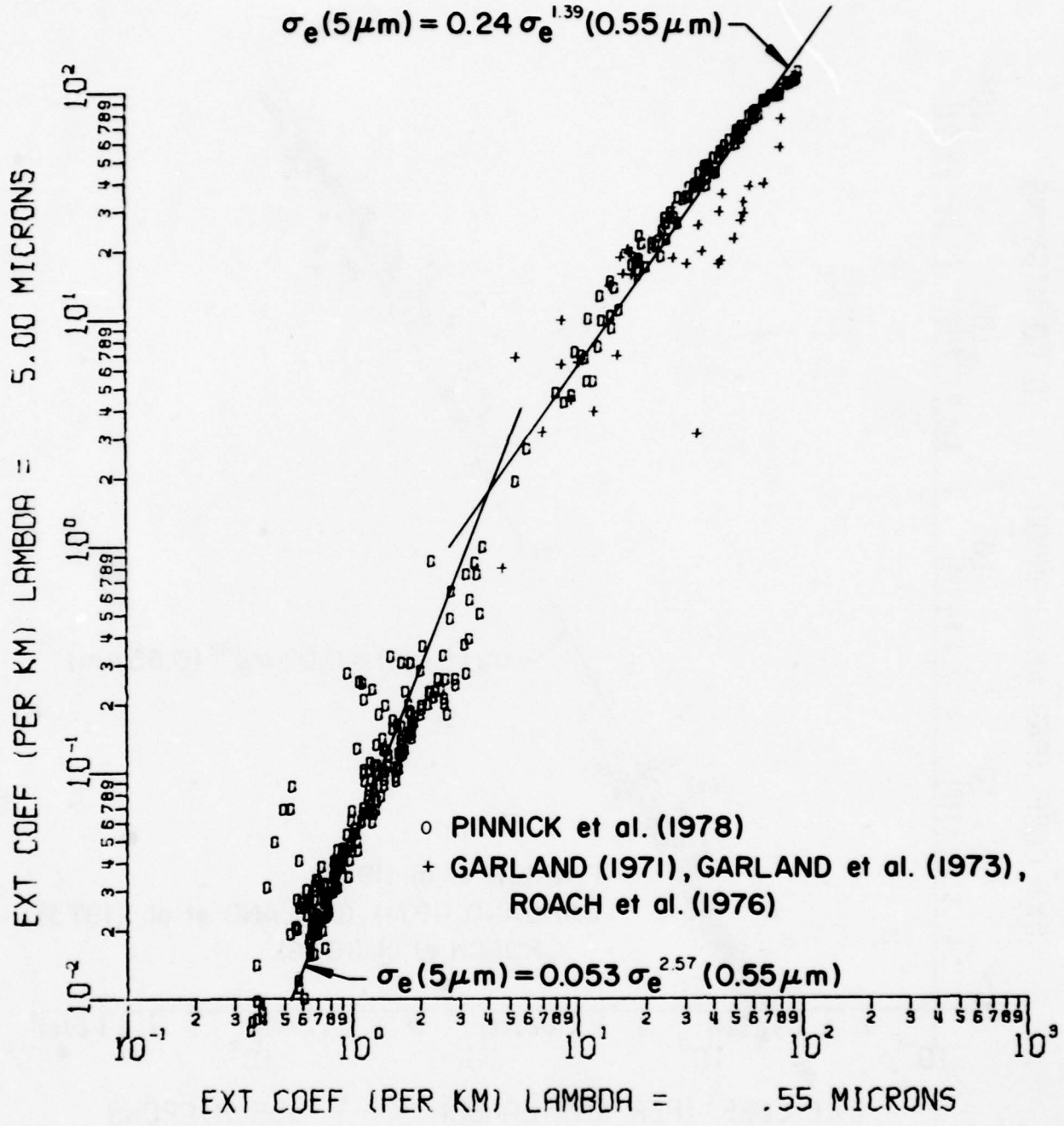

Figure A-8. Same as figure A-5 except for the infrared wavelength λ = 5μm.

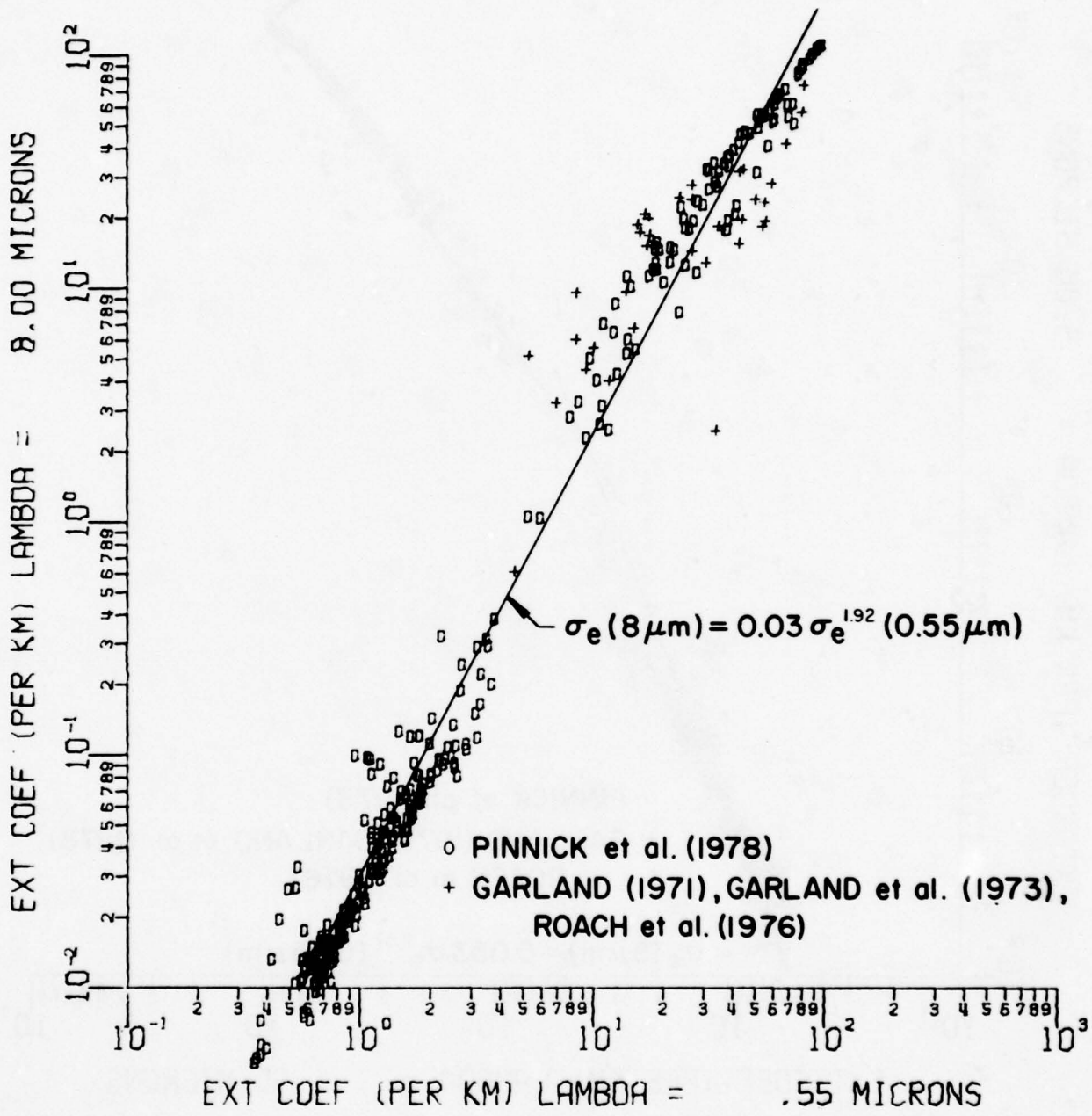

Figure A-9. Same as figure A-5 except for the infrared wavelength λ = 8μm.

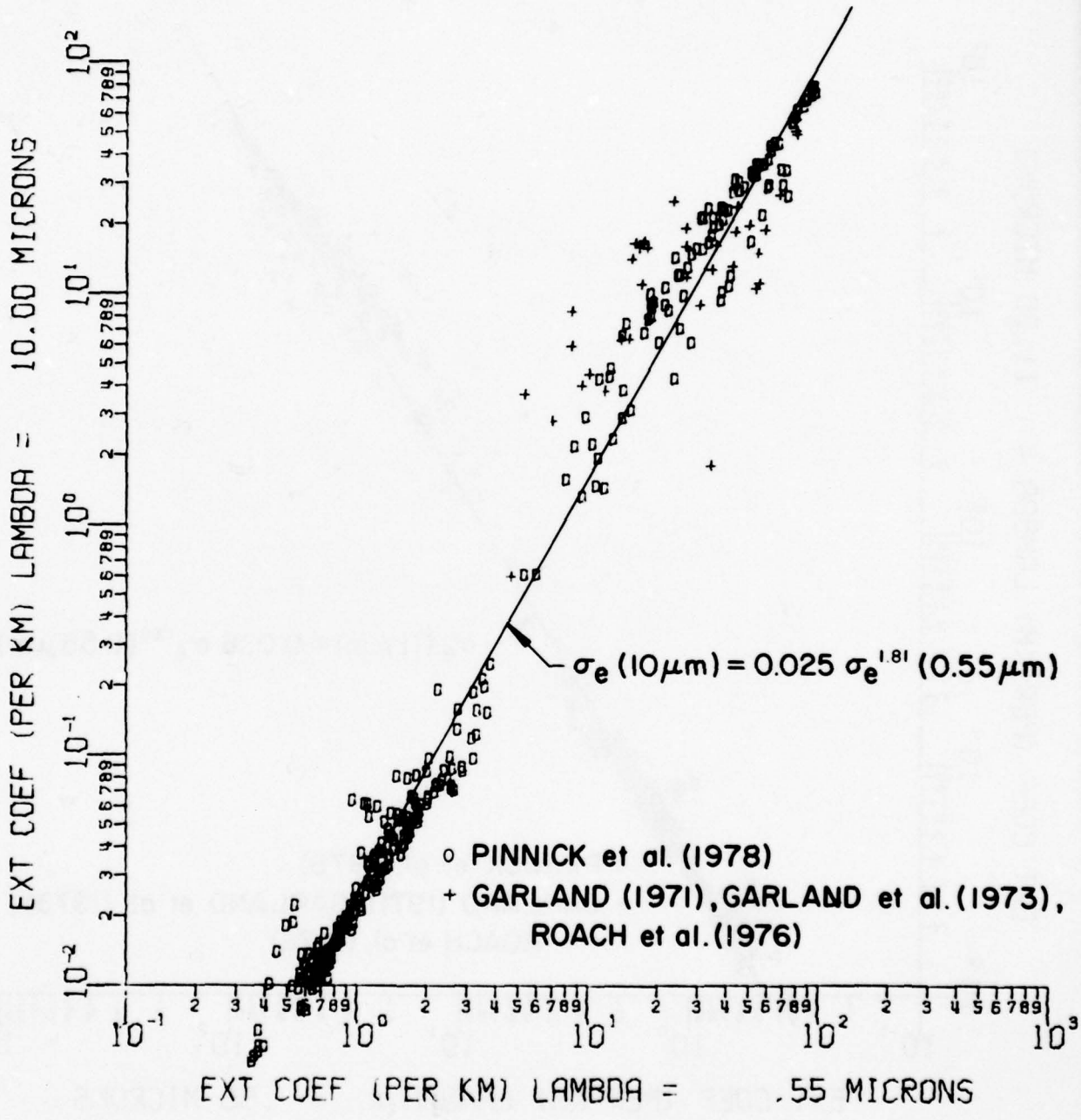

Figure A-10. Same as figure A-5 except for the infrared wavelength λ = 10μm.

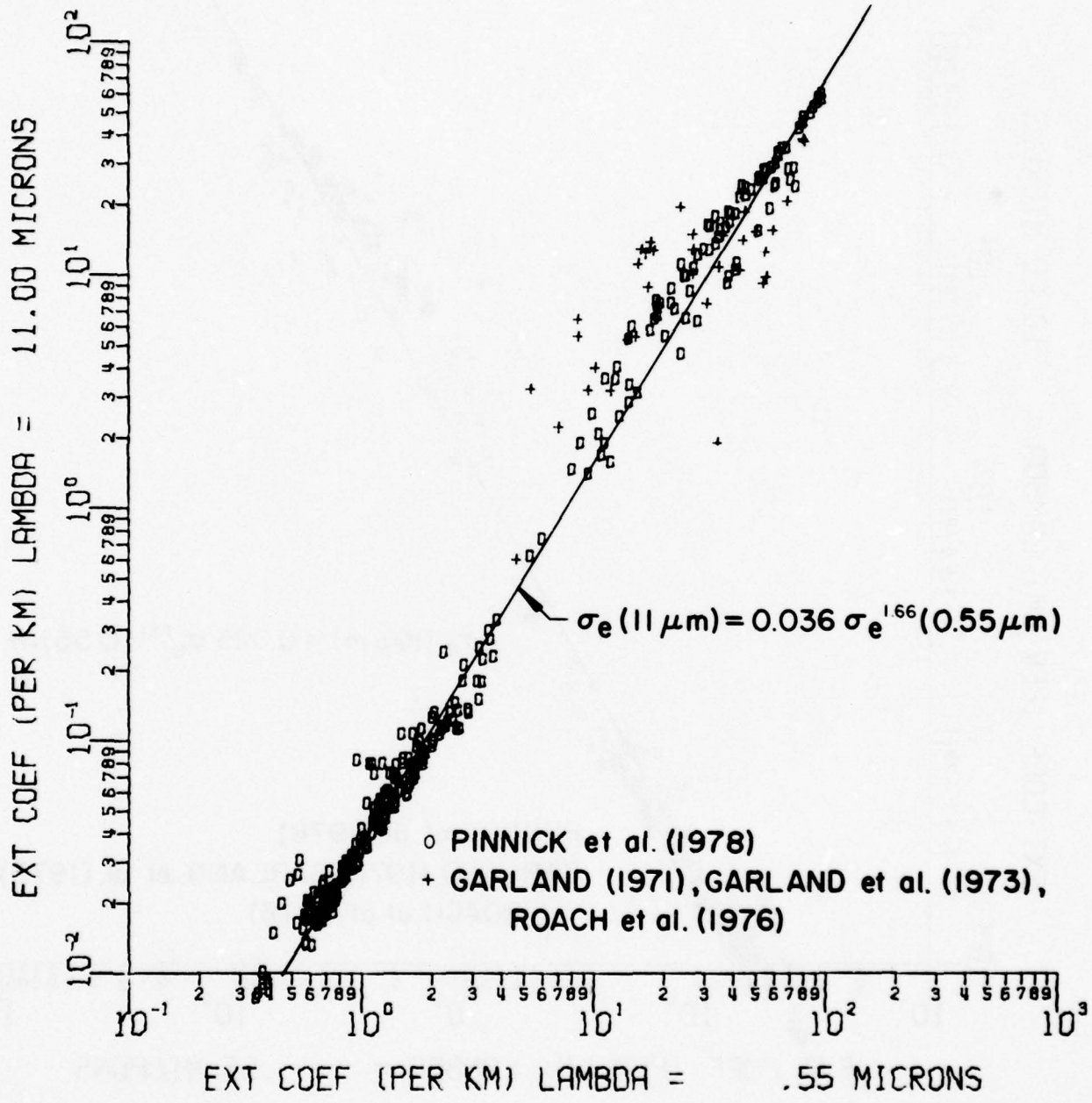

Figure A-11. Same as figure A-5 except for the infrared wavelength λ = 11μm.

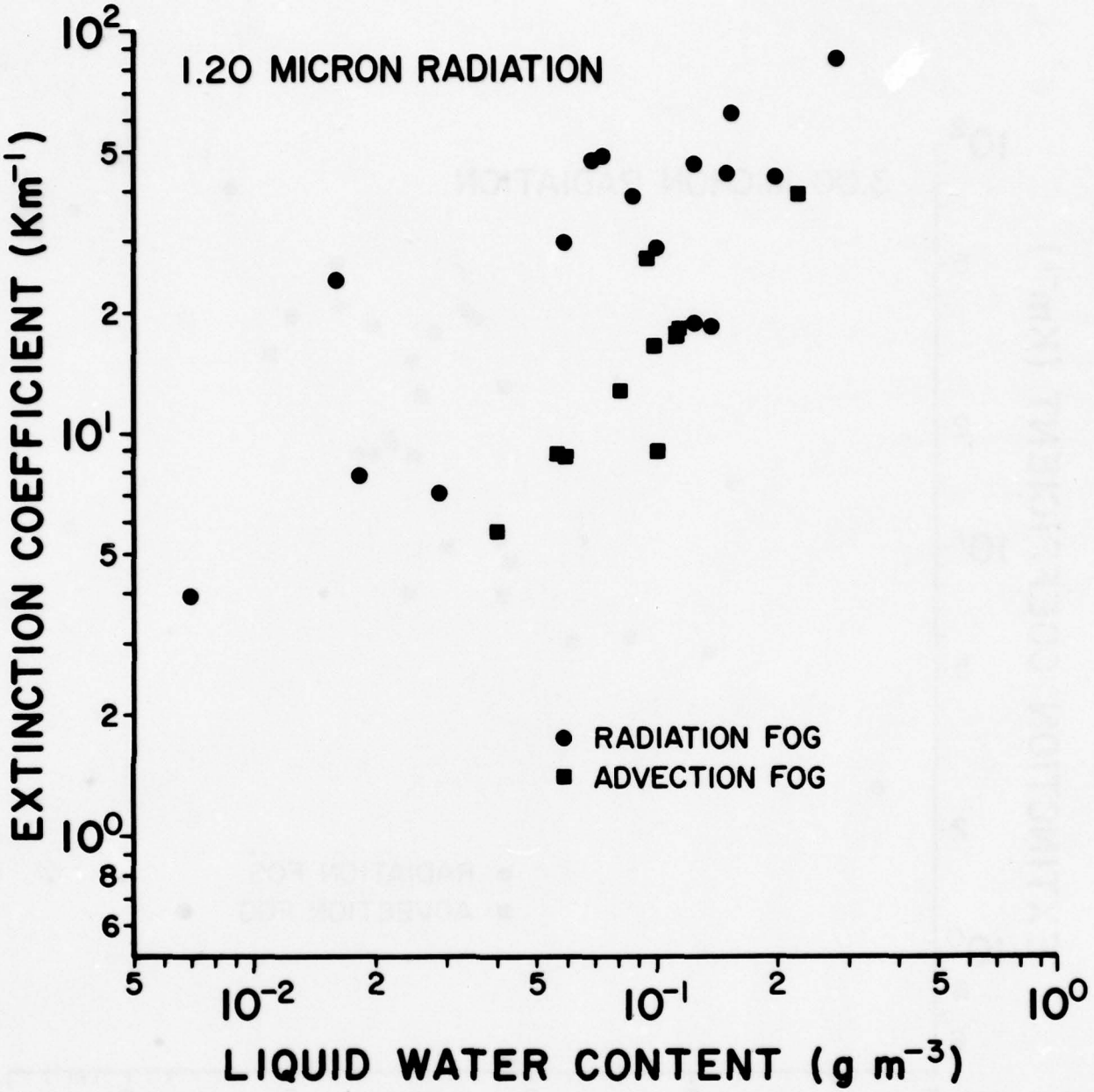

Figure A-12. Variation of extinction coefficient (at λ = 1.2μm) with liquid water content in atmospheric fog for 26 size distribution measurements made over an approximate 5-year period under a variety of meteorological conditions in England. The large spread of the points in the graph shows that the extinction coefficient is a function of the size distribution as well as of the liquid water content. The extinction and liquid water contents calculated from the measured size distributions are divided according to radiation (circles) or advection (squares) fog. We see from the figure that radiation fogs are generally more effective scatterers than advection fogs with the same liquid water content.

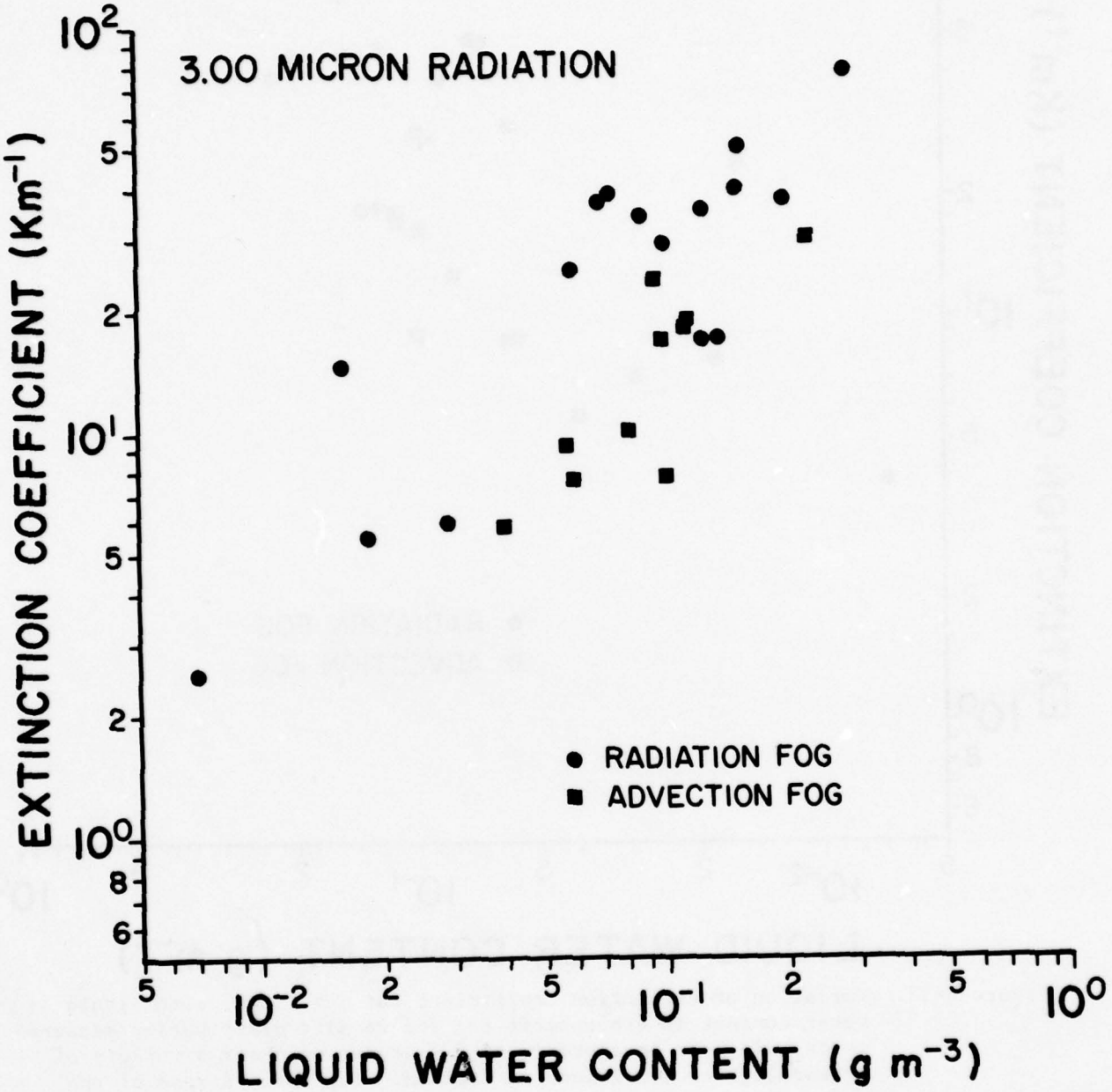

Figure A-13. Same as figure A-12 except for = 3.m.

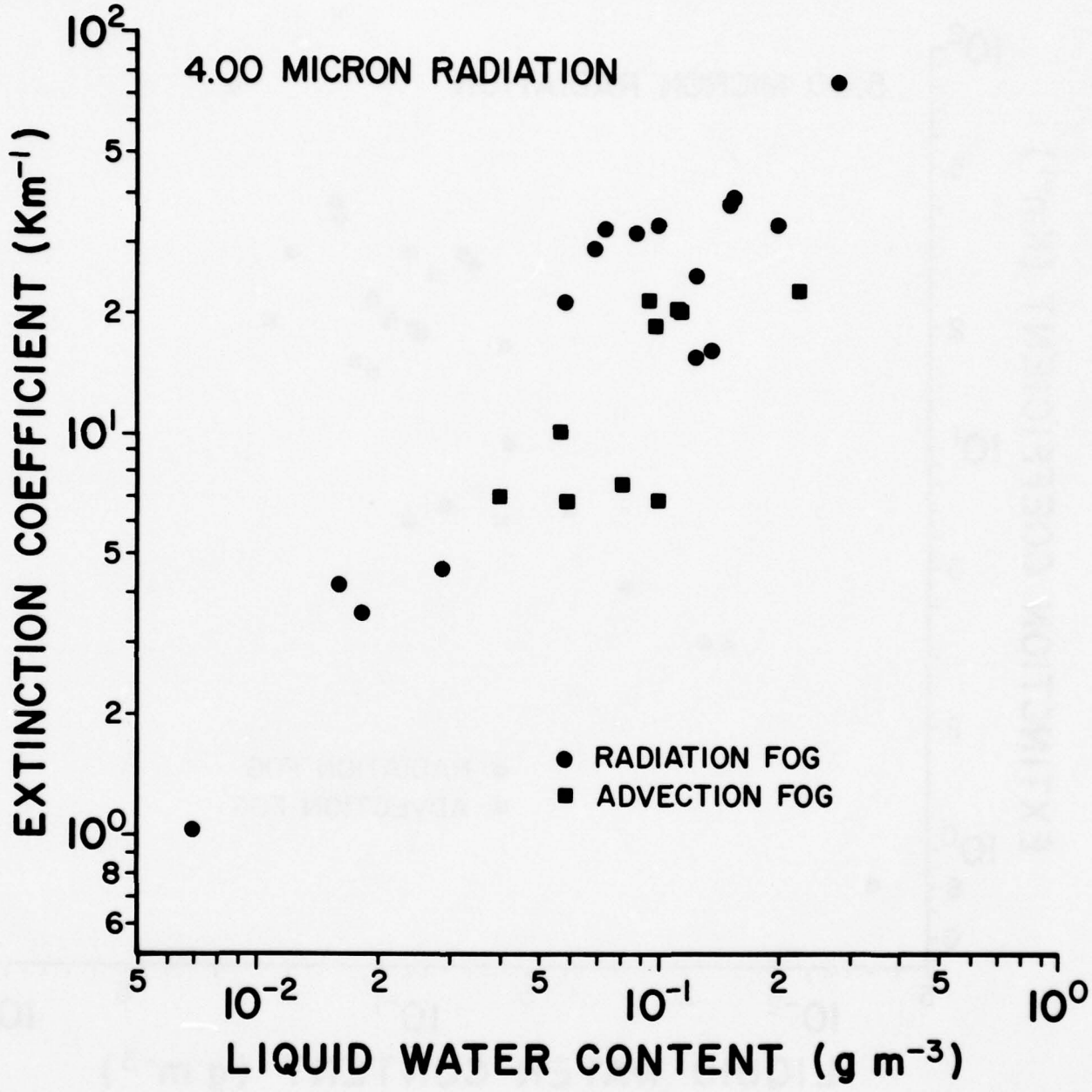

Figure A-14. Same as figure A-12 except for λ = 4μm.

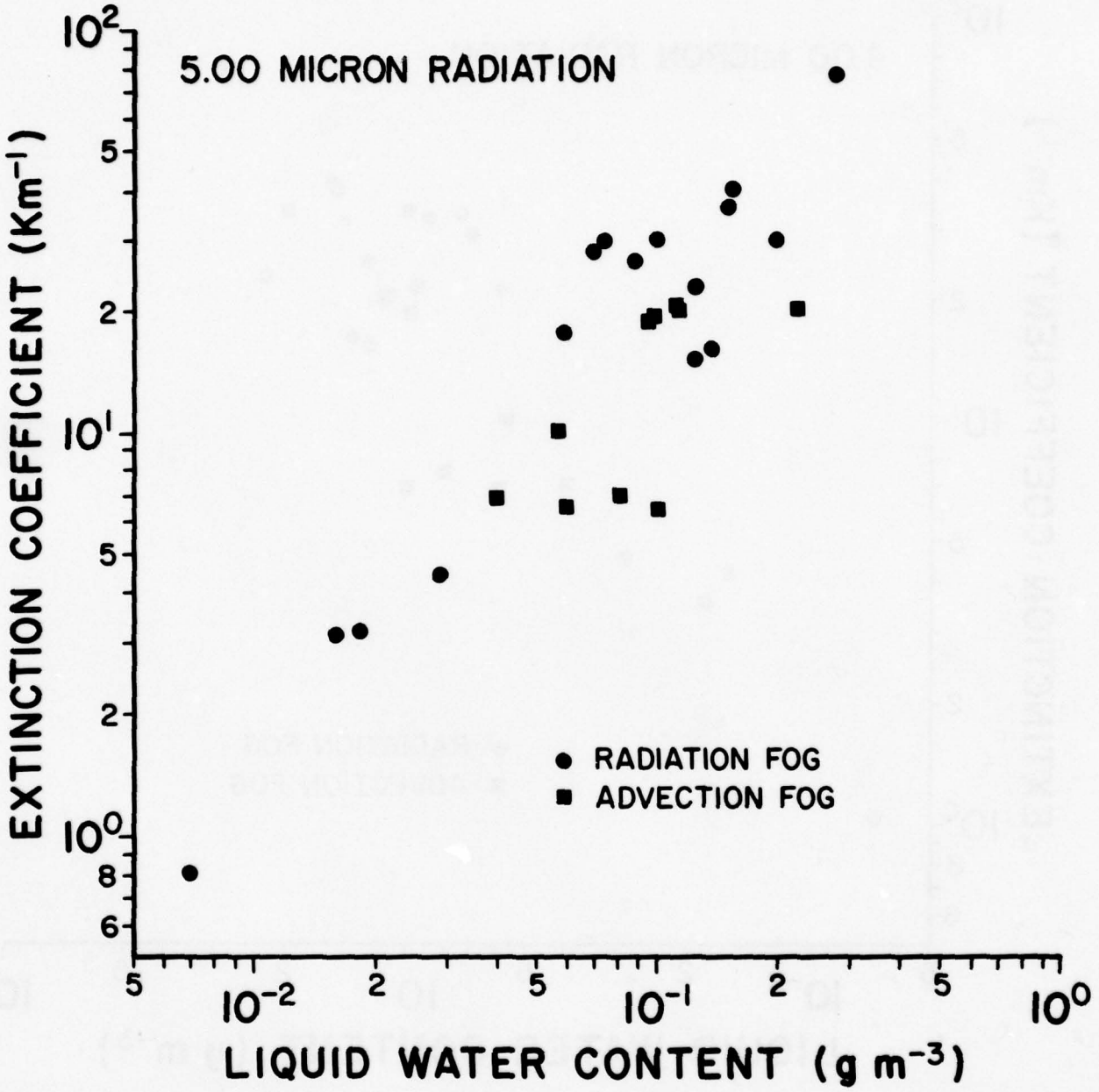

Figure A-15. Same as figure A-12 except for λ = 5μm.

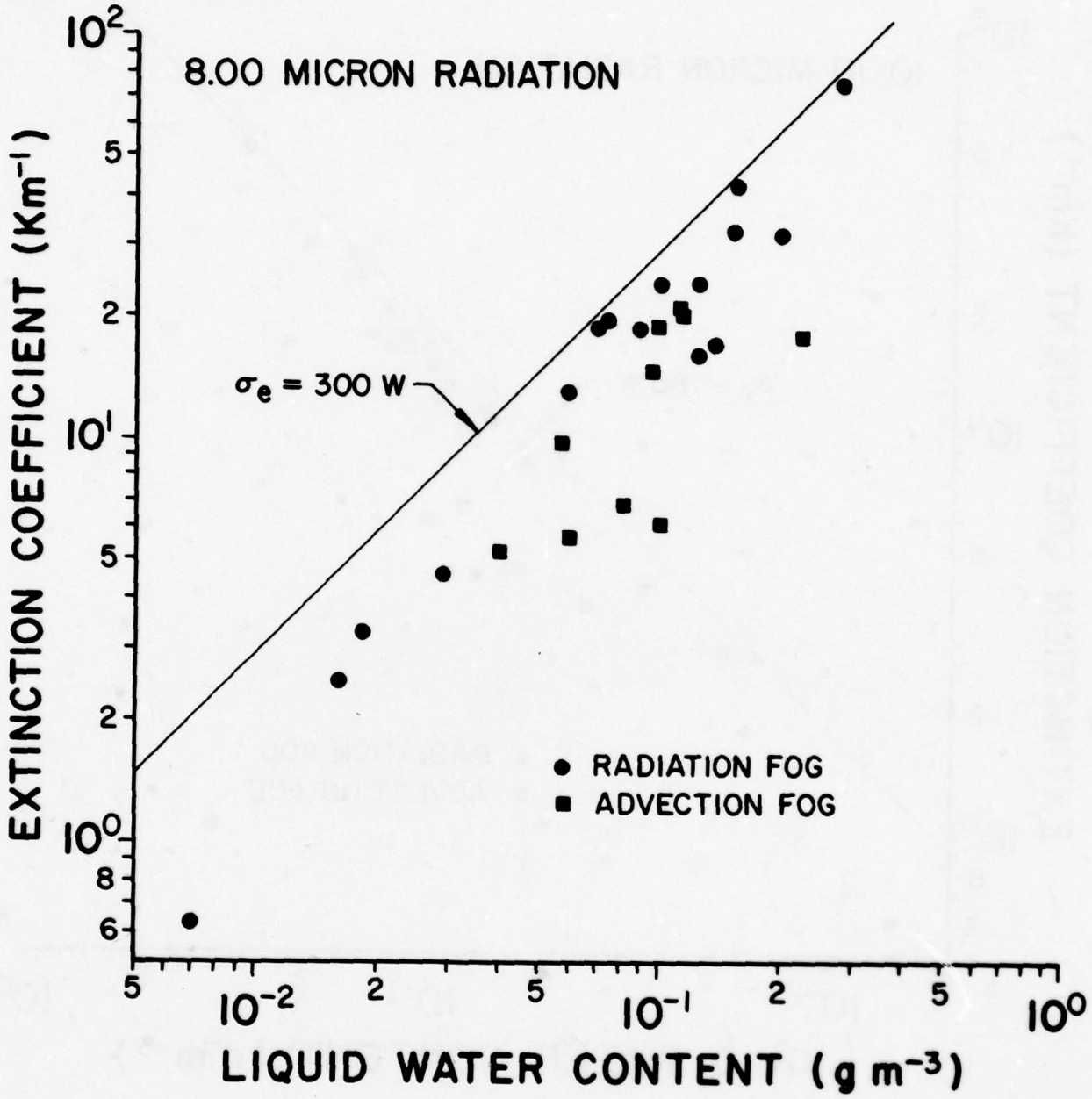

Figure A-16. Same as figure A-12 except for λ = 8μm. The predicted relation between extinction and liquid water content given by eq. (1) is shown by the straight line. Because the $Q_e = \alpha x$ approximation is generally better satisfied for radiation fogs, those points fall closer to the straight line prediction.

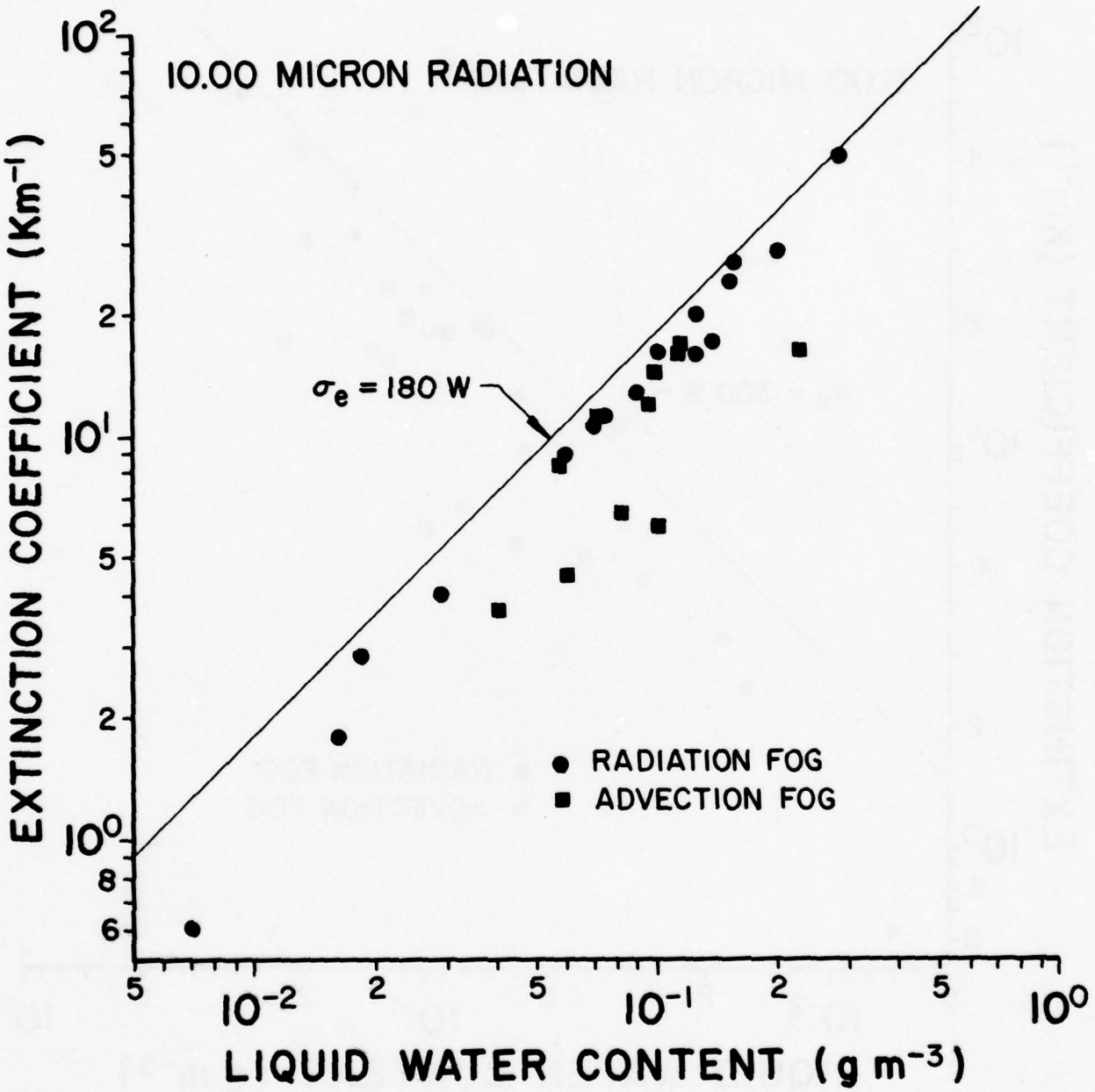

Figure A-17. Same as figure A-16 except for λ = 10μm.

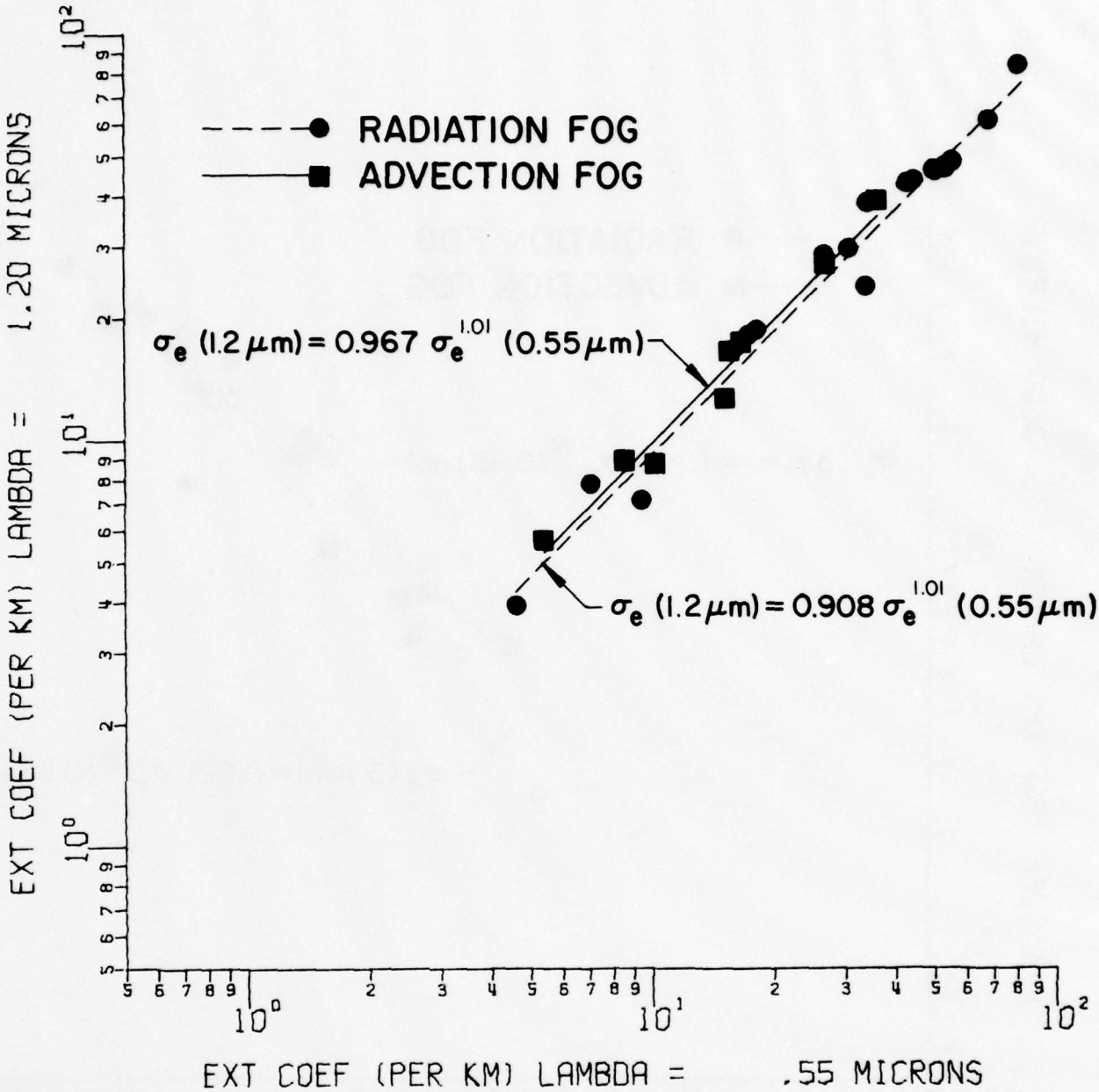

Figure A-18. Variation of the infrared extinction coefficient at λ = 1.2μm with visible extinction coefficient (λ = 0.55μm) in atmospheric fog for 26 size distribution measurements made over an approximate 5-year period under a variety of meteorological conditions in England. The spread of the points in the graph shows that the infrared extinction coefficient is a function of the size distribution as well as of the visible extinction coefficient. Also shown are empirical power-law relationships (one for radiation fog and one for advection fog) determined by doing least-square fits to the Mie-calculated points for radiation fogs (circles) and advection fogs (squares).

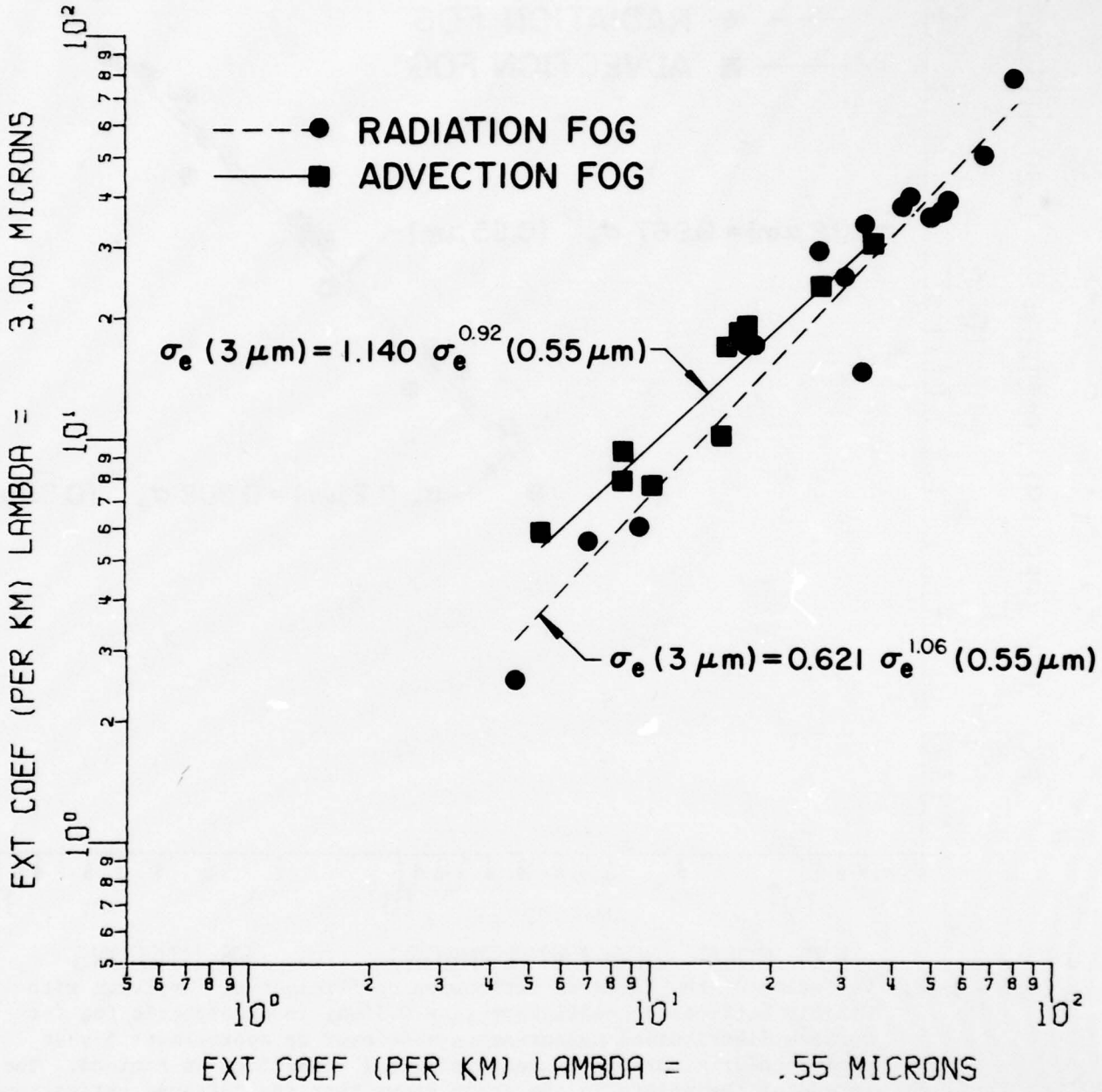

Figure A-19. Same as figure A-18 except for the infrared wavelength λ = 3μm.

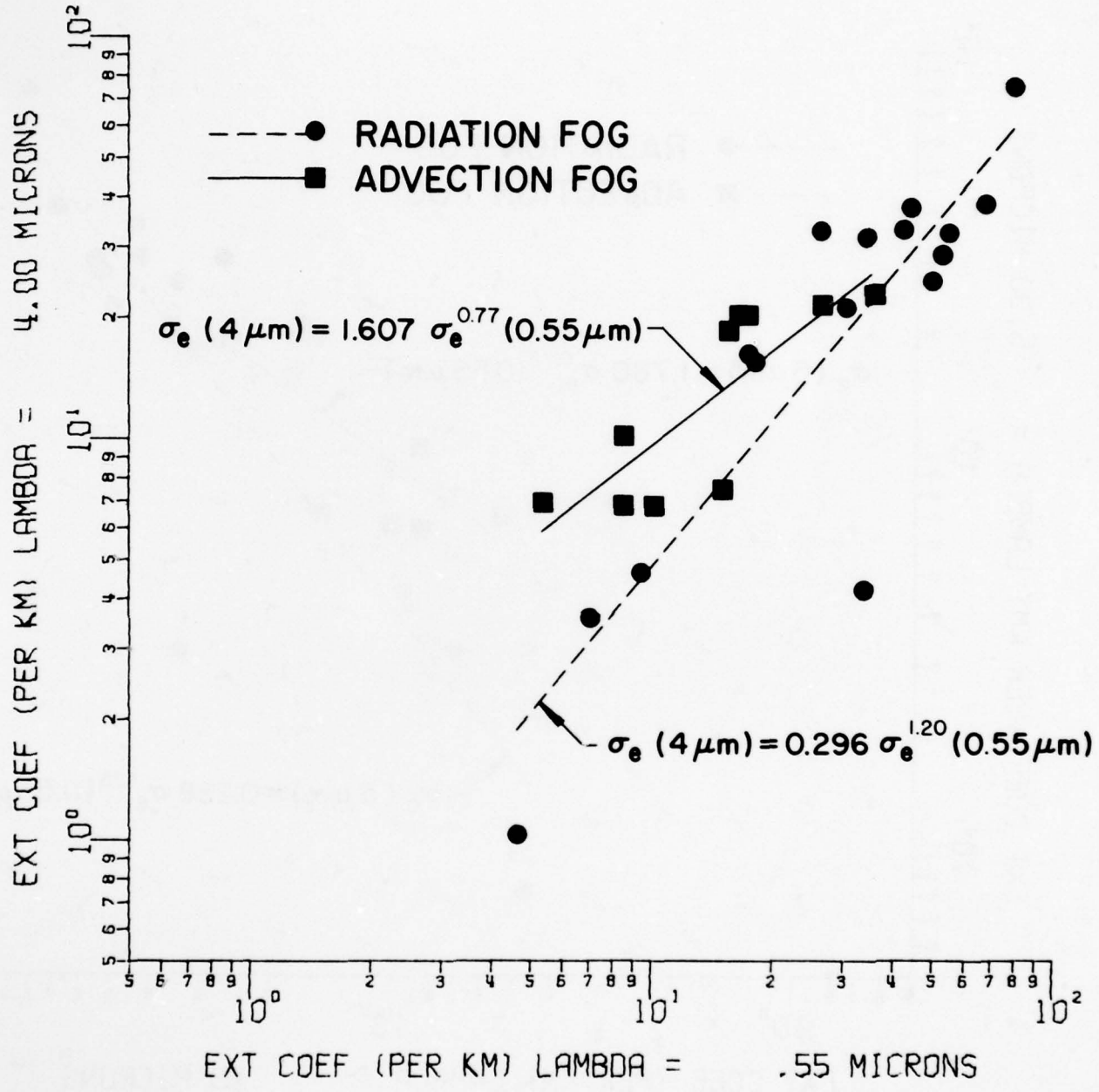

Figure A-20. Same as figure A-18 except for the infrared wavelength λ = 4μm.

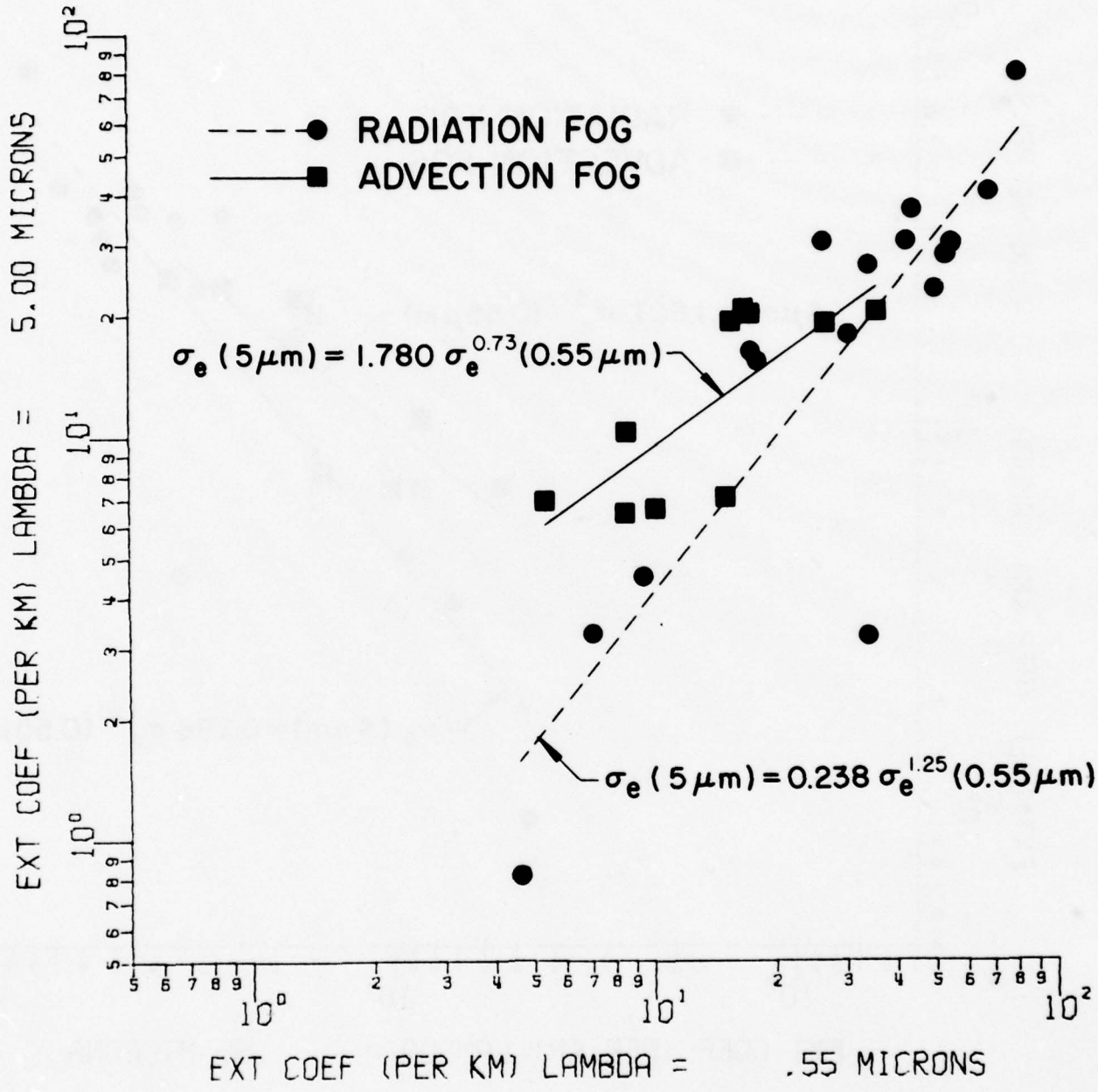

Figure A-21. Same as figure A-18 except for the infrared wavelength λ = 5μm.

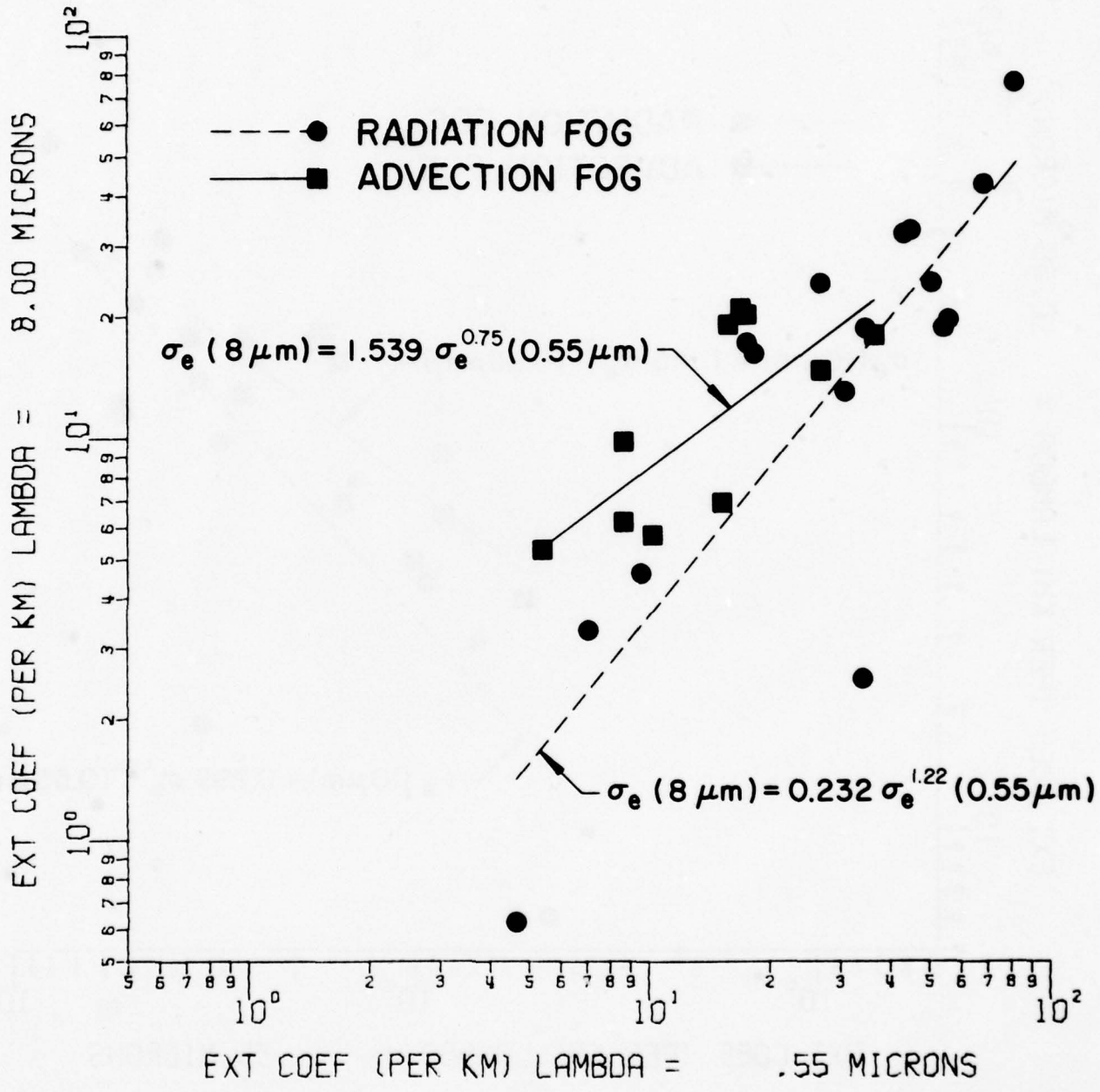

Figure A-22. Same as fig. A-18 except for the infrared wavelength λ = 8μm.

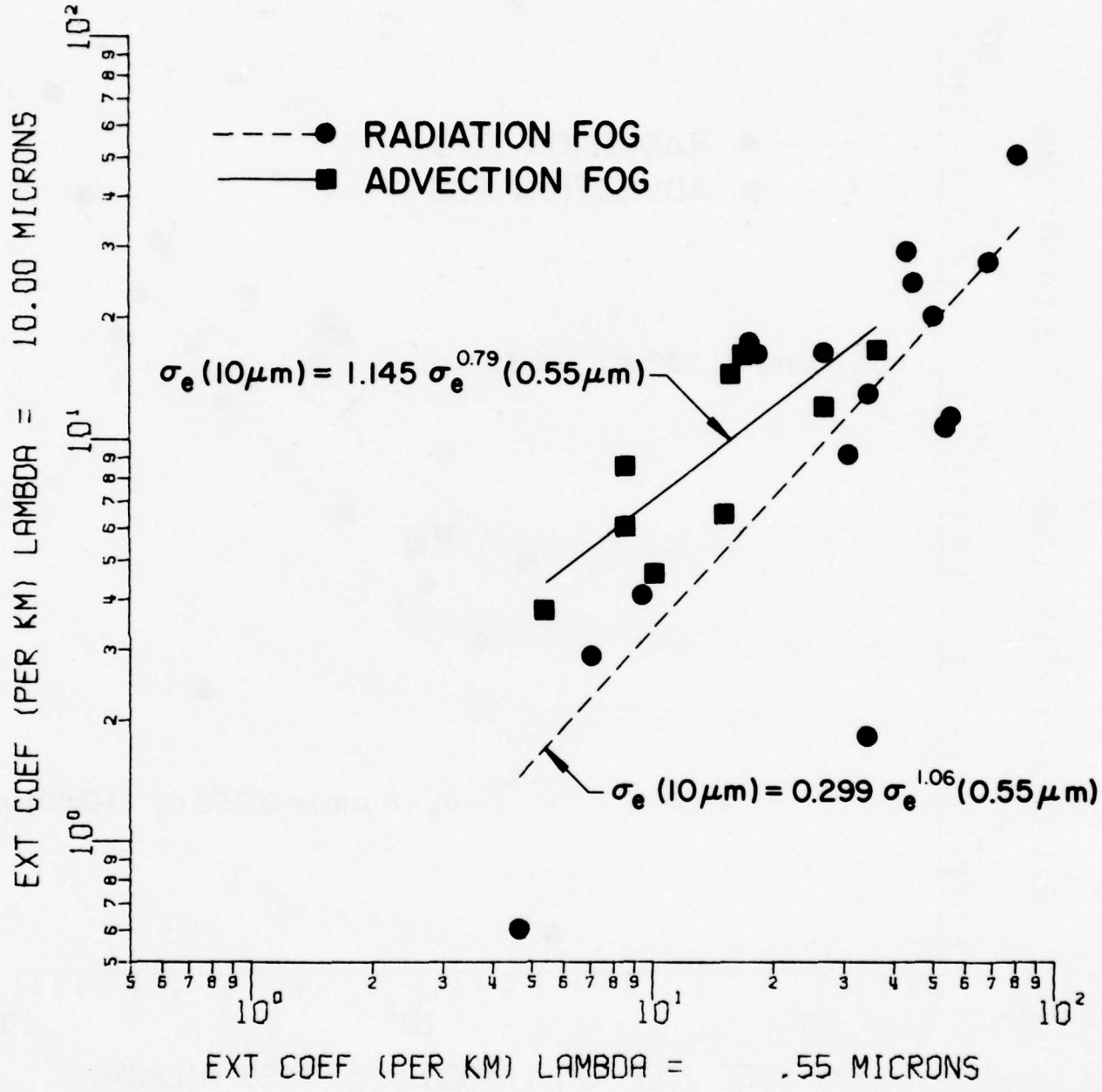

Figure A-23. Same as fig. A-18 except for the infrared wavelength λ = 10μm.

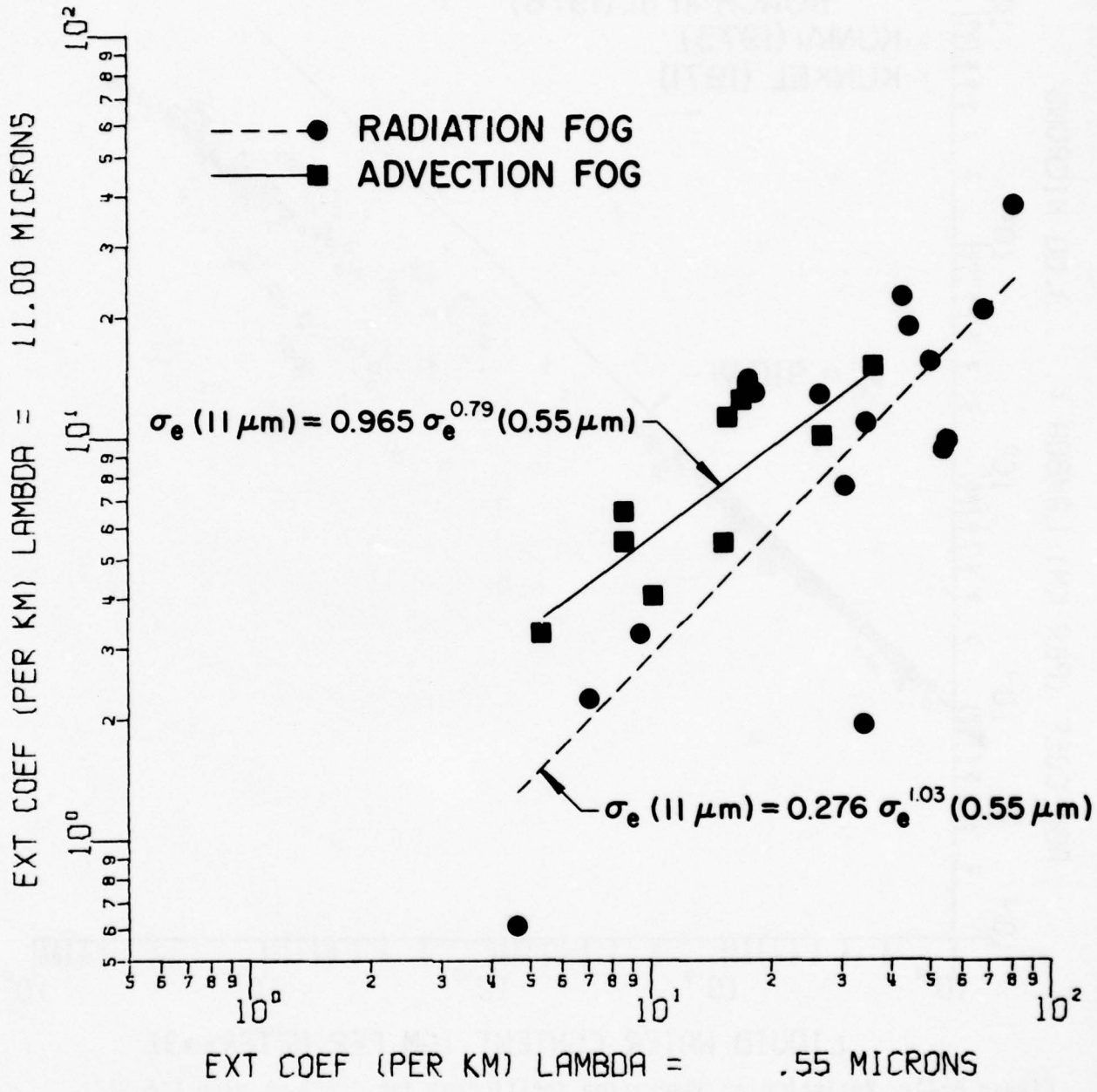

Figure A-24. Same as fig. A-18 except for the infrared wavelength λ = 11μm.

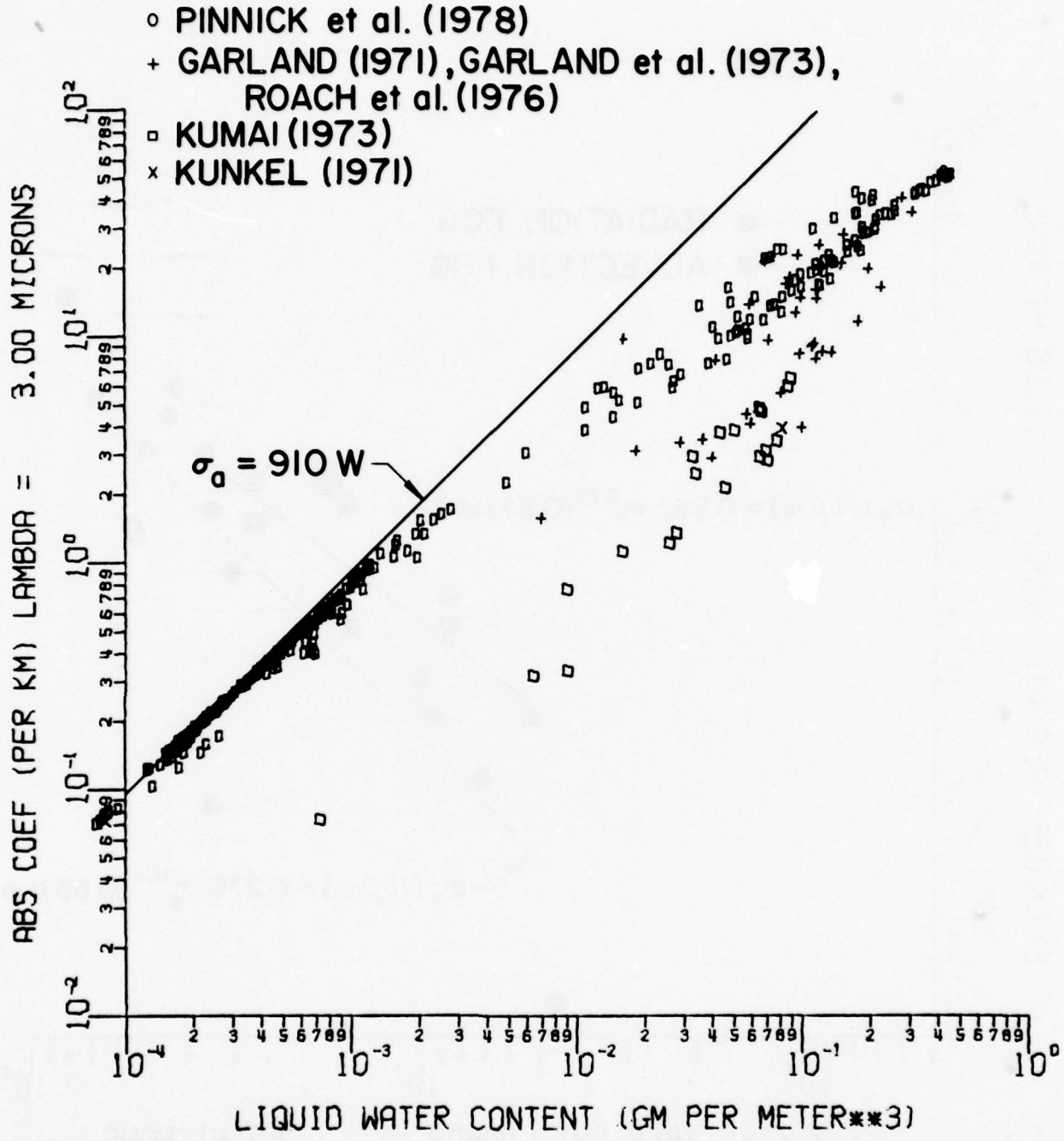

Figure A-25. Variation of absorption coefficient (at λ = 3μm) with liquid water content in atmospheric fog and haze for 341 size distribution measurements made at different geographic locales and under a variety of meteorological conditions. The spread of the points in the graph shows the absorption coefficient is a function of the size distribution as well as of the liquid water content. The predicted relation between absorption σ_a and liquid water content W according to eq. (7) is shown by the straight line, where σ_a is in km^{-1} and W is in g m^{-3}.

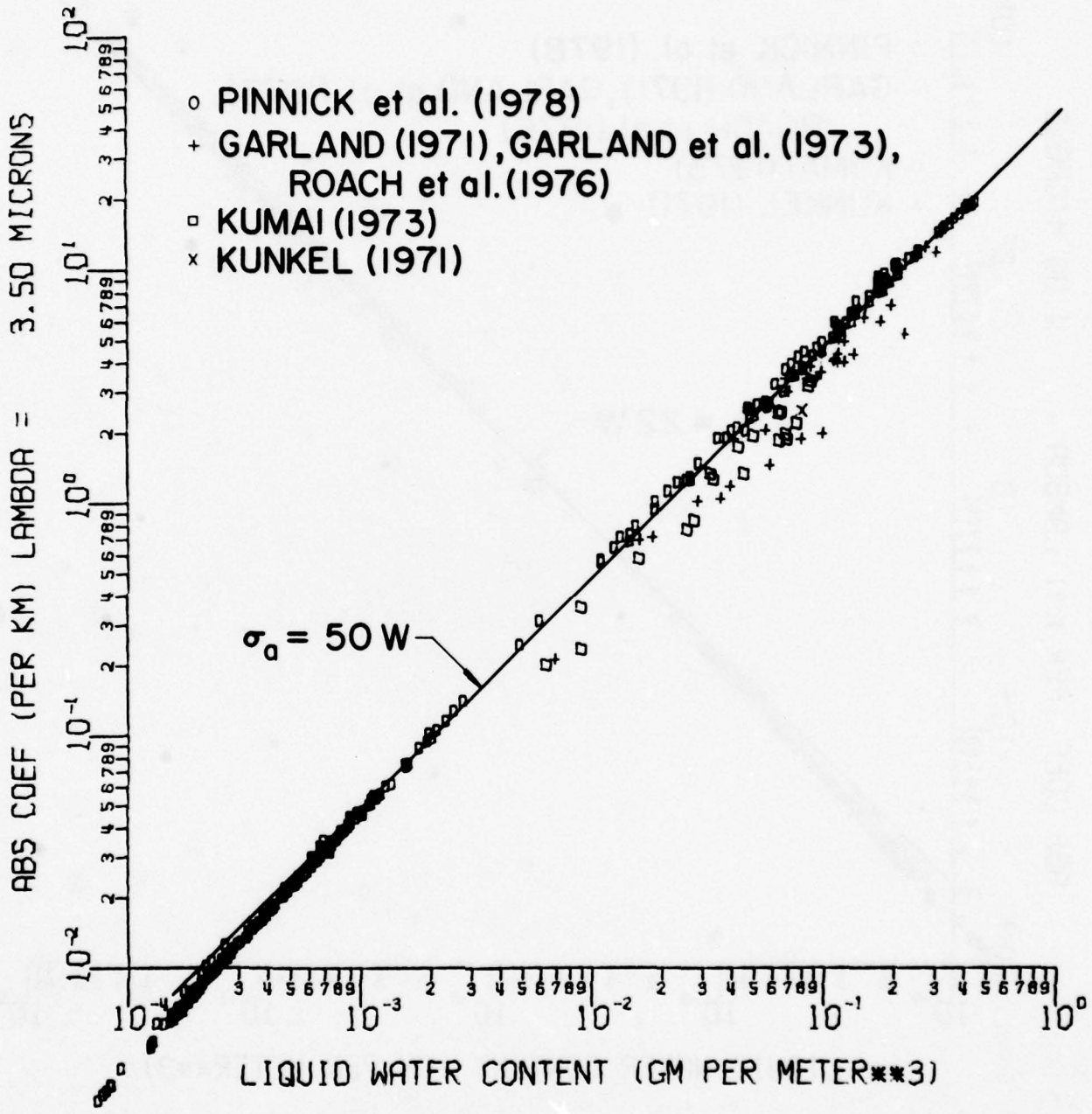

Figure A-26. Same as figure A-25 except for λ = 3.5μm.

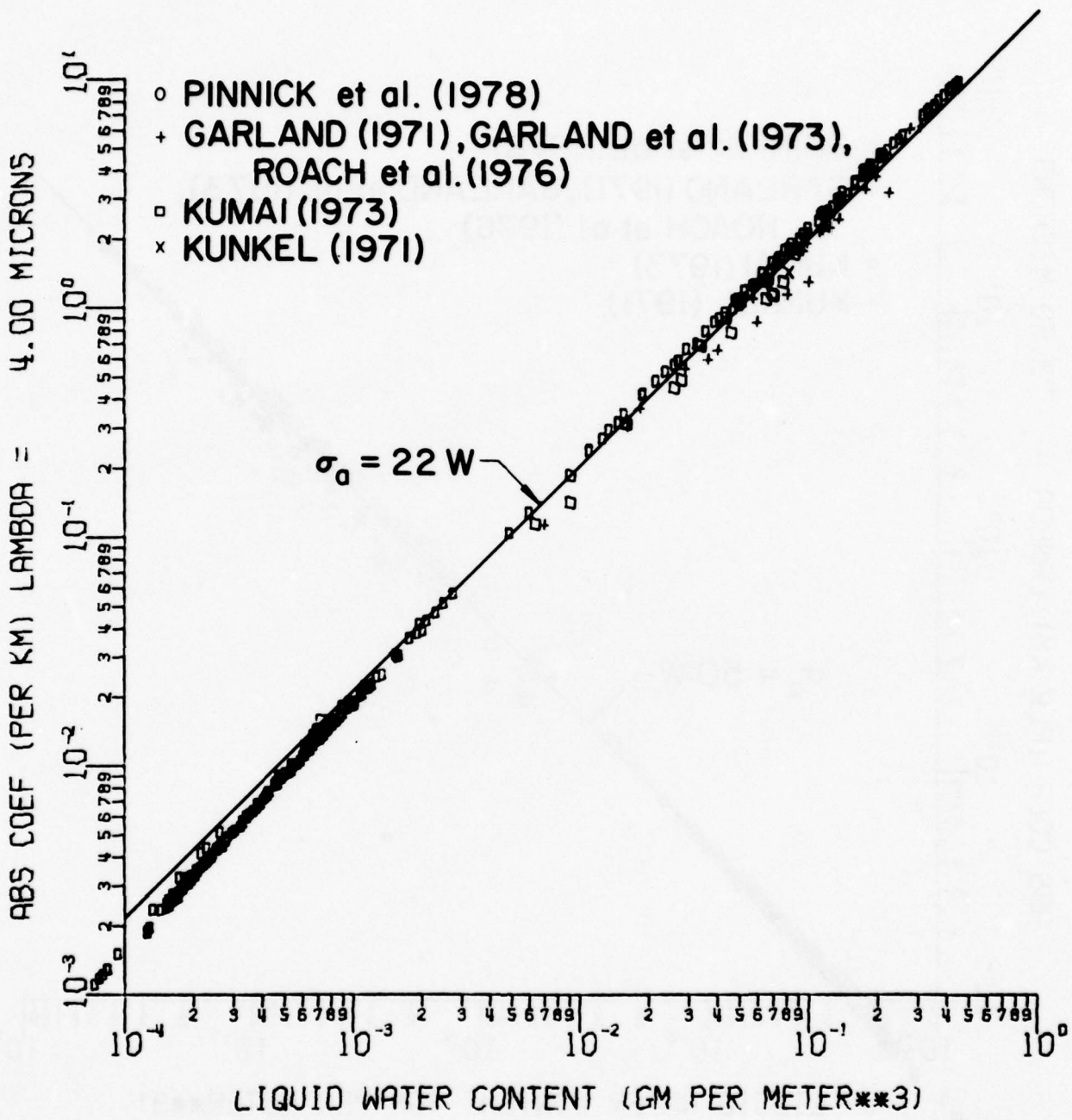

Figure A-27. Same as figure A-25 except for λ = 4μm.

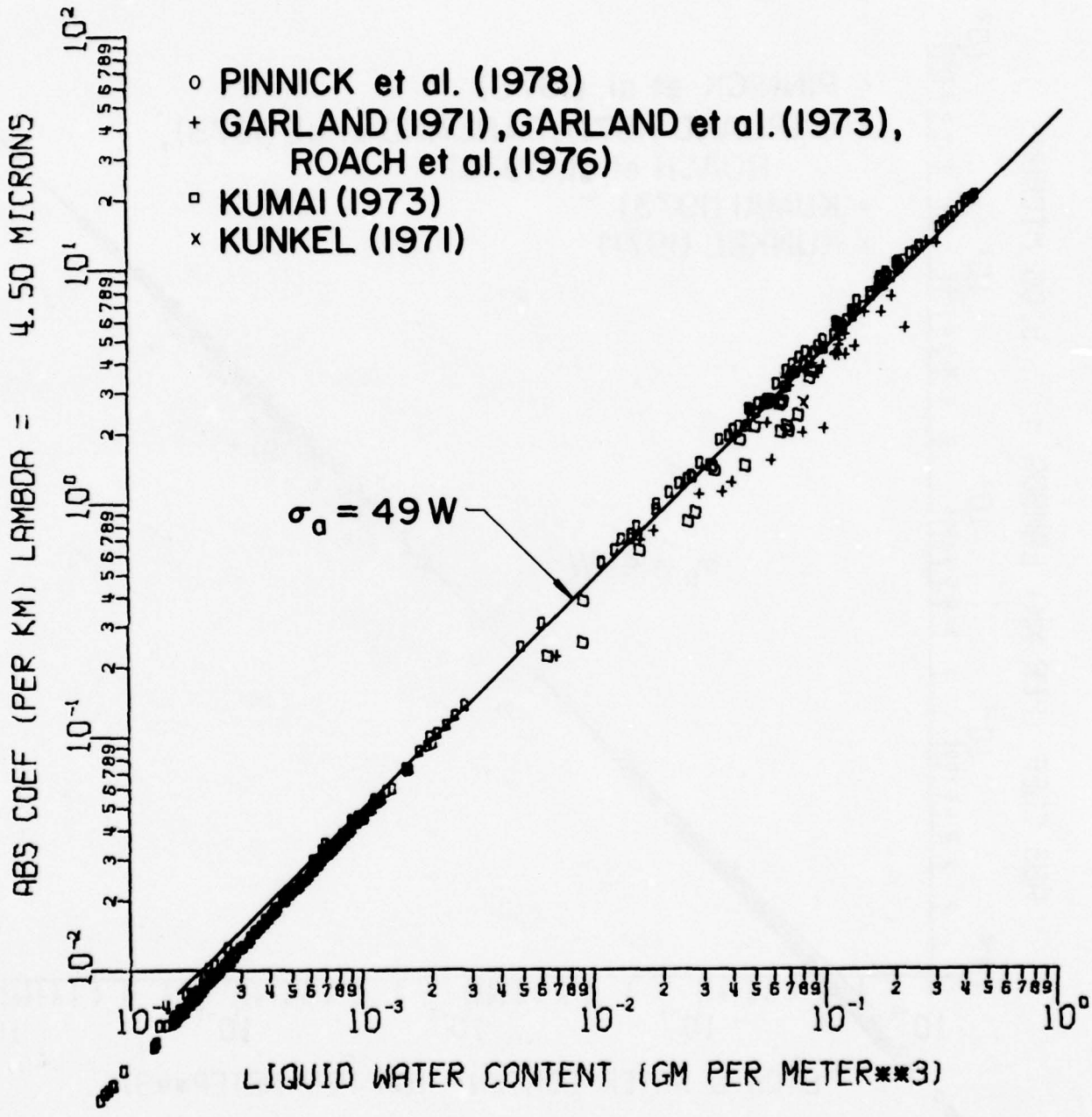

Figure A-28. Same as figure A-25 except for λ = 4.5μm.

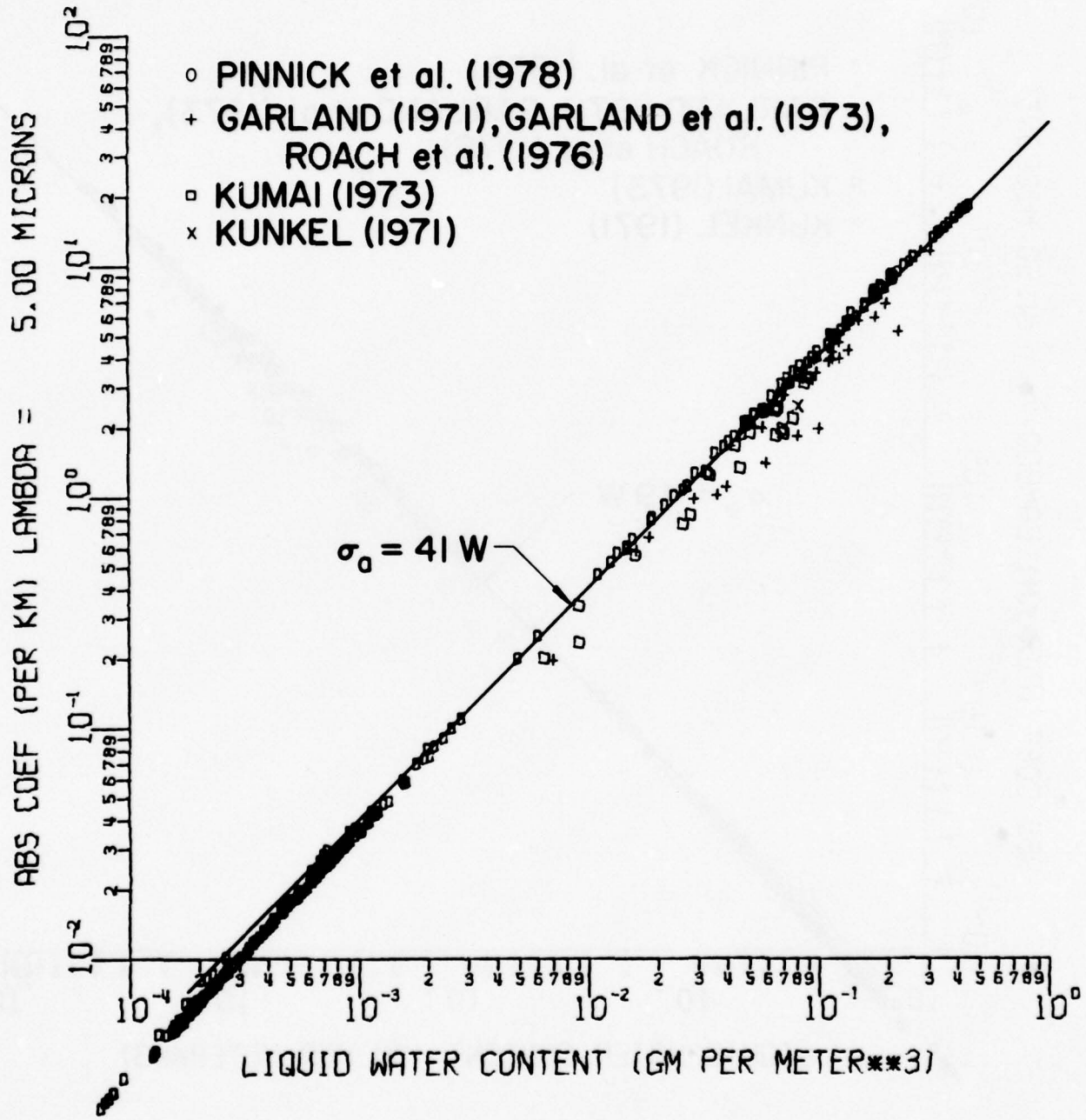

Figure A-29. Same as figure A-25 except for λ = 5μm.

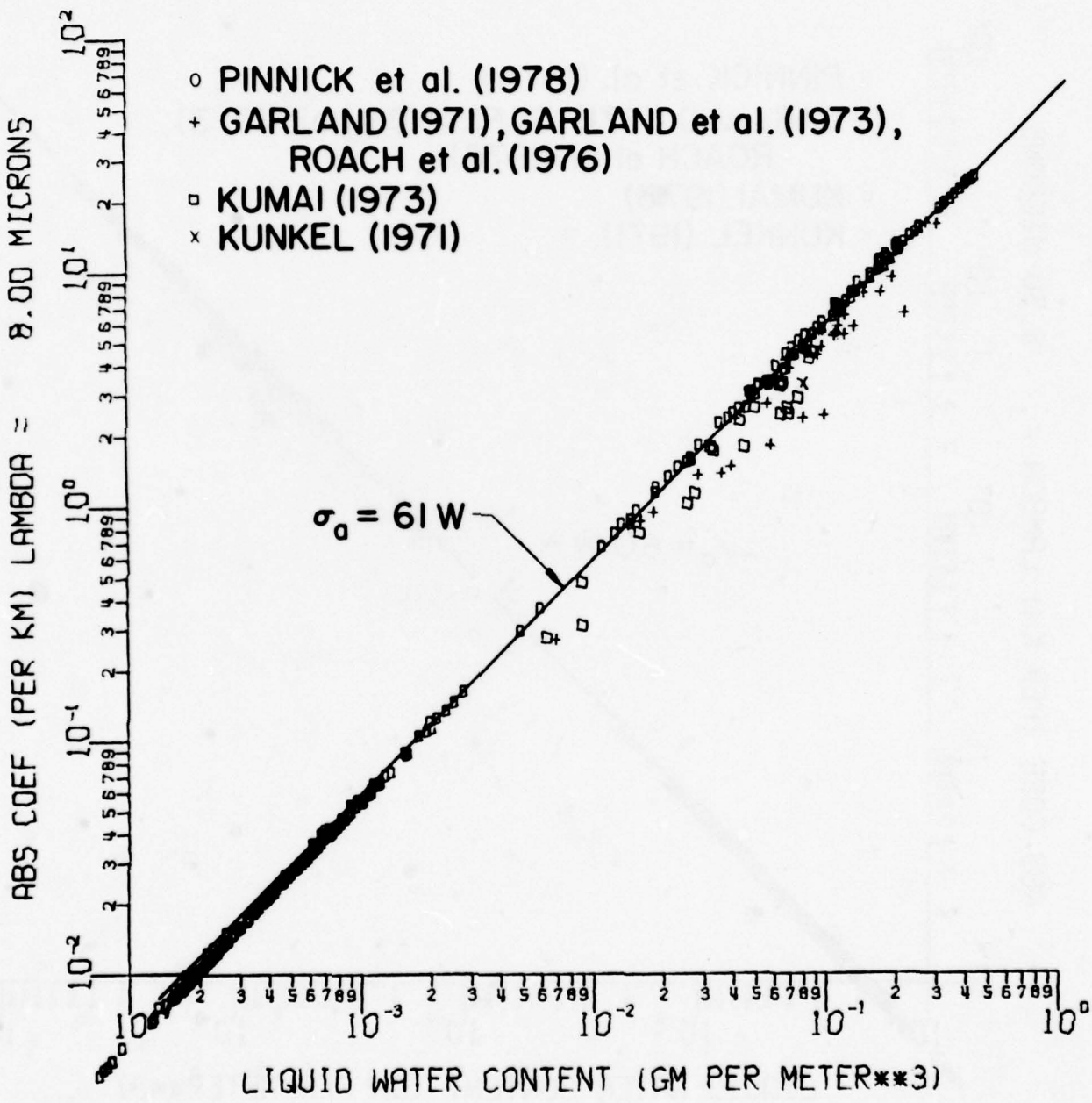

Figure A-30. Same as figure A-25 except for λ = 8μm.

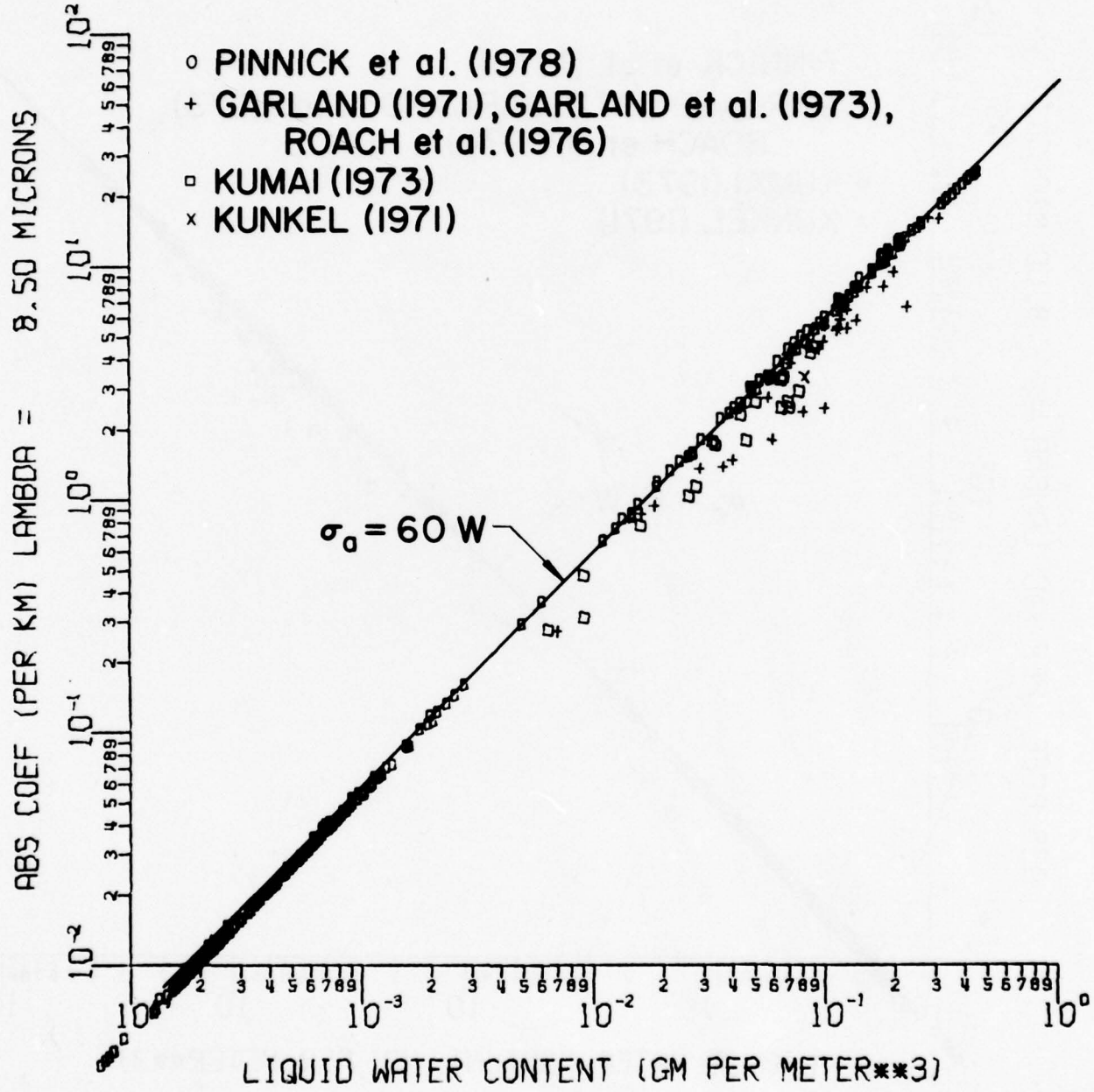

Figure A-31. Same as figure A-25 except for λ = 8.5μm.

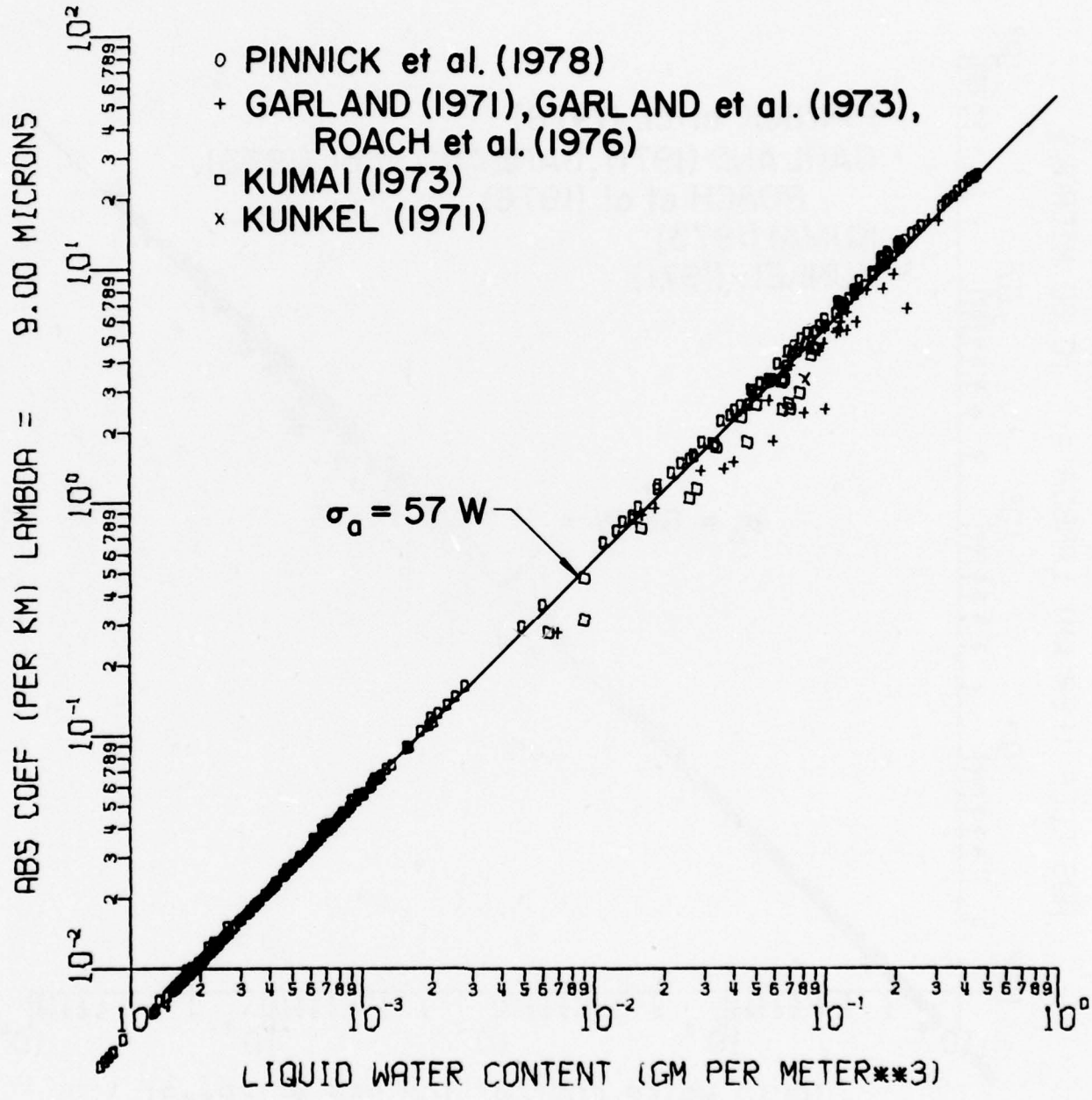

Figure A-32. Same as figure A-25 except for λ = 9μm.

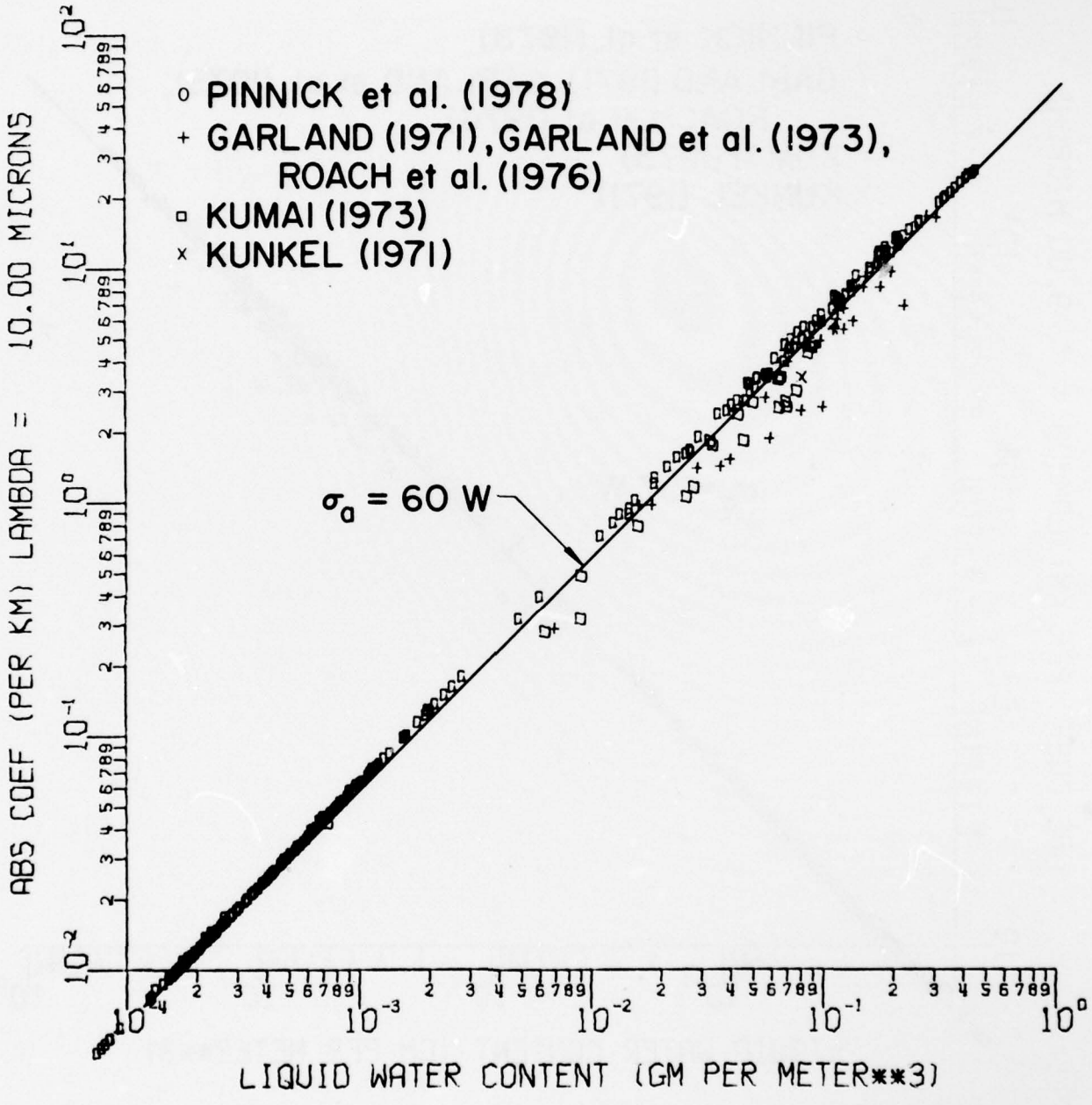

Figure A-33. Same as figure A-25 except for λ = 10μm.

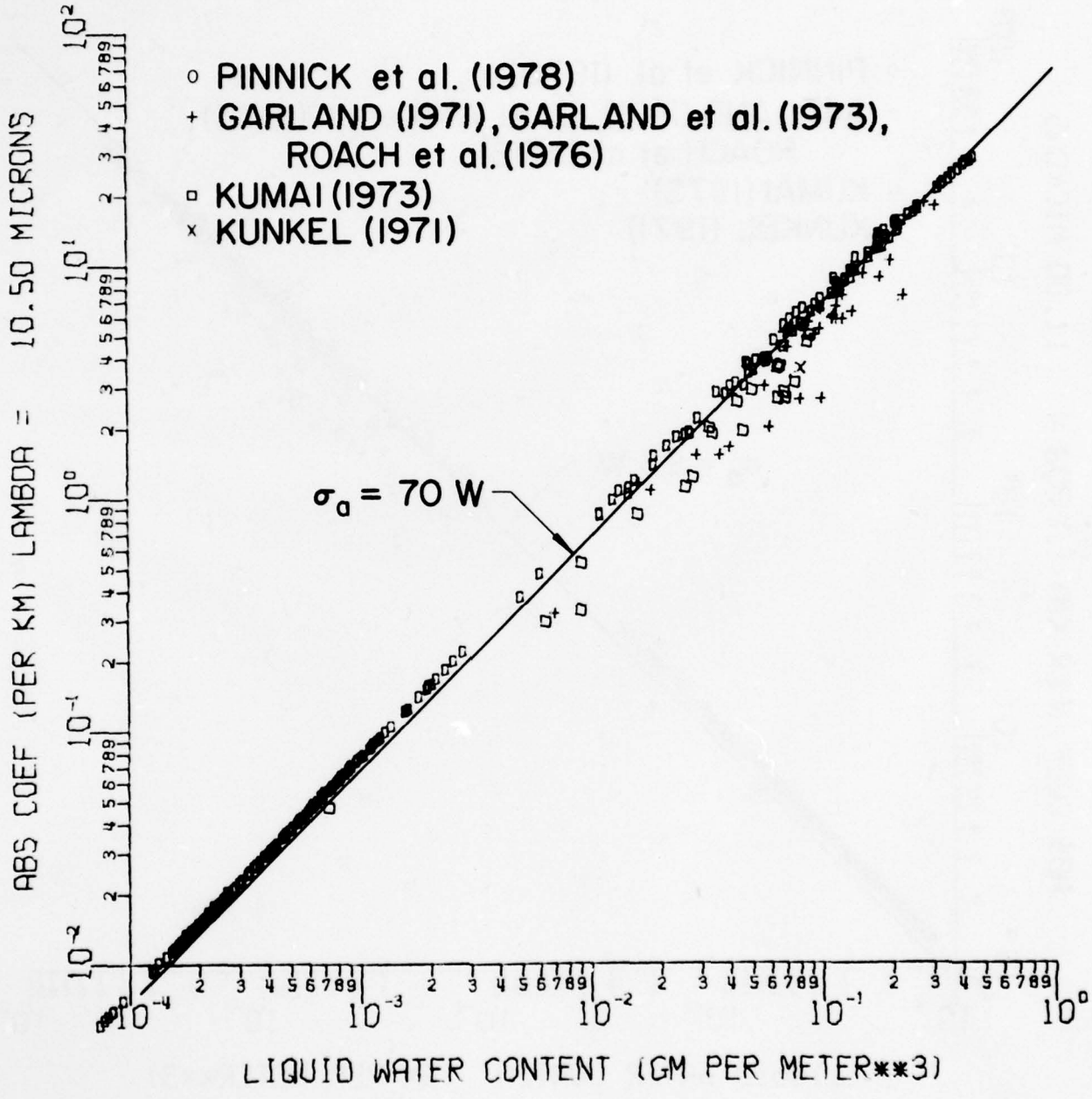

Figure A-34. Same as figure A-25 except for λ = 10.5μm.

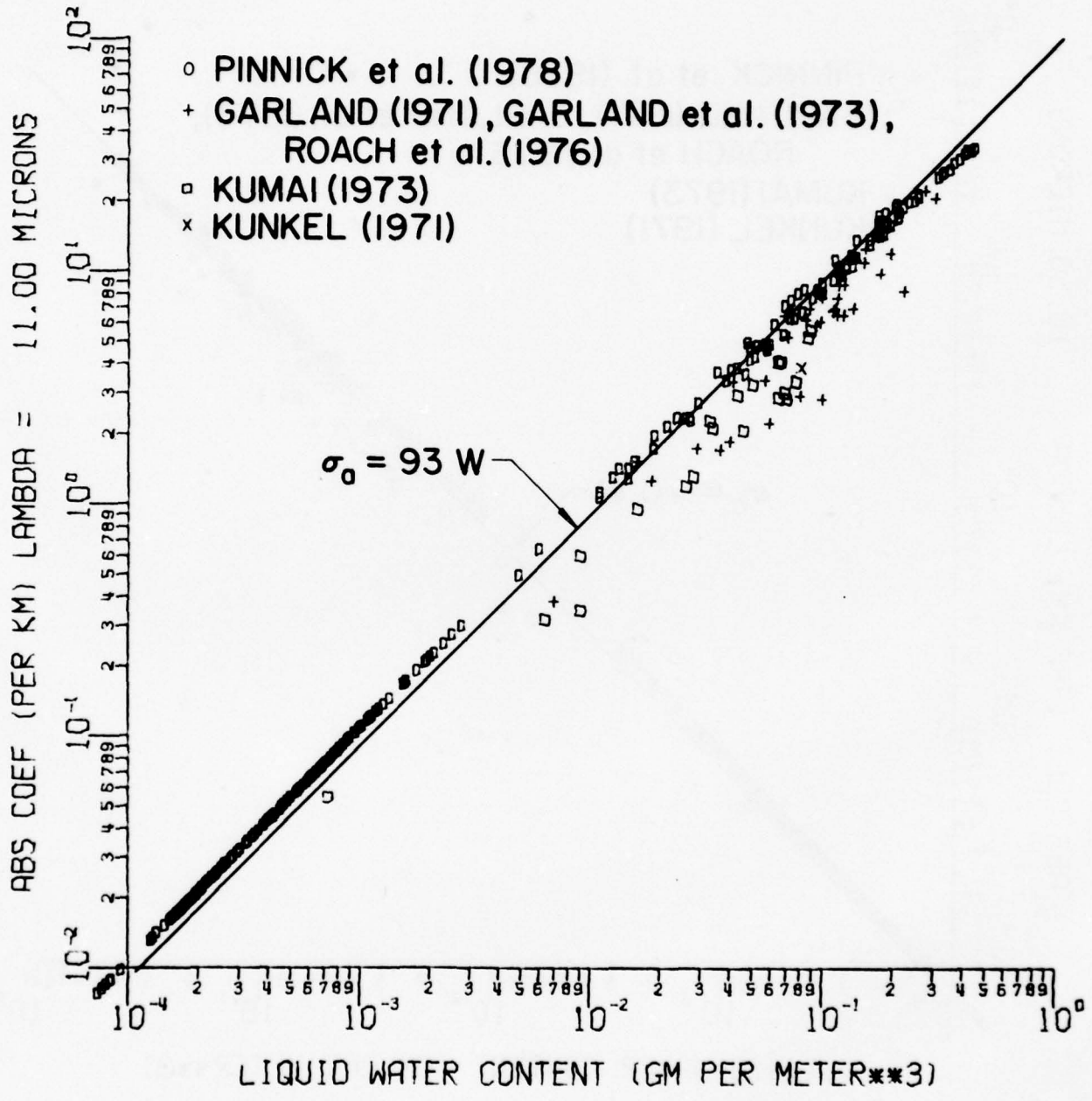

Figure A-35. Same as figure A-25 except for λ = 11μm.

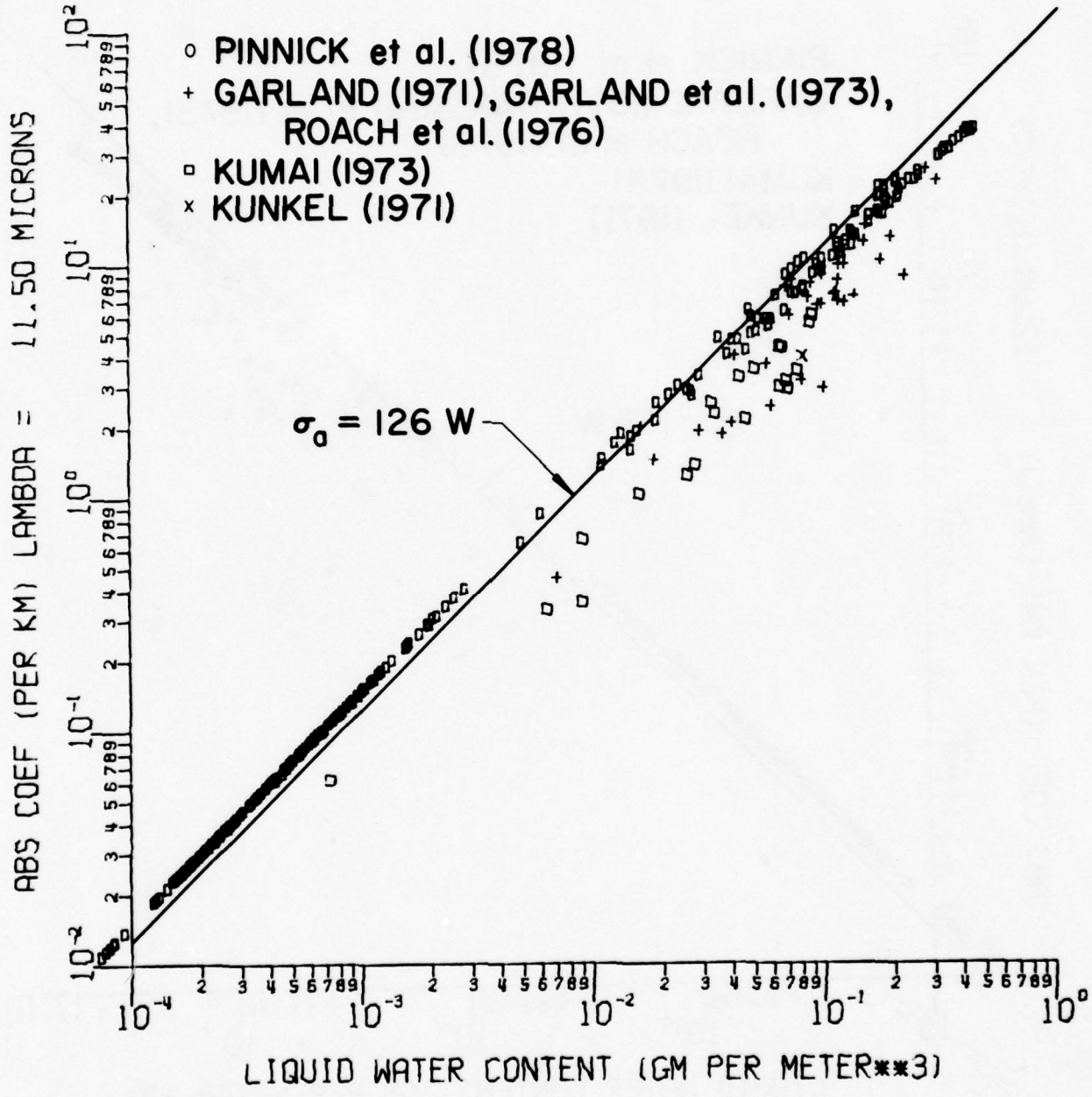

Figure A-36. Same as figure A-25 except for λ = 11.5μm.

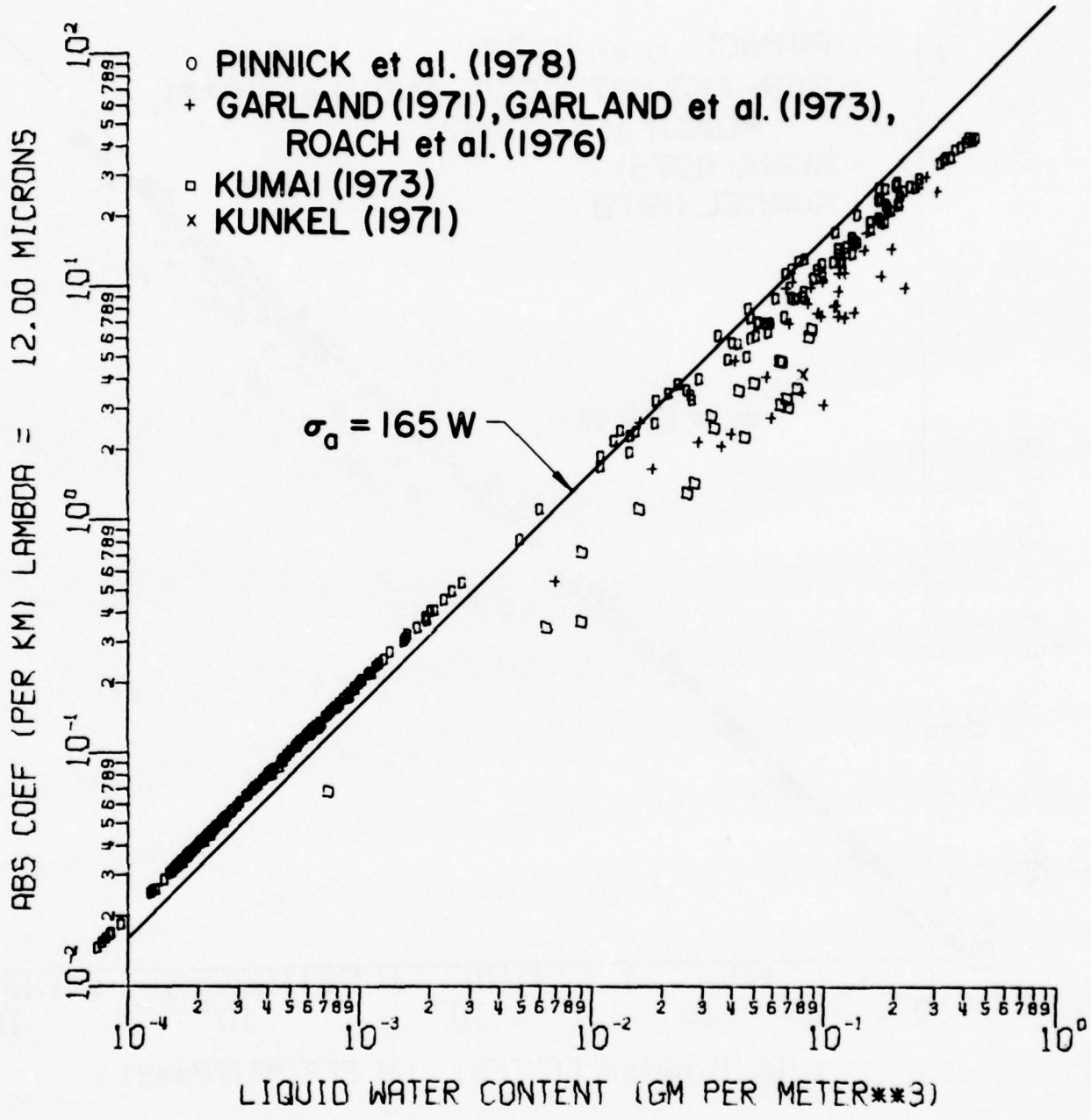

Figure A-37. Same as figure A-25 except for λ = 12μm.

ATMOSPHERIC SCIENCES RESEARCH PAPERS

1. Lindberg, J.D., "An Improvement to a Method for Measuring the Absorption Coefficient of Atmospheric Dust and other Strongly Absorbing Powders, " ECOM-5565, July 1975.
2. Avara, Elton, P., "Mesoscale Wind Shears Derived from Thermal Winds," ECOM-5566, July 1975.
3. Gomez, Richard B., and Joseph H. Pierluissi, "Incomplete Gamma Function Approximation for King's Strong-Line Transmittance Model," ECOM-5567, July 1975.
4. Blanco, A.J., and B.F. Engebos, "Ballistic Wind Weighting Functions for Tank Projectiles," ECOM-5568, August 1975.
5. Taylor, Fredrick J., Jack Smith, and Thomas H. Pries, "Crosswind Measurements through Pattern Recognition Techniques," ECOM-5569, July 1975.
6. Walters, D.L., "Crosswind Weighting Functions for Direct-Fire Projectiles," ECOM-5570, August 1975.
7. Duncan, Louis D., "An Improved Algorithm for the Iterated Minimal Information Solution for Remote Sounding of Temperature," ECOM-5571, August 1975.
8. Robbiani, Raymond L., "Tactical Field Demonstration of Mobile Weather Radar Set AN/TPS-41 at Fort Rucker, Alabama," ECOM-5572, August 1975.
9. Miers, B., G. Blackman, D. Langer, and N. Lorimier, "Analysis of SMS/GOES Film Data," ECOM-5573, September 1975.
10. Manquero, Carlos, Louis Duncan, and Rufus Bruce, "An Indication from Satellite Measurements of Atmospheric CO2 Variability," ECOM-5574, September 1975.
11. Petracca, Carmine, and James D. Lindberg, "Installation and Operation of an Atmospheric Particulate Collector," ECOM-5575, September 1975.
12. Avara, Elton P., and George Alexander, "Empirical Investigation of Three Iterative Methods for Inverting the Radiative Transfer Equation," ECOM-5576, October 1975.
13. Alexander, George D., "A Digital Data Acquisition Interface for the SMS Direct Readout Ground Station — Concept and Preliminary Design," ECOM-5577, October 1975.
14. Cantor, Israel, "Enhancement of Point Source Thermal Radiation Under Clouds in a Nonattenuating Medium," ECOM-5578, October 1975.
15. Norton, Colburn, and Glenn Hoidale, "The Diurnal Variation of Mixing Height by Month over White Sands Missile Range, N.M," ECOM-5579, November 1975.
16. Avara, Elton P., "On the Spectrum Analysis of Binary Data," ECOM-5580, November 1975.
17. Taylor, Fredrick J., Thomas H. Pries, and Chao-Huan Huang, "Optimal Wind Velocity Estimation," ECOM-5581, December 1975.
18. Avara, Elton P., "Some Effects of Autocorrelated and Cross-Correlated Noise on the Analysis of Variance, " ECOM-5582, December 1975.
19. Gillespie, Patti S., R.L. Armstrong, and Kenneth O. White, "The Spectral Characteristics and Atmospheric CO2 Absorption of the Ho^{+3}:YLF Laser at 2.05μm," ECOM-5583, December 1975.
20. Novlan, David J. "An Empirical Method of Forecasting Thunderstorms for the White Sands Missile Range," ECOM-5584, February 1976.
21. Avara, Elton P., "Randomization Effects in Hypothesis Testing with Autocorrelated Noise," ECOM-5585, February 1976.
22. Watkins, Wendell R., "Improvements in Long Path Absorption Cell Measurement," ECOM-5586, March 1976.
23. Thomas, Joe, George D. Alexander, and Marvin Dubbin, "SATTEL — An Army Dedicated Meteorological Telemetry System," ECOM-5587. March 1976.
24. Kennedy, Bruce W., and Delbert Bynum, "Army User Test Program for the RDT&E-XM-75 Meteorological Rocket," ECOM-5588, April 1976.

25. Barnett, Kenneth M., "A Description of the Artillery Meteorological Comparisons at White Sands Missle Range, October 1974 - December 1974 ('PASS' - Prototype Artillery [Meteorological] Subsystem)," ECOM-5589, April 1976.
26. Miller, Walter B., "Preliminary Analysis of Fall-of-Shot From Project 'PASS'," ECOM-5590, April 1976.
27. Avara, Elton P., "Error Analysis of Minimum Information and Smith's Direct Methods for Inverting the Radiative Transfer Equation," ECOM-5591, April 1976.
28. Yee, Young P., James D. Horn, and George Alexander, "Synoptic Thermal Wind Calculations from Radiosonde Observations Over the Southwestern United States," ECOM-5592, May 1976.
29. Duncan, Louis D., and Mary Ann Seagraves, "Applications of Empirical Corrections to NOAA-4 VTPR Observations," ECOM-5593, May 1976.
30. Miers, Bruce T., and Steve Weaver, "Applications of Meterological Satellite Data to Weather Sensitive Army Operations,"ECOM-5594, May 1976.
31. Sharenow, Moses, "Redesign and Improvement of Balloon ML-566," ECOM-5595, June, 1976.
32. Hansen, Frank V., "The Depth of the Surface Boundary Layer," ECOM-5596, June 1976.
33. Pinnick, R.G., and E.B. Stenmark, "Response Calculations for a Commercial Light-Scattering Aerosol Counter," ECOM-5597, July 1976.
34. Mason, J., and G.B. Hoidale, "Visibility as an Estimator of Infrared Transmittance," ECOM-5598, July 1976.
35. Bruce, Rufus E., Louis D. Duncan, and Joseph H. Pierluissi, "Experimental Study of the Relationship Between Radiosonde Temperatures and Radiometric-Area Temperatures," ECOM-5599, August 1976.
36. Duncan, Louis D., "Stratospheric Wind Shear Computed from Satellite Thermal Sounder Measurements," ECOM-5800, September 1976.
37. Taylor, F., P. Mohan, P. Joseph and T. Pries, "An All Digital Automated Wind Measurement System," ECOM-5801, September 1976.
38. Bruce, Charles, "Development of Spectrophones for CW and Pulsed Radiation Sources," ECOM-5802, September 1976.
39. Duncan, Louis D., and Mary Ann Seagraves,"Another Method for Estimating Clear Column Radiances," ECOM-5803, October 1976.
40. Blanco, Abel J., and Larry E. Taylor, "Artillery Meteorological Analysis of Project Pass," ECOM-5804, October 1976.
41. Miller, Walter, and Bernard Engebos," A Mathematical Structure for Refinement of Sound Ranging Estimates," ECOM-5805, November, 1976.
42. Gillespie, James B., and James D. Lindberg, "A Method to Obtain Diffuse Reflectance Measurements from 1.0 to 3.0 μm Using a Cary 17I Spectrophotometer," ECOM-5806, November 1976.
43. Rubio, Roberto, and Robert O. Olsen,"A Study of the Effects of Temperature Variations on Radio Wave Absorption,"ECOM-5807, November 1976.
44. Ballard, Harold N., "Temperature Measurements in the Stratosphere from Balloon-Borne Instrument Platforms, 1968-1975," ECOM-5808, December 1976.
45. Monahan, H.H., "An Approach to the Short-Range Prediction of Early Morning Radiation Fog," ECOM-5809, January 1977.
46. Engebos, Bernard Francis, "Introduction to Multiple State Multiple Action Decision Theory and Its Relation to Mixing Structures," ECOM-5810, January 1977.
47. Low, Richard D.H.,"Effects of Cloud Particles on Remote Sensing from Space in the 10-Micrometer Infrared Region," ECOM-5811, January 1977.
48. Bonner, Robert S., and R. Newton, "Application of the AN/GVS-5 Laser Rangefinder to Cloud Base Height Measurements," ECOM-5812, February 1977.
49. Rubio, Roberto, "Lidar Detection of Subvisible Reentry Vehicle Erosive Atmospheric Material," ECOM-5813, March 1977.
50. Low, Richard D.H., and J.D. Horn, "Mesoscale Determination of Cloud-Top Height: Problems and Solutions," ECOM-5814, March 1977.

51. Duncan, Louis D., and Mary Ann Seagraves, "Evaluation of the NOAA-4 VTPR Thermal Winds for Nuclear Fallout Predictions," ECOM-5815, March 1977.
52. Randhawa, Jagir S., M. Izquierdo, Carlos McDonald and Zvi Salpeter, "Stratospheric Ozone Density as Measured by a Chemiluminescent Sensor During the Stratcom VI-A Flight," ECOM-5816, April 1977.
53. Rubio, Roberto, and Mike Izquierdo, "Measurements of Net Atmospheric Irradiance in the 0.7- to 2.8-Micrometer Infrared Region," ECOM-5817, May 1977.
54. Ballard, Harold N., Jose M. Serna, and Frank P. Hudson Consultant for Chemical Kinetics, "Calculation of Selected Atmospheric Composition Parameters for the Mid-Latitude, September Stratosphere," ECOM-5818, May 1977.
55. Mitchell, J.D., R.S. Sagar, and R.O. Olsen, "Positive Ions in the Middle Atmosphere During Sunrise Conditions," ECOM-5819, May 1977.
56. White, Kenneth O., Wendell R. Watkins, Stuart A. Schleusener, and Ronald L. Johnson, "Solid-State Laser Wavelength Identification Using a Reference Absorber," ECOM-5820, June 1977.
57. Watkins, Wendell R., and Richard G. Dixon, "Automation of Long-Path Absorption Cell Measurements," ECOM-5821, June 1977.
58. Taylor, S.E., J.M. Davis, and J.B. Mason, "Analysis of Observed Soil Skin Moisture Effects on Reflectance," ECOM-5822, June 1977.
59. Duncan, Louis D. and Mary Ann Seagraves, "Fallout Predictions Computed from Satellite Derived Winds," ECOM-5823, June 1977.
60. Snider, D.E., D.G. Murcray, F.H. Murcray, and W.J. Williams, "Investigation of High-Altitude Enhanced Infrared Backround Emissions" (U), SECRET, ECOM-5824, June 1977.
61. Dubbin, Marvin H. and Dennis Hall, "Synchronous Meteorlogical Satellite Direct Readout Ground System Digital Video Electronics," ECOM-5825, June 1977.
62. Miller, W., and B. Engebos, "A Preliminary Analysis of Two Sound Ranging Algorithms," ECOM-5826, July 1977.
63. Kennedy, Bruce W., and James K. Luers, "Ballistic Sphere Techniques for Measuring Atomspheric Parameters," ECOM-5827, July 1977.
64. Duncan, Louis D., "Zenith Angle Variation of Satellite Thermal Sounder Measurements," ECOM-5828, August 1977.
65. Hansen, Frank V., "The Critical Richardson Number," ECOM-5829, September 1977.
66. Ballard, Harold N., and Frank P. Hudson (Compilers), "Stratospheric Composition Balloon-Borne Experiment," ECOM-5830, October 1977.
67. Barr, William C., and Arnold C. Peterson, "Wind Measuring Accuracy Test of Meteorological Systems," ECOM-5831, November 1977.
68. Ethridge, G.A. and F.V. Hansen, "Atmospheric Diffusion: Similarity Theory and Empirical Derivations for Use in Boundary Layer Diffusion Problems," ECOM-5832, November 1977.
69. Low, Richard D.H., "The Internal Cloud Radiation Field and a Technique for Determining Cloud Blackness," ECOM-5833, December 1977.
70. Watkins, Wendell R., Kenneth O. White, Charles W. Bruce, Donald L. Walters, and James D. Lindberg, "Measurements Required for Prediction of High Energy Laser Transmission," ECOM-5834, December 1977.
71. Rubio, Robert, "Investigation of Abrupt Decreases in Atmospherically Backscattered Laser Energy," ECOM-5835, December 1977.
72. Monahan, H.H. and R.M. Cionco, "An Interpretative Review of Existing Capabilities for Measuring and Forecasting Selected Weather Variables (Emphasizing Remote Means)," ASL-TR-0001, January 1978.
73. Heaps, Melvin G., "The 1979 Solar Eclipse and Validation of D-Region Models," ASL-TR-0002, March 1978.

74. Jennings, S.G., and J.B. Gillespie, "M.I.E. Theory Sensitivity Studies - The Effects of Aerosol Complex Refractive Index and Size Distribution Variations on Extinction and Absorption Coefficients Part II: Analysis of the Computational Results," ASL-TR-0003, March 1978.
75. White, Kenneth O. et al, "Water Vapor Continuum Absorption in the 3.5μm to 4.0μm Region," ASL-TR-0004, March 1978.
76. Olsen, Robert O., and Bruce W. Kennedy, "ABRES Pretest Atmospheric Measurements," ASL-TR-0005, April 1978.
77. Ballard, Harold N., Jose M. Serna, and Frank P. Hudson, "Calculation of Atmospheric Composition in the High Latitude September Stratosphere," ASL-TR-0006, May 1978.
78. Watkins, Wendell R. et al, "Water Vapor Absorption Coefficients at HF Laser Wavelengths," ASL-TR-0007, May 1978.
79. Hansen, Frank V., "The Growth and Prediction of Nocturnal Inversions," ASL-TR-0008, May 1978.
80. Samuel, Christine, Charles Bruce, and Ralph Brewer, "Spectrophone Analysis of Gas Samples Obtained at Field Site," ASL-TR-0009, June 1978.
81. Pinnick, R.G. et al., "Vertical Structure in Atmospheric Fog and Haze and its Effects on IR Extinction," ASL-TR-0010, July 1978.
82. Low, Richard D.H., Louis D. Duncan, and Richard B. Gomez, "The Microphysical Basis of Fog Optical Characterization," ASL-TR-0011, August 1978.
83. Heaps, Melvin G., "The Effect of a Solar Proton Event on the Minor Neutral Constituents of the Summer Polar Mesosphere," ASL-TR-0012, August 1978.
84. Mason, James B., "Light Attenuation in Falling Snow," ASL-TR-0013, August 1978.
85. Blanco, Abel J., "Long-Range Artillery Sound Ranging: "PASS" Meteorological Application," ASL-TR-0014, September 1978.
86. Heaps, M.G., and F.E. Niles, "Modeling the Ion Chemistry of the D-Region: A case Study Based Upon the 1966 Total Solar Eclipse," ASL-TR-0015, September 1978.
87. Jennings, S.G., and R.G. Pinnick, "Effects of Particulate Complex Refractive Index and Particle Size Distribution Variations on Atmospheric Extinction and Absorption for Visible Through Middle-Infrared Wavelengths," ASL-TR-0016, September 1978.
88. Watkins, Wendell R., Kenneth O. White, Lanny R. Bower, and Brian Z. Sojka, " Pressure Dependence of the Water Vapor Continuum Absorption in the 3.5- to 4.0-Micrometer Region," ASL-TR-0017, September 1978.
89. Miller, W.B., and B.F. Engebos, "Behavior of Four Sound Ranging Techniques in an Idealized Physical Enviroment," ASL-TR-0018, September 1978.
90. Gomez, Richard G., "Effectiveness Studies of the CBU-88/B Bomb, Cluster, Smoke Weapon" (U), CONFIDENTIAL ASL-TR-0019, September 1978.
91. Miller, August, Richard C. Shirkey, and Mary Ann Seagraves, "Calculation of Thermal Emission from Aerosols Using the Doubling Technique," ASL-TR-0020, November, 1978.
92. Lindberg, James D. et al., "Measured Effects of Battlefield Dust and Smoke on Visible, Infrared, and Millimeter Wavelengths Propagation: A Preliminary Report on Dusty Infrared Test-I (DIRT-I)," ASL-TR-0021, January 1979.
93. Kennedy, Bruce W., Arthur Kinghorn, and B.R. Hixon, "Engineering Flight Tests of Range Meteorological Sounding System Radiosonde," ASL-TR-0022, February 1979.
94. Rubio, Roberto, and Don Hoock, "Microwave Effective Earth Radius Factor Variability at Wiesbaden and Balboa," ASL-TR-0023, February 1979.
95. Low, Richard D.H., "A Theoretical Investigation of Cloud/Fog Optical Properties and Their Spectral Correlations," ASL-TR-0024, February 1979.

96. Pinnick, R.G., and H.J. Auvermann, "Response Characteristics of Knollenberg Light-Scattering Aerosol Counters," ASL-TR-0025, February 1979.
97. Heaps, Melvin G., Robert O. Olsen, and Warren W. Berning, "Solar Eclipse 1979, Atmospheric Sciences Laboratory Program Overview," ASL-TR-0026 February 1979.
98. Blanco, Abel J., "Long-Range Artillery Sound Ranging: 'PASS' GR-8 Sound Ranging Data," ASL-TR-0027, March 1979.
99. Kennedy, Bruce W., and Jose M. Serna, "Meteorological Rocket Network System Reliability," ASL-TR-0028, March 1979.
100. Swingle, Donald M., "Effects of Arrival Time Errors in Weighted Range Equation Solutions for Linear Base Sound Ranging," ASL-TR-0029, April 1979.
101. Umstead, Robert K., Ricardo Pena, and Frank V. Hansen, "KWIK: An Algorithm for Calculating Munition Expenditures for Smoke Screening/Obscuration in Tactical Situations," ASL-TR-0030, April 1979.
102. D'Arcy, Edward M., "Accuracy Validation of the Modified Nike Hercules Radar," ASL-TR-0031, May 1979.
103. Rodriguez, Ruben, "Evaluation of the Passive Remote Crosswind Sensor," ASL-TR-0032, May 1979.
104. Barber, T.L., and R. Rodriguez, "Transit Time Lidar Measurement of Near-Surface Winds in the Atmosphere," ASL-TR-0033, May 1979.
105. Low, Richard D.H., Louis D. Duncan, and Y.Y. Roger R. Hsiao, "Microphysical and Optical Properties of California Coastal Fogs at Fort Ord," ASL-TR-0034, June 1979.
106. Rodriguez, Ruben, and William J. Vechione, "Evaluation of the Saturation Resistant Crosswind Sensor," ASL-TR-0035, July 1979
107. Ohmstede, William D., "The Dynamics of Material Layers," ASL-TR-0036, July 1979.
108. Pinnick, R.G., S.G. Jennings, Petr Chýlek, and H.J. Auvermann "Relationships between IR Extinction, Absorption, and Liquid Water Content of Fogs," ASL-TR-0037, August 1979

ELECTRO-OPTICS DIVISION DISTRIBUTION LIST

Commander
US Army Aviation Center
ATTN: ATZQ-D-MA
Fort Rucker, AL 36362

Commander
US Army Aviation School
Fort Rucker, AL 36362

Ballistic Missile Defense Advanced
Technology Center
ATTN: ATC-R
PO Box 1500
Huntsville, AL 35807

Lockheed-Huntsville Msl & Space Co.
ATTN: Dr. Lary W. Pinkley
PO Box 1103
West Station
Huntsville, AL 35807

Chief, Atmospheric Sciences Div
Code ES-81, NASA
Marshall Space Flight Center,
AL 35812

Project Manager
Patriot Missile Systems
ATTN: DRCPM-MD-T
Redstone Arsenal, AL 35809

Commander
US Army Missile R&D Command
ATTN: DRDMI-CGA (B. W. Fowler)
Redstone Arsenal, AL 35809

Redstone Scientific Information Center
ATTN: DRDMI-TBD
US Army Missile R&D Command
Redstone Arsenal, AL 35809

Commander
US Army Missile R&D Command
ATTN: DRDMI-TEM (R. Haraway)
Redstone Arsenal, AL 35809

Commander
US Army Missile R&D Command
ATTN: DRDMI-TRA (Dr. Essenwanger)
Redstone Arsenal, AL 35809

Commander
US Army Missiles and Munitions
Center & School
ATTN: ATSIC-CD
Redstone Arsenal, AL 35809

Commander
US Army Missile R&D Command
ATTN: DRDMI-REO (Dr. Maxwell Harper)
Redstone Arsenal, AL 35809

Commander
US Army Missile R&D Command
ATTN: DRDMI-RRE (Dr. Julius Lilly)
Redstone Arsenal, AL 35809

Commander
US Army Missile R&D Command
ATTN: DRDMI-TEO (Dr. Gene Widenhofer)
Redstone Arsenal, AL 35809

Commander
US Army Missile R&D Command
ATTN: DRDMI-HRO (Dr. D.B. Guenter)
Redstone Arsenal, AL 35809

Commander
US Army Missile R&D Command
ATTN: DRDMI-TDO (Dr. Hugh Anderson)
Redstone Arsenal, AL 35809

Commander
US Army Missile R&D Command
ATTN: DRDMI-YLA (Mr. W.S. Rich)
Redstone Arsenal, AL 35809

Commander
US Army Missile R&D Command
ATTN: DRDMI-TEG (Dr. George Emmons)
Redstone Arsenal, AL 35809

Commander
HQ, Fort Huachuca
ATTN: Tech Ref Div
Fort Huachuca, AZ 85613

Commander
US Army Intelligence Center & School
ATTN: ATSI-CD
Fort Huachuca, AZ 85613

Commander
US Army Intelligence Center & School
ATTN: ATSI-CD-CS (Mr. Jim Rustenbeck)
Fort Huachuca, AZ 85613

Commander
US Army Intelligence Center & School
ATTN: ATSI-CD-MD
Fort Huachuca, AZ 85613

Commander
US Army Communications Command
Fort Huachuca, AZ 85613

Commander
US Army Yuma Proving Ground
ATTN: Technical Library
Bldg 2100
Yuma, AZ 85364

Northrop Corporation
Electro-Mechanical Division
ATTN: Dr. R. D. Tooley
500 East Orangethorpe Ave
Anaheim, CA 92801

Naval Weapons Center
ATTN: Code 3173 (Dr. A. Shlanta)
China Lake, CA 93555

Hughes Helicopters
ATTN: Charles R. Hill
Centinela and Teale Streets
Culter City, CA 90230

Commander
US Army Combat Dev Evaluation Command
ATTN: ATEC-PL-M (Gary Love)
Fort Ord, CA 93941

SRI International
ATTN: Dr. Ed Uthe
333 Ravenswood Avenue
Menlo Park, CA 94025

SRI International
ATTN: J. E. Van der Laan
333 Ravenswood Avenue
Menlo Park, CA 94025

Sylvania Elec Sys Western Div
ATTN: Technical Reports Library
PO Box 205
Mountain View, CA 94040

Geophysics Officer
PMTC Code 3250
Pacific Missile Test Center
Point Mugu, CA 93042

Commander
Naval Ocean Systems Center
ATTN: Code 4473 (Tech Library)
San Diego, CA 92152

Commander
Naval Ocean Systems Center
ATTN: Code 532 (Dr. Juergen Richter)
San Diego, CA 92152

General Electric -TEMPO
ATTN: Dr. James Thompson
816 State Street
PO Drawer QQ
Santa Barbara, CA 93102

The RAND Corporation
ATTN: Ralph Huschke
1700 Main Street
Santa Monica, CA 90406

National Center for Atmos Research
NCAR Library
PO Box 3000
Boulder, CO 80307

Library-R-51-Tech Reports
NOAA/ERL
320 S. Broadway
Boulder, CO 80302

Wave Propagation Laboratory
NOAA/ERL
ATTN: Dr. Vernon Derr
Boulder, CO 80302

Particle Measuring Systems, Inc.
ATTN: Dr. Robert Knollenberg
1855 South 57th Court
Boulder, CO 80301

US Department of Commerce
Institute for Telecommunication Sciences
ATTN: Dr. H. J. Liebe
Boulder, CO 80303

HQDA (SAUS-OR/Hunter Woodall)
Rm 2E614, Pentagon
Washington, DC 20301

Dr. Herbert Fallin
ODUSA-OR
Rm 2E621, Pentagon
Washington, DC 20301

COL Elbert Friday
OUSDR&E
Rm 3D129, Pentagon
Washington, DC 20301

Defense Communications Agency
Technical Library Center
Code 205
Washington, DC 20305

Director
Defense Nuclear Agency
ATTN: Technical Library
Washington, DC 20305

Director
Defense Nuclear Agency
ATTN: RAAE (MAJ Ed Mueller)
Washington, DC 20305

Director
Defense Nuclear Agency
ATTN: SPAS (Mr. A.T. Hopkins)
Washington, DC 20305

Defense Intelligence Agency
ATTN: Scientific Advisory Committee
Washington, DC 20310

HQDA (DAMA-ARZ-D/Dr. Verderame)
Washington, DC 20310

HQDA (DAMI-ISP/Mr. Beck)
Washington, DC 20310

Department of the Army
Deputy Chief of Staff for
Operations and Plans
ATTN: DAMO-RQ
Washington, DC 20310

Department of the Army
Director of Telcommunications and
Command and Control
ATTN: DAMO-TCZ
Washington, DC 20310

Department of the Army
Deputy Chief of Staff for Research,
Development and Acquisition
ATTN: DAMA-AR
Washington, DC 20310

Department of the Army
Assistant Chief of Staff for Intelligence
ATTN: DAMI-TS
Washington, DC 20310

HQDA (DAEN-RDM/Dr. de Percin)
Forrestal Building
Washington, DC 20314

Director
Naval Research Laboratory
ATTN: Code 5530
Washington, DC 20375

Director
Naval Research Laboratory
ATTN: Code 2627
Washington, DC 20375

Director
Naval Research Laboratory
ATTN: Code 1409
(Dr. J. M. MacCallum)
Washington, DC 20375

Director
Naval Research Laboratory
ATTN: Code 5567
(Dr. James A. Dowling)
Washington, DC 20375

Director
Naval Research Laboratory
ATTN: Code 5567
(Dr. Steve Hanley)
Washington, DC 20375

Director
Naval Research Laboratory
ATTN: Code 8320
(Dr. L.H. Ruhnke)
Washington, DC 20375

The Library of Congress
ATTN: Exchange & Gift Div
Washington, DC 20540
2

Head, Atmos Rsch Section
Div Atmospheric Science
National Science Foundation
1800 G. Street, NW
Washington, DC 20550

ADTC/DLODL
Eglin AFB, FL 32542

Naval Training Equipment Center
ATTN: Technical Library
Orlando, FL 32813

Georgia Institute of Technology
ATTN: Dr. James Wiltse
Atlanta, GA 30332

Georgia Institute of Technology
ATTN: Dr. Robert McMillan
Atlanta, GA 30332

Georgia Institute of Technology
ATTN: Mr. James Gallagher
Atlanta, GA 30332

Commander
US Army Infantry Center
Fort Benning, GA 31805

Commander
US Army Infantry Center
ATTN: AT2B-CD
Fort Benning, GA 31805

US Army Signal School
ATTN: ATSN-CD
Fort Gordon, GA 30905

USAFETAC
Scott AFB, IL 62225

Commander
Air Weather Service
ATTN; DNPP (LTC Donald Hodges)
Scott AFB, IL 62269

Commander
US Army Combined Arms Center
ATTN: ATCA-CAA-Q (Kent Pickett)
Fort Leavenworth, KS 66027

Commander
US Army Combined Arms Center
ATTN: ATCA-CS
Fort Leavenworth, KS 66027

Commander
US Army Combined Arms Center
ATTN: ATCA-CCC
Fort Leavenworth, KS 66027

Commander
US Army Combined Arms Center
ATTN: ATCA-CDC
Fort Leavenworth, KS 66027

Commander
US Army Combined Arms Center
ATTN: ATCA-CDE
Fort Leavenworth, KS 66027

Commander
US Army Combined Arms Center
ATTN: ATCA-CCM
Fort Leavenworth, KS 66027

Commander
US Army Armor Center
ATTN: ATZK-AE-TA
(Dr. Charles Leake)
Fort Knox, KY 40121

Commander
US Army Armor Center
ATTN: ATZK-CD
Fort Knox, KY 40121

Aerodyne Research Inc.
ATTN: Dr. John Ebersole
Bedford Research Park
Crosby Drive
Bedford, MA 01730

Commander
Air Force Geophysical Laboratory
ATTN: OPI (Dr. R.A. McClatchey)
Hanscom AFB, MA 01731

Commander
Air Force Geophysical Laboratory
ATTN: OPI (Dr. R. Fenn)
Hanscom AFB, MA 01731

Commander
US Army Ordnance Center and School
ATTN: ATSL-CD
Aberdeen Proving Ground, MD 21005

Commander
US Army Ordnance & Chemical Center
and School
ATTN: ATSL-CLC (Dr. Thomas Welch)
Aberdeen Proving Ground, MD 21005

Commander
US Army Ballistic Rsch Laboratory
ATTN: Dr. Robert Eichelberge
Aberdeen Proving Ground, MD 21005

Commander
US Army Ballistic Rsch Laboratory
ATTN: Mr. Alan Downs
Aberdeen Proving Ground, MD 21005

Commander
US Army Ballistic Rsch Laboratory
ATTN: DRDAR-BLB (Mr. Arthur LaGrange)
Aberdeen Proving Ground, MD 21005

Commander
US Army Ballistic Research Laboratory
ATTN: Mr. Richard McGee
Aberdeen Proving Ground, MD 21005

Project Manager
Smoke/Obscurants
ATTN: DRDPM-SMC (COL H. Shelton)
Aberdeen Proving Ground, MD 21005

Project Manager
Smoke/Obscurants
ATTN: DRDPM-SMC (Dr. T. Van de Wal Jr.)
Aberdeen Proving Ground, MD 21005

Project Manager
Smoke/Obscurants
ATTN: DRDPM-SMC (Mr. G. Bowman)
Aberdeen Proving Ground, MD 21005

Project Manager
Smoke/Obscurants
ATTN: DRDPM-SMC (Mr. J. Steedman)
Aberdeen Proving Ground, MD 21005

Commander
US Army Test & Evaluation Command
ATTN: DRSTE-AD-M (Mr. Warren M. Baily)
Aberdeen Proving Ground, MD 21005

Director
US Army Material Systems Analysis Activity
ATTN: DRXSY-LA (Mr. Paul Frossell)
Aberdeen Proving Ground, MD 21005

Director
US Army Material Systems Analysis Activity
ATTN: DRXSY-LA (Mr. Michael Starks)
Aberdeen Proving Ground, MD 21005

Director
US Army Material Systems Analysis Activity
ATTN: DRXSY-LA (Mr. William Smith)
Aberdeen Proving Ground, MD 21005

Director
US Army Material Systems Analysis Activity
ATTN: DRXSY-LA (Dr. Keats Pullen)
Aberdeen Proving Ground, MD 21005

Commander
US Army Armor Center
ATTN: ATZK-CD
Fort Knox, KY 40121

Aerodyne Research Inc.
ATTN: Dr. John Ebersole
Bedford Research Park
Crosby Drive
Bedford, MA 01730

Commander
Air Force Geophysical Laboratory
ATTN: OPI (Dr. R.A. McClatchey)
Hanscom AFB, MA 01731

Commander
Air Force Geophysical Laboratory
ATTN: OPI (Dr. R. Fenn)
Hanscom AFB, MA 01731

Commander
US Army Ordnance Center and School
ATTN: ATSL-CD
Aberdeen Proving Ground, MD 21005

Commander
US Army Ordnance & Chemical Center
and School
ATTN: ATSL-CLC (Dr. Thomas Welch)
Aberdeen Proving Ground, MD 21005

Commander
US Army Ballistic Rsch Laboratory
ATTN: Dr. Robert Eichelberge
Aberdeen Proving Ground, MD 21005

Commander
US Army Ballistic Rsch Laboratory
ATTN: Mr. Alan Downs
Aberdeen Proving Ground, MD 21005

Commander
US Army Ballistic Rsch Laboratory
ATTN: DRDAR-BLB (Mr. Arthur LaGrange)
Aberdeen Proving Ground, MD 21005

Commander
US Army Ballistic Research Laboratory
ATTN: Mr. Richard McGee
Aberdeen Proving Ground, MD 21005

Project Manager
Smoke/Obscurants
ATTN: DRDPM-SMC (COL H. Shelton)
Aberdeen Proving Ground, MD 21005

Project Manager
Smoke/Obscurants
ATTN: DRDPM-SMC (Dr. T. Van de Wal Jr.)
Aberdeen Proving Ground, MD 21005

Project Manager
Smoke/Obscurants
ATTN: DRDPM-SMC (Mr. G. Bowman)
Aberdeen Proving Ground, MD 21005

Project Manager
Smoke/Obscurants
ATTN: DRDPM-SMC (Mr. J. Steedman)
Aberdeen Proving Ground, MD 21005

Commander
US Army Test & Evaluation Command
ATTN: DRSTE-AD-M (Mr. Warren M. Baily)
Aberdeen Proving Ground, MD 21005

Director
US Army Material Systems Analysis Activity
ATTN: DRXSY-LA (Mr. Paul Frossell)
Aberdeen Proving Ground, MD 21005

Director
US Army Material Systems Analysis Activity
ATTN: DRXSY-LA (Mr. Michael Starks)
Aberdeen Proving Ground, MD 21005

Director
US Army Material Systems Analysis Activity
ATTN: DRXSY-LA (Mr. William Smith)
Aberdeen Proving Ground, MD 21005

Director
US Army Material Systems Analysis Activity
ATTN: DRXSY-LA (Dr. Keats Pullen)
Aberdeen Proving Ground, MD 21005

Director
US Army Material Systems Analysis Activity
ATTN: DRXSY-GI (Mr. Sid Geraud)
Aberdeen Proving Ground, MD 21005

Director
US Army Armament R&D Command
Chemical Systems Laboratory
ATTN: DRDAR-CLB-PS (Dr. Ed Stuebing)
Aberdeen Proving Ground, MD 21010

Director
US Army Armament R&D Command
Chemical Systems Laboratory
ATTN: DRDAR-CLB-PS (Mr. Joseph Vervier)
Aberdeen Proving Ground, MD 21010

Director
US Army Armament R&D Command
Chemical Systems Laboratory
ATTN: DRDAR-CLY-A (Mr. Ron Pennsyle)
Aberdeen Proving Ground, MD 21010

Commander
Harry Diamond Laboratories
ATTN: Dr. William Carter
2800 Powder Mill Road
Adelphi, MD 20783

Commander
Harry Diamond Laboratories
ATTN: DELHD-RAC (Dr. R.G. Humphrey)
2800 Powder Mill Road
Adelphi, MD 20783

Commander
Harry Diamond Laboratories
ATTN: Dr. Ed Brown
2800 Powder Mill Road
Adelphi, MD 20783

Commander
Harry Diamond Laboratories
ATTN: Dr. Stan Kulpa
2800 Powder Mill Road
Adelphi, MD 20783

Commander
ERADCOM
ATTN: DRDEL-AP
2800 Powder Mill Road
Adelphi, MD 20783
2

Commander
ERADCOM
ATTN: DRDEL-CG/DRDEL-DC/DRDEL-CS
2800 Powder Mill Road
Adelphi, MD 20783

Commander
ERADCOM
ATTN: DRDEL-CT
2800 Powder Mill Road
Adelphi, MD 20783

Commander
ERADCOM
ATTN: DRDEL-EA
2800 Powder Mill Road
Adelphi, MD 20783

Commander
ERADCOM
ATTN: DRDEL-PA/DRDEL-ILS/DRDEL-E
2800 Powder Mill Road
Adelphi, MD 20783

Commander
ERADCOM
ATTN: DRDEL-PAO (S. Kimmel)
2800 Powder Mill Road
Adelphi, MD 20783

Commander
ERADCOM
ATTN: DRDEL-PAO (Paul Case)
2800 Powder Mill Road
Adelphi, MD 20783

Commander
HQ, AFSC/DLCAA
ATTN: LTC Glen Warner
Andrews AFB, MD 20334

AFSC
ATTN: WER (Mr. Richard F. Picanso)
Andrews AFB, MD 20334

Commander
Concepts Analysis Agency
ATTN: MOCA-SMC (Hal E. Hock)
8120 Woodmont Ave
Bethesda, MD 20014

Martin Marietta Laboratories
ATTN: Jar Mo Chen
1450 South Rolling Road
Baltimore, MD 21227

Commander
US Army Intelligence Agency
Fort George G. Meade, MD 20755

Director
National Security Agency
ATTN: R52/Woods
Fort George G. Meade, MD 20755

Chief
Intelligence Materiel Dev & Support Ofc
ATTN: DELEW-WL-I
Bldg 4554
Fort George G. Meade, MD 20755

Acquisitions Section, IRDB-D823
Library & Info Service Div, NOAA
6009 Executive Blvd
Rockville, MD 20852

Naval Surface Weapons Center
ATTN: Code WR42 (Dr. Barry Katz)
White Oak Library
Silver Spring, MD 20910

The Environmental Research
Institute of MI
ATTN: IRIA Library
PO Box 8618
Ann Arbor, MI 48107

Science Applications Inc.
ATTN: Dr. Robert E. Meredith
15 Research Drive
PO Box 7329
Ann Arbor, MI 48107

Science Applications Inc.
ATTN: Dr. Robert E. Turner
15 Research Drive
PO Box 7329
Ann Arbor, MI 48107

Commander
US Army Tank-Automative R&D Command
Warren, MI 48090

Dr. A. D. Belmont
Research Division
PO Box 1249
Control Data Corp
Minneapolis, MN 55440

Commander
US Army Aviation Systems Command
St. Louis, MO 63166

Director
Naval Oceanography & Meteorology
NSTL Station
Bay St Louis, MS 39529

Director
US Army Engr Waterways Experiment Sta
ATTN: Library
PO Box 631
Vicksburg, MS 39180

Director
US Army Engr Waterways Experiment Sta
ATTN: WESFT (Dr. Bob Penn)
PO Box 631
Vicksburg, MS 39180

Director
US Army Engr Waterways Experiment Sta
ATTN: WESFT (Mr. Jerry Lundien)
PO Box 631
Vicksburg, MS 39180

US Army Research Office
ATTN: DRXRO-PP
PO Box 12211
Research Triangle Park, NC 27709

US Army Research Office
ATTN: DRXRO-GS (Dr. Arthur V. Dodd)
PO Box 12211
Research Triangle Park, NC 27709

Commander
US Army Cold Regions Rsch & Engr Lab
ATTN: Mr. Roger Berger
Hanover, NH 03755

Commander
US Army Cold Regions Rsch & Engr Lab
ATTN: Mr. George Aitken
Hanover, NH 03755

Commander
US Army Cold Regions Rsch & Engr Lab
ATTN: CRREL-RD (Dr. K.F. Sterrett)
Hanover, NH 03755

Commander
US Army Armament R&D Command
ATTN: DRDAR-TSS (Bldg 59)
Dover, NJ 07801

Commander
US Army Armament R&D Command
ATTN: DRDAR-AC (J. Greenfield)
Dover, NJ 07801

Project Manager
Cannon Artillery Weapons Systems
ATTN: DRCPM-CAWS
Dover, NJ 07801

Project Manager
Cannon Artillery Weapons Systems
ATTN: DRCPM-CAWS-GP (G.H. Waldron)
Dover, NJ 07801

Commander
HQ, US Army Avionics R&D Activity
ATTN: DAVAA-O
Fort Monmouth, NJ 07703

Commander/Director
US Army Combat Surveillance & Target
Acquisition Laboratory
ATTN: DELCS-D
Fort Monmouth, NJ 07703

Director
US Army Electronics Technology &
Devices Laboratory
ATTN: DELET-D
Fort Monmouth, NJ 07703

Commander
US Army Electronic Warfare Laboratory
ATTN: DELEW-D (Mr. George Haber)
Fort Monmouth, NJ 07703

Commander
US Army Night Vision &
Electro-Optics Laboratory
ATTN: DELNV-L (Dr. Rudolf Buser)
Fort Monmouth, NJ 07703

Commander
US Army Night Vision &
Electro-Optics Laboratory
ATTN: DELNV-L (Dr. Robert Rodhe)
Fort Monmouth, NJ 07703

Commander
ERADCOM Technical Support Activity
ATTN: DELSD-L
Fort Monmouth, NJ 07703

Project Manager, FIREFINDER
ATTN: DRCPM-FF
Fort Monmouth, NJ 07703

Project Manager, REMBASS
ATTN: DRCPM-RBS
Fort Monmouth, NJ 07703

Commander
US Army Satellite Comm Agency
ATTN: DRCPM-SC-3
Fort Monmouth, NJ 07703

Commander
ERADCOM Scientific Advisor
ATTN: DRDEL-SA
Fort Monmouth, NJ 07703

Project Manager
Army Tactical Data Systems
ATTN: DRCPM-TDS
Fort Monmouth, NJ 07703

6585 TG/WE
Holloman AFB, NM 88330

AFWL/WE
Kirtland, AFB, NM 87117

AFWL/Technical Library (SUL)
Kirtland AFB, NM 87117

Commander
US Army Test & Evaluation Command
ATTN: STEWS-AD-L
White Sands Missile Range, NM 88002

Chief
US Army Electronics R&D Command
Office of Missile Electronic Warfare
ATTN: DELEW-M-STE (Dr. Steven Kovel)
White Sands Missile Range, NM 88002

US Army Office of the Test Director
Joint Services EO GW CM Test Program
ATTN: DRXDE-TD (Mr. Weldon Findley)
White Sands Missile Range, NM 88002

Commander
TRASANA
ATTN: ATAA-D (Dr. Wilbur Payne)
White Sands Missile Range, NM 88002

Commander
TRASANA
ATTN: ATAA-TDB (Louis Dominquez)
White Sands Missile Range, NM 88002

Commander
TRASANA
ATTN: ATAA-PL (Dolores Anguiano)
White Sands Missile Range, NM 88002

Commander
TRASANA
ATTN: ATAA-TOP (Roger Willis)
White Sands Missile Range, NM 88002

Commander
TRASANA
ATTN: ATAA-TGC (Dr. Alfonso Diaz)
White Sands Missile Range, NM 88002

Commander
TRASANA
ATTN: ATAA-TGA (Mr. Edward Henry)
White Sands Missile Range, NM 88002

Grumman Aerospace Corporation
Research Dept - MS A08-35
ATTN: John E. A. Selby
Bethpage, NY 11714

Rome Air Development Center
ATTN: Documents Library
TSLD (Bette Smith)
Griffiss AFB, NY 13441

Commander
US Army Tropic Test Center
ATTN: STETC-TD (Info Center)
APO New York 09827

Commander
US Army R&D Coordinator
US Embassy, Bonn, Box 165
APO New York 09080

HQ
USAREUR & Seventh Army
APO New York, NY 09403

Air Force Avionics Laboratory
ATTN: AFAL/RWI-3 (Cpt James Pryce)
Wright-Patterson AFB, OH 45433

Air Force Air Systems Laboratory
ATTN: AFAL/RWI-e (Dr. George Mavko)
Wright-Patterson AFB, OH 45433

Commandant
US Army Field Artillery School
ATTN: ATSF-CD-R (Mr. Farmer)
Fort Sill, OK 73503

Commandant
US Army Field Artillery School
ATTN: ATSF-CF-R
Fort Sill, OK 73503

Director CFD
US Army Field Artillery School
ATTN: Met Division
Fort Sill, OK 73503

Commandant
US Army Field Artillery School
ATTN: Morris Swett Library
Fort Sill, OK 73503

Commander
US Army Combined Arms Center
ATTN: ATCA-CAT-V (R. DeKinder, Jr.)
Fort Sill, OK 73503

US Army Field Artillery School
ATTN: ATSF-CD
Fort Sill, OK 73503

Commander
273rd Transportation Company
(Heavy Helicopter)
W44CCQ
ATTN: CW4 J. Kard
Fort Sill, OK 73503

Commander
Naval Air Development Center
ATTN: Code 202 (Mr. Thomas Shopple)
Warminster, PA 18974

University of Texas at El Paso
Electrical Engineering Department
ATTN: Dr. Joseph H. Pierluissi
El Paso, TX 79968

US Army Air Defense School
ATTN: ATSA-CD
Fort Bliss, TX 79916

Commander
3rd Armored Cavalry Regiment
ATTN: AFVF-SO
Fort Bliss, TX 79916

Commander
TRADOC Combined Arms Test Activity
ATTN: ATCAT-OP-Q (Wayland Smith)
Fort Hood, TX 76544

Commander
TRADOC Combined Arms Test Activity
ATTN: Technical Library
Fort Hood, TX 76544

Commander
TRADOC Combined Arms Test Activity
ATTN: ATCAT-SCI (Darrell Collin)
Fort Hood, TX 76544

MAJ Joseph Caruso
HQ, TRADOC Combined Arms Test Activity
ATTN: ATCAT-CA
Fort Hood, TX 76544

Commandant
US Army Air Defense School
ATTN: Mr. Blanchett
Fort Bliss, TX 79916

Commander
US Army Dugway Proving Ground
ATTN: STEDP-MT-DA-L
Dugway, UT 84022

Commander
US Army Dugway Proving Ground
ATTN: STEDP-MT-DA-S (John Treatheway)
Dugway, UT 84022

Commander
US Army Dugway Proving Ground
ATTN: STEDP-MT-DA-M (Paul Carlson)
Dugway, UT 84022

Commander
US Army Dugway Proving Ground
ATTN: STEDP-MT-DA-T (William Peterson)
Dugway, UT 84022

Defense Documentation Center
ATTN: DDC-TCA
Cameron Station Bldg 5
Alexandria, VA 22314
12

Ballistic Missile Defense Program Office
ATTN: DACS-BMT
5001 Eisenhower Avenue
Alexandria, VA 22333

Commander
US Army Materiel Dev & Readiness Command
ATTN: DRCLDC (Mr. James Bender)
5001 Eisenhower Ave
Alexandria, VA 22333

Commander
US Army Materiel Dev & Readiness Command
ATTN: DRCBSI
5001 Eisenhower Ave
Alexandria, VA 22333

Institute for Defense Analysis
ATTN: Mr. Lucian Biberman
Arlington, VA 22202

Institute for Defense Analysis
ATTN: Dr. Robert Roberts
Arlington, VA 22202

Director
ARPA
1400 Wilson Blvd
Arlington, VA 22209

Defense Advanced Rsch Projects Agency
ATTN: Steve Zakanyez
1400 Wilson Blvd
Arlington, VA 22209

Defense Advanced Rsch Projects Agency
ATTN: Dr. Carl Thomas
1400 Wilson Blvd
Arlington, VA 22209

Defense Advanced Rsch Projects Agency
ATTN: Dr. James Tegnelia
1400 Wilson Blvd
Arlington, VA 22209

Commander
US Army Security Agency
ATTN: IARD-MF
Arlington Hall Station
Arlington, VA 22212

USA Intelligence & Security Command
ATTN: E. A. Speakman,
Science Advisor
Arlington Hall Station
Arlington, VA 22212

Commander
US Army Foreign Sci & Tech Center
ATTN: DRXST-IS1
220 7th Street, NE
Charlottesville, VA 22901

Commander
US Army Foreign Sci & Tech Center
ATTN: Dr. Orville Harris
220 7th Street, NE
Charlottesville, VA 22901

Commander
US Army Foreign Sci & Tech Center
ATTN: Dr. Bertram Smith
220 7th Street, NE
Charlottesville, VA 22901

Naval Surface Weapons Center
ATTN: Code G65
Dahlgren, VA 22448

Commander
Operational Test & Evaluation Agency
Columbia Pike Bldg
5600 Columbia Pike
Falls Church, VA 22041

Commander
US Army Night Vision
& Electro-Optics Lab
ATTN: DELNV-D (Mr. John Johnson)
Fort Belvoir, VA 22060

Commander
US Army Night Vision
& Electro-Optics Lab
ATTN: DELNV-VI (Mr. J.R. Moulton)
Fort Belvoir, VA 22060

Commander
US Army Night Vision
& Electro-Optics Lab
ATTN: DELNV-VI (Luanne Overt)
Fort Belvoir, VA 22060

Commander
US Army Night Vision
& Electro-Optics Lab
ATTN: DELNV-VI (Tom Cassidy)
Fort Belvoir, VA 22060

Commander
US Army Night Vision
& Electro-Optics Lab
ATTN: DELNV-VI (Richard Bergemann)
Fort Belvoir, VA 22060

Commander
US Army Night Vision
& Electro-Optics Lab
ATTN: DELNV-VI (Dr. John Ratches)
Fort Belvoir, VA 22060

Commander
US Army Night Vision
& Electro-Optics Lab
ATTN: DELNV-FIR (Fred Petito)
Fort Belvoir, VA 22060

Commander
US Army Engineering Topographic Lab
ATTN: ETL-TD-MB
Fort Belvoir, VA 22060

US Army Engineer School
ATTN: ATSE-CD
Fort Belvoir, VA 22060

Commandant
US Army Engineering Center & School
Directorate of Combat Developments
Fort Belvoir, VA 22060

Commander
US Army Mobility Equip R&D Command
ATTN: DRDME-RT (Mr. Fred Kezer)
Fort Belvoir, VA 22060

Director
Applied Technology Laboratory
ATTN: DAVDL-EU-TSD (Tech Library)
Fort Eustis, VA 23604

Department of the Air Force
OL-C, 5WW
Fort Monroe, VA 23651

Commander
HQ, TRADOC
ATTN: ATCD-PM
Fort Monroe, VA 23651

Commander
US Army Training & Doctrine Command
Fort Monroe, VA 23651

Commander
US Army Training & Doctrine Command
ATTN: ATCD-IE-R (Mr. Dave Ingram)
Fort Monroe, VA 23651

Commander
US Army Training & Doctrine Command
ATTN: ATCD-STE
Fort Monroe, VA 23651

Commander
US Army Training & Doctrine Command
ATTN: ATCD-CF (Chris O'Conner)
Fort Monroe, VA 23651

Commander
US Army Training & Doctrine Command
ATTN: ATCD-AN-TD (Seymour Goldbert)
Fort Monroe, VA 23651

Commander
US Army Training & Doctrine Command
ATTN: ATCD-TA (M. P. Pastel)
Fort Monroe, VA 23651

Commander
US Army Training & Doctrine Command
ATTN: Tech Library
Fort Monroe, VA 23651

Department of the Air Force
5WW/DN
Langley AFB, VA 23665

Commander
US Army INSCOM/QRC
6845 Elm Street - S407
McLean, VA 22101

MITRE Corporation
ATTN: Robert Finkelstein
1820 Dolley Madison Blvd
McLean, VA 22101

Science Applications, Inc.
8400 Westpark Drive
ATTN: Dr. John E. Cockayne
McLean, VA 22101

Director
Development Center MCDEC
ATTN: Firepower Division
Quantico, VA 22134

US Army Nuclear & Chemical Agency
ATTN: MONA-WE (Dr. Jack Berberet)
7500 Backlick Road
Springfield, VA 22150

Director
US Army Signals Warfare Laboratory
ATTN: DELSW-OS (Dr. R. Burkhardt)
Vint Hill Farms Station
Warrenton, VA 22186

Commander
US Army Cold Regions Test Center
ATTN: STECR-OP-PM
APO Seattle, WA 98733

Effects Technology Inc.
ATTN: Jack Carlyle
5383 Hollister Avenue
Santa Barbara, CA 93111

Raytheon Company
Electro-Optics Department
ATTN: Dr. Charles M. Sonnenschein
Boston Post Road
Wayland, MA 01778

Norden Systems
ATTN: Estelle Thurman, Librarian
Norwalk, CT 06856

MIT Lincoln Laboratory
ATTN: Dr. T. Goblick, D-447
PO Box 73
Lexington, MA 02173

Commander/Director
US Army Combat Surveillance & Target
Acquisition Laboratory
ATTN: DELCS-R (Mr. David Longinotti)
Fort Monmouth, NJ 07703

General Research Corporation
ATTN: Dr. Ralph Zirkind
7655 Old Springhouse Road
McLean, VA 22101

Commander
MIRADCOM
ATTN: DRDMI-TE (Mr. W. J. Lindberg)
Huntsville, AL 35807

Teledyne Brown Engineering
ATTN: Bruce Tully, Mail Stop 19
Cummings Research Park
Huntsville, AL 35807

Applied Physics Laboratory
John Hopkins University
ATTN: Dr. Michael Lun
John Hopkins Road
Laurell, MD 20810

☆ U.S.GOVERNMENT PRINTING OFFICE: 1979 — 677-017/22